

Dissertation zur Erlangung des Doktorgrades
der Fakultät für Chemie und Pharmazie
der Ludwig-Maximilians-Universität München

**Development of an Aqueous Suspension of
Recombinant Human Bone Morphogenetic
Protein-2 (rhBMP-2)**

**Entwicklung einer wässrigen Suspension des rekombinanten
menschlichen Knochenwachstumsproteins-2 (rhBMP-2)**

vorgelegt von

Daniel Hans Schwartz

aus Pegnitz

München, 2005

ERKLÄRUNG

Diese Dissertation wurde im Sinne von § 13 Abs. 3 bzw. 4 der Promotionsordnung vom 29. Januar 1998 von Herrn Prof. Dr. W. Frieß betreut.

EHRENWÖRTLICHE VERSICHERUNG

Diese Dissertation wurde selbstständig, ohne unerlaubte Hilfe angefertigt.

München, am 18.03.2005

.....
Daniel Hans Schwartz

Dissertation eingereicht am: 5.4.2005

1. Gutachter: Prof. Dr. W. Frieß

2. Gutachter: Prof. Dr. G. Winter

Tag der mündlichen Prüfung: 31.5.2005

TO MY MOTHER

In love and perpetual gratefulness

„Geschrieben steht: „Im Anfang war das *Wort!*“
Hier stock ich schon! Wer hilft mir weiter fort?
Ich kann das *Wort* so hoch unmöglich schätzen,
ich muß es anders übersetzen,
Wenn ich vom Geiste recht erleuchtet bin.
Geschrieben steht: Im Anfang war der *Sinn*.
Bedenke wohl die erste Zeile,
das deine Feder sich nicht übereile!
Ist es der *Sinn*, der alles wirkt und schafft?
Es sollte stehn: Im Anfang war die *Kraft!*
Doch auch indem ich dieses niederschreibe,
Schon warnt mich was, dass ich dabei nicht bleibe.
Mir hilft der Geist! Auf einmal seh ich Rat
Und schreibe getrost: Im Anfang war die *Tat!*“

Goethe, Faust, 1224-1237

Acknowledgements

The present thesis has been acquired at the Institute for Pharmacy and Food Chemistry, Department of Pharmaceutical Technology, at the Friedrich-Alexander University of Erlangen-Nuernberg and the Department of Pharmacy, Pharmaceutical Technology and Biopharmaceutics at the Ludwig-Maximilians-University of Munich.

I am mostly indebted to my supervisor Prof. Dr. W. Frieß, to give me the opportunity to join his working group and to prepare this thesis. I very much appreciated his scientific advice and his ongoing interest in the progress of my work. His great personality and his soft skills make it a pleasure to work with him.

I also want to express my thanks to Prof. Dr. J. Lee, the chairman of the Department of Pharmaceutical Technology in Erlangen, who accorded me an excellent technological education and granted relief during my first time as a PhD student. From the kind and collegial working group in Erlangen, I want to set apart PhD Monika Geiger, my “pre-decessor”, who introduced me in the secrets of BMP and provided ongoing mentor- and friendship beyond her time at the university – thanks a lot!

At the University of Munich, the chairman and co-referee, Prof. Winter, is greatly acknowledged. By his personal leadership, he managed to create a very pleasant working atmosphere, and his door was always open for both scientific and personal advice.

I would like to thank all my colleagues who warmly welcomed me in Munich and who greatly contribute to the excellent atmosphere (mirrored, e.g. in the legendary “Weißwurstfrühstück” in the “Fürstenegger”, in trips through the “Schickeria” of Munich with Richard Fuhrherr, or in the dancing contest in the “Soul” between our group and the group of Prof. E. Wagner). I want to express my gratitude to Iris Metzmacher and Andreas Rutz who shared the lab with me. Thanks for the pleasant time and your friendship – the indefatigable helpfulness of Andreas is greatly acknowledged.

Outside the university, great thanks are addressed to Wyeth BioPharm, Andover, MA, USA for funding and supporting the work with material. Special thanks go to Susan Sofia for her engagement, her ongoing support across the ocean and for critical proofreading the final work. I am also indebted to all whom I meet and worked with during my visit in the USA and to the working groups who performed the animal testing and the cell culture studies for me. I am also much obliged to Andrea Schmitt from Brucker Optics for her support with FTIR-measurements, and to Klaus Hellerbrand, Scill Biomedicals, for the opportunity to use the μ DSC.

Within the period of almost 4 years at two different locations, I had the pleasure to collaborate with a lot of people, who to mention all would go beyond the scope of this acknowledgement. This is particularly true for all who did a great job in the background – the secretary, the technical staff, the cleaners and engineers. So ‘thanks’ to all who contributed in one way or another to this work, but were not explicitly listed.

Table of Contents

Table of Contents	I
List of Abbreviations	V
1 Introduction	1
1.1 Bone Morphogenetic Proteins	1
1.1.1 Milestones in History	1
1.1.2 Biochemistry	2
1.1.2.1 BMP-2 and its Family	2
1.1.2.2 Features of rhBMP-2	3
1.1.2.3 Signaling Pathway	5
1.1.2.4 Pharmacokinetics of rhBMP-2	7
1.1.3 Biologic Activity: Mechanism of Ossification	7
1.1.4 Delivery Systems	8
1.1.5 Applications of BMPs	9
1.1.5.1 Use of rhBMP-2 in Spinal Fusion Applications	9
1.1.5.2 Use of rhBMP in the Treatment of Non-unions	14
1.1.5.3 Further Potential Applications	14
1.2 Formation of Protein Particles by Precipitation	17
1.2.1 Formation of Dry Particles by Standard Methods	17
1.2.2 Protein Precipitation: Definition and Principles	19
1.2.3 Precipitation Methods	19
1.2.3.1 Crystallization	20
1.2.3.2 Isoelectric Precipitation	20
1.2.3.3 Salt-induced Precipitation: Salting-out	21
1.2.3.4 Miscible Organic Solvent Precipitation	24
1.2.3.5 Precipitation by Non-ionic Polymers	25
1.2.3.6 Precipitation by Metal Ions	26
1.2.3.7 Protein Binding Dyes	27
1.2.3.8 Precipitation by Ionic (Poly)-Electrolytes	27
1.2.3.9 Affinity Precipitation	29

1.2.4	Precipitate Formation	29
1.2.5	Precipitation Process Conditions.....	30
2	Objectives of the Work	31
3	Materials and Methods	32
3.1	Materials.....	32
3.1.1	rhBMP-2.....	32
3.1.2	Reagents and Substances	32
3.2	Methods	35
3.2.1	Focus on the Protein	35
3.2.1.1	Dialysis of Bulk Formulation.....	35
3.2.1.2	Ultrafiltration.....	35
3.2.1.3	Concentration Determination	36
3.2.1.4	High Molecular Weight Species and Aggregation	36
3.2.1.5	Monitoring of Oxidation and Isomerization	37
3.2.1.6	Peptide Mapping	37
3.2.1.7	Proteins' Secondary Structure Integrity.....	38
3.2.1.8	Differential Scanning Calorimetry.....	38
3.2.1.9	(ATR) FT-IR Measurements.....	38
3.2.2	Focus on the Formulation	39
3.2.2.1	Preparation Methods.....	39
3.2.2.2	Additional Operations.....	40
3.2.3	Particle Characterization	41
3.2.3.1	Photon Correlation Spectroscopy	41
3.2.3.2	Laser Light Diffraction	42
3.2.3.3	Light Microscopy	42
3.2.3.4	Laser Light Blockade	42
3.2.3.5	Environmental Scanning Electron Microscopy	42
3.2.4	In-vitro Release	43
3.2.5	Bioactivity Testing	43
3.2.5.1	Determination of Bioactivity in Cell Culture	43
3.2.5.2	Efficacy Study in an Animal Model.....	43

4	Results and Discussion.....	45
4.1	Formulation Development.....	45
4.1.1	Initial Precipitation Process Development.....	45
4.1.1.1	Considerations and Setup	45
4.1.1.2	Particle Size Distribution of Initial Formulation.....	47
4.1.1.3	Effect of Centrifugation	49
4.1.1.4	Influence of Lyophilization	49
4.1.1.5	Influence of Protein Concentration and Batch Volume	50
4.1.1.6	Variations of Mixing Technique and Protein Concentration .	51
4.1.2	Optimization of Formulation Composition	54
4.1.2.1	Solubility in Different Phosphate Buffer Systems.....	54
4.1.2.2	Particle Size Distribution of Optimized Formulation.....	56
4.1.2.3	Phase Contrast Microscopic Imaging of Microparticles	58
4.1.2.4	Laser Light Blockade Measurements	60
4.1.2.5	Effect of Polymers and Surfactants	61
4.1.2.6	Gel Formulations	63
4.1.3	Scanning Electronic Microscopy	64
4.1.4	Mechanistic Studies on Particle Formation with PCS	66
4.1.5	Summary	69
4.2	Protein Integrity.....	69
4.2.1	Process Stability of Precipitation.....	69
4.2.1.1	Aggregation	70
4.2.1.2	Conformational Stability.....	70
4.2.1.3	Bioactivity of Redissolved Microparticles in Cell Culture	80
4.2.1.4	Summary	81
4.2.2	Storage Stability of rhBMP-2 in Microparticles.....	82
4.2.2.1	Study Design	82
4.2.2.2	Oxidation	83
4.2.2.3	Isomerization	87
4.2.2.4	Aggregation	91
4.2.3	Summary	100

4.3	In-vitro Release from rhBMP-2 Microparticles	102
4.3.1	Considerations and Setup	102
4.3.2	Analytic Development	103
4.3.3	Calibration of Concentration Determination with SDS-PAGE....	105
4.3.4	In-Vitro Release of rhBMP-2 from Microparticles in Serum	106
4.3.5	Summary	108
4.4	Efficacy Study in the Rabbit Distal Femur Intraosseous Model	109
4.4.1	Study Design.....	109
4.4.2	Study Outcome	109
5	Summary	110
6	References	110

List of Abbreviations

Ala	alanin
Arg	arginin
ASES	aerosol solvent extraction system
Asn	asparagin
Asp	aspartic acid
ATR	attenuated total reflection
BESTT	BMP-2 evaluation in surgery for tibia trauma
BCP	biphasic calcium phosphate
CDMPs	cartilage derived morphogenetic proteins
Cys	cystein
DME	Dulbecco's modified Eagle's medium
DNA	deoxyribonucleic acid
ESEM	environmental scanning electron microscopy
FBS	fetal bovine serum
FDA	Food and Drug Administration
FTIR	Fourier transform infrared spectroscopy
GDF	growth and differentiation factor
Gln	glutamine
Glu	glutamic acid
Gly	glycine
His	histidine
HDE	human device exemption
HMWs	high molecular weight species
INN	international nonproprietary name
Ile	isoleucine
IM	intramuscular
LLD	laser light diffraction
LDL	low-density lipoprotein
LDS	lithiumdodecyl-sulfate

Leu	leucine
LT	lumbar tapered
Lys	lysine
Met	methionine
MOPS	4-morpholine-propanesulfonic acid
OP	ostogenetic protein
PCMC	protein-coated microcrystals
PAGE	polyacrylamide gel electrophoresis
PCS	photon correlation spectroscopy
PEG	poly-ethylene glycol
PLA	poly-lactide acid
PLGA	poly-lactide-co-glycolic acid
PMA	premarked approval
pl	isoelectric point
rhBMP-2	recombinant human bone morphogenetic protein 2
RPM	rounds per minute
SQ	subcutaneous
SCF	supercritical fluids
Ser	serine
SOC	standard of care
TCA	trichloroacetic acid
Thr	thyrosine
Trp	tryptophane
Val	valine
Vgr	vegetal related
VLDL	very low-density lipoprotein

1 Introduction

1.1 Bone Morphogenetic Proteins

1.1.1 Milestones in History

As it seems typical for ground breaking discoveries, the key find triggering an avalanche of intense research was made by chance, based on a failed experiment of Marshall Urist in 1965. He demineralized rabbit and rat bone matrix with 0.6 M HCl, treated some of the samples with CaCl_2 to create nucleation sites and implanted both the treated as well as the untreated control samples intramuscularly in rodents. Surprisingly, the control samples exhibited the formation of new bone within few weeks after implantation [Urist, 1965]. What happened? The demineralized bone matrix seems to contain substance(s) responsible for the observed morphogenesis. Morphogenesis describes the complex process of differentiation and growth of the structure of a part of or the whole organism – herein the development of a vascularized spherical ossicle with functioning bone marrow. Urist attributed this phenomenon to certain bone matrix derived proteins, coining the term “bone morphogenetic protein” to describe them, and in the following years, he succeeded in corroboration of his hypothesis [Urist et al., 1971] by identification of the protein fraction responsible for the effect.

The isolation and characterization of bone morphogenetic proteins (BMPs) was hampered by the minimal amounts present in bone as 1 kg bone only contains approximately 1-2 μg BMPs [Wang et al., 1988]. Consequently, laborious purification procedures were necessary to obtain at least partially purified extracts. The introduction of dissociative extractants [Sampath et al., 1981] led to an improvement of the extraction technique, increasing the availability of highly purified bone inducing proteins. The development of a satisfactory bioassay and advances in molecular biotechnology made it possible to encode the amino-acid sequences of purified bovine bone extracts. In 1988, Wang and coworkers succeeded in isolation and characterization of three polypeptides subsequently named BMP-1, BMP-2 and BMP-3 [Wang et al., 1988]. Knowing their amino acid sequence, oligonucleotide probes could be synthesized and used to screen the human genes for the encoding DNA sequences [Wang et al., 1987]. Transfection of the full length cDNA via mammalian expression vectors into Chinese hamster ovary cells finally led to the production of the first recombinant human bone morphogenetic proteins (rhBMPs) [Wang et al., 1989].

1.1.2 Biochemistry

1.1.2.1 BMP-2 and its Family

BMP-2 is only one representative of the large bone morphogenetic protein family. BMPs are highly conserved across different animal species. At least 15 individual human BMPs are currently recognized (Figure 1-1) [Einhorn, 2003]. RhoBMP-2 and rhoBMP-4 to rhoBMP-7 have proven to be osteoinductive in the rat subcutaneous assay. Interestingly, BMP-3, which is most abundant in bone, failed to develop new bone and is believed to represent an inhibitor [Bahamonde et al., 2001]. With the exception of BMP-1, that has proven to be a metalloproteinase [Hofbauer et al., 1996], BMPs are multifunctional cytokines belonging to the large group of the Transforming Growth Factor β gene superfamily, currently including approximately 45 genes [Rueger, 2002]. They are synthesized as large precursors consisting of an N-terminal signal sequence, a poorly conserved prodomain and a mature domain at the carboxy terminus. The latter contains 7 highly conserved cysteine residues. Six of them join in three intramolecular disulfide bridges, building the cystine-knot folding motif: two cysteine bridges form a ring-like structure with the main chain, wide enough for the third disulfide bridge to pass through [Scheufler et al., 1999]. The remaining cysteine participates in a disulfide bridge with the cysteine of another molecule, enabling the formation of homodimers in case of linkage with an identical monomer or heterodimers by dimerization of two different members.

Table 1-1: BMP family (modified from Reddi, 2000)

BMP Subfamily	generic name	BMP designation
BMP-2/4	BMP-2A	BMP-2
	BMP-2B	BMP-4
BMP-3	Osteogenin	BMP-3
	GDF-10 (growth/differentiation factor)	BMP-3B
OP-1 (ostogenetic protein)/BMP-7	BMP-5	BMP-5
	Vgr-1 (vegetal related)	BMP-6
	OP-1	BMP-7
	OP-2	BMP-8
	OP-3	BMP-8B
	GDF-11	BMP-11

BMP Subfamily	generic name	BMP designation
CDMP (cartilage derived morphogenetic protein)	CDMP-1/GDF-5	BMP-14
	CDMP-2/GDF-6	BMP-13
	CDMP-3/GDF-7	BMP-12
others	BMP-9	BMP-9
	BMP-10	BMP-10
	BMP-15	BMP-15
	BMP-16	BMP-16

1.1.2.2 Features of rhBMP-2

RhBMP-2 is secreted by genetically engineered CHO (Chinese hamster ovary) cells as a dimeric glycoprotein of approx. 30 KDa [Wozney et al., 1988]. The carbohydrate moiety has proven to be not important for biological activity [Rueger, 2002], and methods to produce active BMP-2 in *Escherichia coli* are also described [Ruppert et al., 1996, Zhao et al., 2002]. The structure of a BMP-2 monomer is descriptively associated with a 'hand' consisting of two 'fingers' of antiparallel β -strands and a α -helical region at the 'wrist' (Figure 1-1a, b) [Rueger, 2002]. Dimer formation can illustrative be figured as a handshake. Beside the covalent disulfide bond, interactions between the α -helix and the β -sheets of the neighboring molecule further support the intersubunit contact. RhBMP-2 dimer formation involves three monomer variants: the mature monomer (Q), consisting of 114 amino acids, an extended form with a prolonged sequence of 17 amino acids at the N-terminus (T), and an alteration of the mature form, with isomerization of the N-terminal glutamine into the pyroglutamate form (<Q) [Friess, 2000]. Consequently, 6 dimeric isoforms are possible (Figure 1-2). All of them have proven to be active in an in vitro cell culture assay.

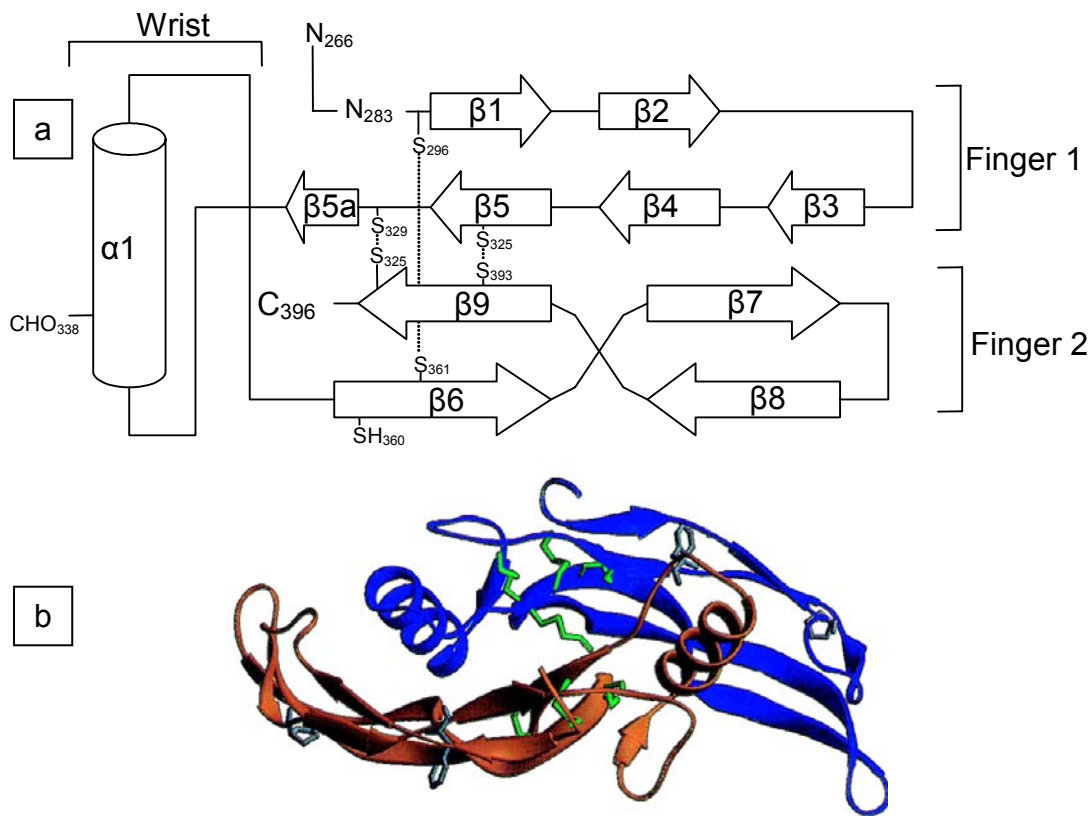


Figure 1-1: Topology diagrams of BMP-2: (a) schematic drawing: Helices are indicated as cylinders, β -strands as arrows; disulfide bridges are dotted (modified from Friess 2000 and Scheufler et al. 1999) (b) three dimensional folding of the native BMP-2 dimer: α -helices are indicated as spiral, β -strands as arrow (modified from Scheufler et al. 1999)

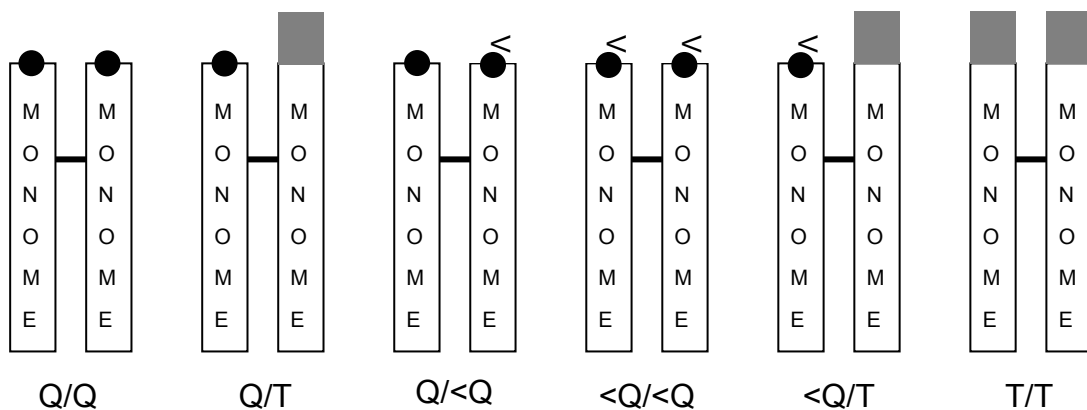


Figure 1-2: Combination among 3 different monomers, the mature monomer (Q), an isomerized pyro-glutamate mature form (<Q) and an extended form (T) leads to 6 dimeric isoforms.

With an isoelectric point (pI) of 8.2 ± 0.4 , BMP-2 is a highly basic protein [Abbatiello et al., 1997]. The need of chaotropic agents for satisfied extraction of

natural occurring BMPs underlines its limited solubility in water. The highly hydrophobic surface of the dimer, as it can be seen in Figure 1-3a, provides an explanation for this (modified from Scheufler et al., 1999). Furthermore, BMP-2 exhibits a unique solubility profile (Figure 1-3b): increasing the ionic strength initially causes a rapid decrease in solubility, being minimal at approx. 0.15 M, followed by an increase at intermediate ionic strengths. Above approx. 0.5 M, classic salting-out is observed [Abbatiello et al., 1997]. The fact that solubility is minimal at physiologic conditions is thought to be relevant for its pharmacologic effect.

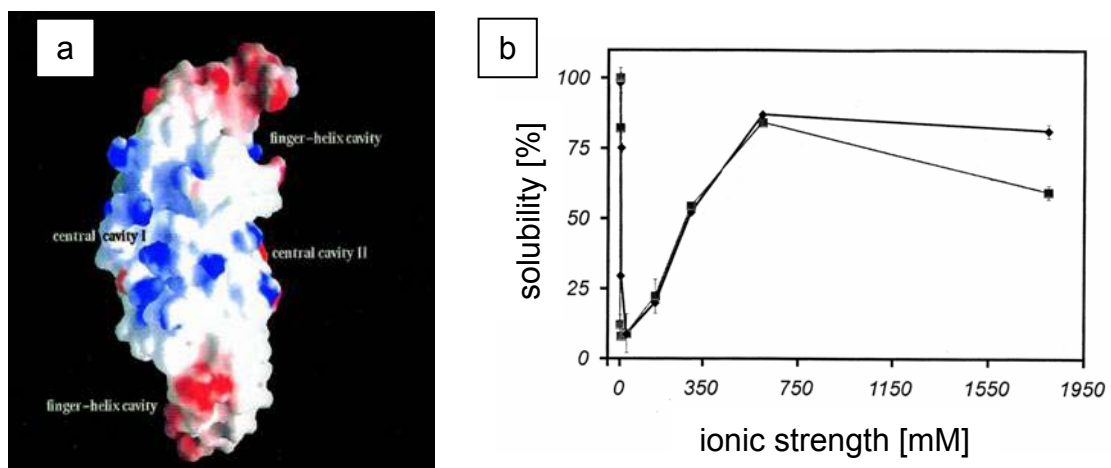


Figure 1-3: (a) Solvent accessible surface of BMP-2: white areas depict hydrophobic, blue positive and red areas negative surface charges (modified from Scheufler et al., 1999); (b) solubility behavior of rhBMP-2 at pH 7.2 for NaCl (♦) and Na₂SO₄ (■): before approx. 500 mM, solubility correlates to the ionic strength, at higher concentrations, salt specific salting out is observed in pH given (adapted from Abbatiello et al., 1997).

1.1.2.3 Signaling Pathway

Two different BMP receptors, BMPR-I and BMPR-II are known. The individual receptors have a weak affinity for the BMP dimer, but binding to both types occurs with high affinity leading to the formation of a heteromeric complex (Figure 1-4a). Within this complex, the constitutively active BMPR-II receptor kinase phosphorylates the GS domain of BMPR-I. In the 'canonical' pathway, intracellular signaling is mediated by Smad proteins. The Smads can be divided into three subclasses: receptor-regulated Smads (R-Smads), common-mediator Smads (Co-Smads, i.e. Smad 4) and inhibitory Smads (I-Smads, i.e. Smad 6 and 7). Upon BMP receptor activation, R-Smads (Smad 1, 5, and 8) are phosphorylated and form heteromeric complexes with Co-Smad 4. The trimeric Smad complex translocates to the nucleus and activates the transcription of early BMP-responsive genes. I-Smads (Smad 6 and 7) display their negative regulation by inhibition of the phosphorylation of R-Smads (Figure 1-4b). The 'noncanonical', mitogen-activated protein kinase (BMP-MAPK) pathway is

thought to be responsible for BMP induced apoptosis and inhibition of transcription factors [Botchkarev, 2003]. Extracellularly, the activity of BMPs is modulated by diffusible antagonists (noggin, chordin, follistatin), preventing their binding.

Despite the increased knowledge about the receptors and the signaling pathways, the understanding of the complex interplay of different growth factors during bone formation and bone repair is still limited. There is general consensus that there must be a so-called cross talk between the various signaling pathways, but the elucidation of the underlying mechanisms is still in its early stages [Lieberman et al., 2002].

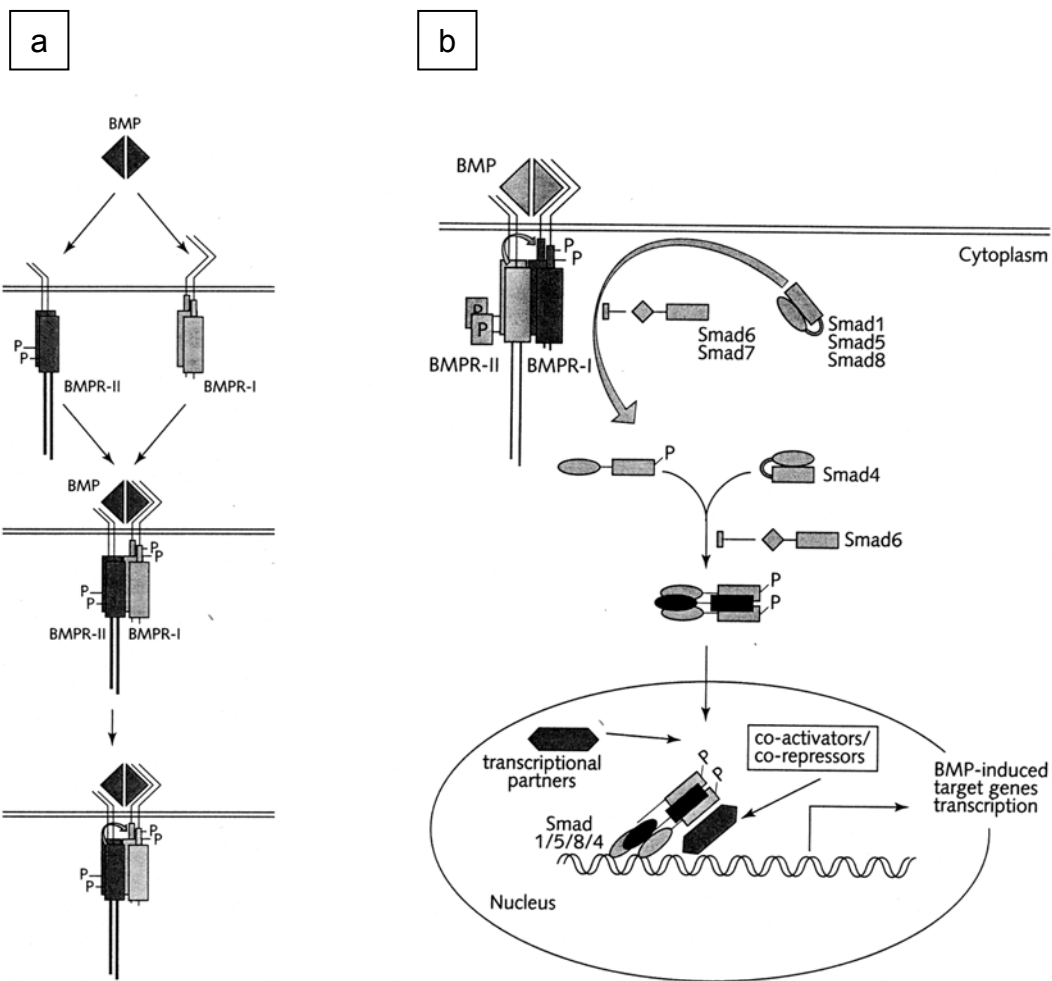


Figure 1-4: (a) Receptor activation; (b) intracellular signalling cascade of the 'canonical' pathway (modified from Korchynsky et al., 2002)

1.1.2.4 Pharmacokinetics of rhBMP-2

Due to its short serum half life, BMP is usually combined with a carrier (1.1.4). Therefore, a discussion of the release profile of BMP from different carriers must consider the property of BMP to bind to various materials, e.g. hydroxylapatite/tricalcium phosphate [Friess et al., 1997] or collagen [Friess, 2000], explaining its incomplete release from these systems. The existence of a binding site for heparin, which strongly influences its activity, is described by Ruppert [Ruppert et al., 1996]. The in vitro release profile is also strongly influenced by the properties of the release medium, reflecting the dependence of BMP solubility on pH and ionic strength. For collagen sponges, an initial burst is reported, releasing 50-80 % of the dose within the first day [Geiger, 2001]. In vitro studies utilizing serum as release medium demonstrate a sustained release over 14 days [D'Augusta et al., 2000]. In vivo studies in the well established rat ectopic model unclosed a more differentiated picture: an initial, rapid rhBMP-2 loss is followed by a monoexponential decrease of BMP concentration from the sponge [Winn et al., 1998]. Further studies compare the osteoinductive activity of rhBMP-2 with a modified variant (plasmin cleaved rhBMP-2) that shows a stronger initial burst and subsequently lower local levels over time. Although the cleaved BMP variant has a higher activity in cell culture [Abbatiello et al., 1997], its in vivo osteoinductive activity is significantly less than the native rhBMP-2 [Winn et al., 1999]. This observation provides strong evidence that sustained release is a critical pharmacokinetic parameter for osteoactivity. The initial retention at the implant site is also a function of the isoelectric point, with molecules of lower pI disappearing faster [Uludag et al., 2001]. It is hypothesized that 'bound' BMP launches its effect not only in terms of an increased effective local concentration, but also may potentiate its activity by being presented in this form to target cells.

1.1.3 Biologic Activity: Mechanism of Ossification

The development of new bone can follow two different pathways. Endochondral ossification refers to formation of bone with a cartilage intermediate and can be found e.g. in long bone development. Direct bone formation without a cartilaginous intermediate, as it is the case in the skull and the face is called intramembranous ossification [Zhao M. et al., 2002]. The mechanisms determining the ossification pathway are not completely understood. In vitro, bone formation has been shown to be concentration dependent, being endochondral at high and intramembranous at low doses of BMP [Lindholm, 1996]. Preclinical studies suggest that the anatomic site at which BMP is administered also determines the formation pathway [Smith, 1994]. The cascade of events induced by rhBMP-2 applied to a matrix implanted ectopically mimics early stages of embryonic bone formation and postnatal endochondral ossification. RhBMP-2 acts as a growth and differentiation factor [Valentin-Opran et al., 2002]. On a

cellular level, undifferentiated mesenchymal-type cells initially infiltrate the periphery of the matrix by chemotaxis and proliferate. After differentiation into chondroblasts, these cells secrete extracellular matrix and create a cartilaginous template, which hypertrophies. At the same time, vascularization by haematopoietic and endothelial cells occurs, a prerequisite for osteoblast differentiation [Reddi, 2001]. The complex process temporally extends from the periphery toward the center of the implant, potentially connected with degradation of the implant. Remodeling of the cartilage and trabecular bone by osteoblasts and osteoclasts finally results in the formation of woven bone with vivid marrow core [Kirker-Head, 2000, Valentin-Opran et al., 2002]. The described bone formation can be subdivided into two underlying principles: osteoinduction and osteoconduction. Osteoinduction - provided by BMPs present within the matrix - refers to the ability to induce proliferation of undifferentiated mesenchymal-type cells and formation of osteoprogenitor cells with the capacity to form bone. Osteoconduction is a process attributable to the matrix, supporting the ingrowths of capillaries and cells into its three-dimensional scaffold geometry [Einhorn, 2003].

1.1.4 Delivery Systems

Closely associated with the BMP research is the development of an adequate carrier to create a clinical device for the field of bone reconstruction. A lot of different matrixes have been evaluated in numerous studies in combination with osteoinductive BMPs. In the course of this development, a number of general features for an ideal carrier were compiled [Friess, 2000, Geiger, 2001, Kohnert, 2003]:

- biocompatibility, low immunogenicity and antigenicity
- relative insolubility in physiological conditions
- protection against proteolytic activities
- biodegradability
- amenability to sterilization
- adequate compressive and tensile strength
- adequate porosity for cellular invasion and vascularization
- enhancement of cellular attachment
- affinity to BMPs and host bone
- enhancement of osteogenic activity of BMP with a restrictive release of BMP at an effective dose during a period coincident with the accumulation and proliferation of target cells

Collagen-based carriers have proven to be most suitable and were used in clinical settings. The failure to identify a delivery vehicle meeting all the criteria implies that different specific applications define their individual requirements to the matrix. Improvement in minimally invasive surgical techniques, as well as the desire to expand the potential application of BMP, e.g. healing of closed fractures puts emphasis on the development of formulations that can be applied by local injection. Injections of BMPs delivered in buffers have already shown to accelerate healing of closed fractures in rats [Einhorn et al., 2003] and in osteotomy sites in rabbits [Ruhe et al., 2003]. However, the success of pure buffer formulations in large animals is limited due to insufficient responsive cells and insufficient retention at the repair site [Seeherman et al., 2003]. To prolong the retention of BMP at the site of action, different materials are currently under investigation, covering the major categories of inorganic materials (calcium cements), synthetic polymers (PLA, PGLA), natural polymers (hyaluronan) and combinations thereof with embedded ceramics or protein loaded microparticles. Promising results in a rabbit osteotomy model were achieved with calcium phosphate cement as carrier, and large animal and nonhuman studies are awaited to confirm these findings [Ruhe et al., 2003].

1.1.5 Applications of BMPs

Whereas numerous investigations show the potential clinical efficacy of BMPs in the treatment of skeletal disorders, currently only three clinical trials have supported the use of recombinant bone morphogenetic proteins, leading to FDA (Food and Drug Administration) approval for specific indications [Einhorn, 2003].

1.1.5.1 Use of rhBMP-2 in Spinal Fusion Applications

Surgical techniques for spinal fusion and standard of care (SOC):

Spinal fusion describes a surgical treatment aiming the bridging of two (single level) or three (two-level) vertebrae by formation of solid bone between them. This might become necessary when pain in the lower back or the legs arises from irritated nerve endings or even entrapped nerves located at the level of the vertebrae. By fixation, motion across the damaged level is eliminated and so is the trigger for pain. Indications for such a surgical procedure are disorders of the spine, such as recurrent disc herniation, lumbar spondylolisthesis, scoliosis, severe disc degeneration or a traumatic injury of the spine, such as a fracture. (www.spineuniverse.com). According to the procedure, two different types of spine fusion scenarios can be distinguished. In the 'anterior interbody approach', the surgery will be performed from the front via an incision in the patient's abdomen, and the space between the vertebral bodies is targeted to be bridged. The 'posterior spinal fusion', also referred to 'posterolateral approach' is performed from the back and the rigidity of the vertebrae should be

achieved by inducing new bone between the spaces of the transverse processes (www.espineinstitute.com). To establish a novel therapeutic regimen, safety and efficacy have to be proven. Efficacy can be demonstrated by equivalence to SOC [Einhorn, 2003]. Preferred bone graft material is autologous bone, i.e. graft originating from the same individual (autograft). It unites all three prerequisites for new bone formation: It supplies potent bone forming cells, i.e. osteoblasts or its precursors (osteogen), depicts osteoinductive and osteoconductive properties. The main disadvantage of autografts is the necessity to harvest them from the patient in an additional surgery which is accompanied by a number of problems, e.g. donor site pain, increased blood loss during surgery and a higher risk of infection.

Posterolateral approach with rhBMP-2:

In several animal models, reaching from low vertebrates to nonhuman primates, the use of endogenous and recombinant BMP in spinal fusion has been evaluated. In a validated rabbit model posterolateral fusion was aimed, comparing rhBMP-2 with control autograft. A 100 % fusion rate within 4 weeks after implantation was achieved. Bone formation, consolidation and remodeling were greater in the rhBMP-2 treated group, and the fusions were biomechanically stronger and stiffer than the control [Schimandle et al., 1995]. However, transfer of the promising results achieved in low animals to a nonhuman primate animal model initially failed. Martin et al. found out that higher concentrations were necessary in primates, compared to lower animals. Furthermore, his studies revealed the need of compression resistant carriers, as muscle compression of the device take place in the posterolateral fusion application [Martin, Jr. et al., 1999]. In awareness of this data, a compression resistant carrier composed of hydroxylapatite and tricalcium phosphate was developed and demonstrated efficacy of rhBMP-2 in a nonhuman primate model, whereas no fusion could be achieved in the autograft control group [Boden et al., 1999]. The successful components were incorporated into a collagen sponge to obtain a moldable matrix which is loaded with BMP before application. Again, the device has proven 100 % fusion in a rabbit and rhesus monkey model, and comparison with historical controls treated with autograft indicates higher stiffness. Preclinical studies in a nonhuman primate animal model have shown that combinations of an rhBMP-2 soaked absorbable collagen sponge with allograft chips or restorable ceramic granules also leads to 100 % fusion, whereas fusion in control group treated with autograft is only achieved in 33 % [Sandhu et al., 2003].

Up to now two pilot clinical trials in humans were performed with rhBMP-2 loaded biphasic calcium phosphate (BCP) carriers for the posterolateral lumbar fusion environment [Boden et al., 2002]. Both studies suggest the superiority of the artificial BMP/BCP device compared to autograft. A 100 % fusion rate was observed in all BMP-2/BCP treated patients, thus determining effective doses of

BMP for this application. Furthermore, the influence of instrumentation was evaluated and a threshold was defined where fusions can be achieved without additional fixation. Studies including larger patient groups were awaited to confirm these findings, paving the way for approval of an rhBMP-2 carrier in the posterior lumbar fusion environment.

Interbody fusion approach with rhBMP-2:

The first preclinical study, using an interbody cage augmented either with rhBMP-2 or with autogenous iliac-crest bone graft for lumbar interbody fusions in a sheep model showed superiority of the BMP group compared to the autograft control group with respect to histologic evaluation of fusion rate after 6 months (37 % vs. 100 % fusion rate). The rhBMP-2 induced fusions had significantly less fibrous-tissue ingrowths along the cage fenestrations than the control [Sandhu et al., 2002]. Similar outcomes were achieved by Zdeblick in a goat model, comparing titanium fusion cages filled either with an rhBMP-2 soaked collagen sponge or with autograft (95 % vs. 48 % fusion rate) [Zdeblick et al., 1998]. With success evident in lower animals, Boden et al. tested the efficacy of two different concentrations of rhBMP-2 in combination with a collagen sponge entrapped in a titanium fusion cage in rhesus monkeys for spinal fusion. Although both concentrations succeed in bridging, bone formation was quicker and denser in response to the higher concentration of 1.5 mg/ml [Boden et al., 1998]. Comparison of rhBMP-2/collagen carrier with autogenous bone graft, both implanted in combination with allograft dowels in rhesus monkeys for interbody fusion, depicts the inferiority of the latter in respect to fusion rates after 6 months. In addition, the rhBMP-2/collagen/allograft composition had undergone complete remodeling [Hecht et al., 1999]. A recently published study elucidates the effectiveness of rhBMP-2 in combination with a composite sponge (collagen-hydroxylapatite-tricalcium phosphate carrier) in pigs. Herein, a minimally invasive surgical technique in combination with instrumentation was used. The observed bone formation was significantly greater in the BMP treated group. Additionally, the rhBMP-2 containing carrier achieves the best fusion score, followed by nearly similar scores for autografts harvested from either the iliac crest or the rib [Sucato et al., 2004].

The promising results prompted the FDA to give approval to a series of pilot IDE¹ studies in humans [Sandhu et al., 2003]. The first one involved 14 patients. A small control group of 3 people were treated in an open approach with a titanium cage (Lumbar Tapered Cage: LT-Cage[®]) filled with autograft derived from the iliac crest. 11 patients received the LT-Cage[®] filled with an rhBMP-2

¹ Investigational Device Exemption: An IDE approval allows the use of an investigational device in a clinical study to collect safety and effectiveness data required to support a Premarket Approval (PMA) (<http://www.fda.gov/>).

soaked collagen sponge (referred to Infuse[®]), either in an open approach or in a laparoscopic surgery [Boden et al., 2000]. Whereas fusion failed in one of three cases in the control group, successful fusions were achieved in all patients of the experimental cohort. To address the question of antibody formation as possible immune response to either the rhBMP-2 or the bovine derived collagen sponge, serum analyses were performed. No patient treated with rhBMP-2 reveals higher antibody titers after surgery. Three patients had increased antibovine-collagen type I titers, but no relevant side effects were observed.

This study demonstrates the safety of rhBMP-2 in humans and its feasibility to induce bone inside intervertebral fusion cages. Furthermore, it confirms the deployed rhBMP-2 concentrations of 1.5 mg/ml to be effective. Although statistical analysis is precluded due to the small number of patients, the outcome also suggests that the rhBMP-2 device is at least equivalent to SOC, autogenous iliac crest bone graft. Finally, the suitability of the study design was confirmed. These results lay the groundwork for a larger pivotal trial enrolling 415 patients requiring anterior lumbar interbody fusion. 143 patients received the LT-Cage[®] filled with Infuse[®] in a classical open approach. 116 patients received the same device in a laparoscopic, i.e. minimally invasive approach. The control group consists of 116 patients and received the LT-Cage[®] filled with iliac crest derived autograft. The highest fusion rates were obtained in the classic open approach of the Infuse[®] treated cohort, achieving fusion in all patients 24 months after surgery. Beside the fusion rate, a 15 point improvement in the Oswestry score, a self-report questionnaire evaluating disability and pain, was used as criterion of success [Fairbank et al., 1980]. After 12 months, the success rate was 76.9 % (100 of 130) in the open Infuse[®] cohort, 75.2 % (94 of 125) in the autograft cohort, 79.8 % (91 of 114) in the cohort that obtained the Infuse[®]/LT-Cage[®] by laparoscopic insertion. The prevalence of rhBMP-2 antibody formation evaluated 3 months after surgery was below 1 % in all cohorts. Prevalence for antibodies against bovine type-I collagen was highest in the laparoscopic cohort (24.8 %), and similar within the autograft and open Infuse[®] cohort (13.1 % and 12.9 % respectively). However, these antibody responses could not be associated with adverse side effects. Significant improvement in respect to operative time and blood loss were yielded in the Infuse[®] group. Additionally, more than one third of the autograft-harvested patients suffer from donor site pain 2 years following surgery. Consulting the results of a previous study enrolling 266 patients treated with iliac crest filled LT-Cages[®] in a laparoscopic approach, the median time to return to work was 116 days in the Infuse[®] group and 170.5 days in the iliac-crest bone-graft group. This study assessed the safety, efficacy and the therapeutic benefits of Infuse[®] combined with the LT-Cage[®] for spinal fusions and led to FDA approval in USA on July 2002 for the treatment of spinal degenerative disc disease.

Table 1-2: Products approved in the USA and the EU containing rhBMPs (BMP-2 or OP-1)

trade name	approval/ date	description	indication
Osigraft [®] (INN: Eptotermin alfa) Novos	Medicinal product for human use: August 21, 2001	osteogenic protein 1 powder for suspension for intraosseus implantation	treatment of non-union of tibia of at least nine month duration
OP-1 [®] Implant	HDE ² : October 17, 2001	human OP-1 powder and bovine collagen mixed with saline so- lution to form a paste	treatment of fractured bones failed to unite without intervention
Infuse [®] Bone Graft/ LT-CAGE [®] Lumbar Tapered Fusion Device	PMA ³ : July 2, 2002	LT-CAGE: metallic tapered spinal fusion cage; Infuse [®] : rhBMP-2 soaked on an absorbable collagen (bovine type-I) carrier	device to support fusion of vertebrae in the lower spine without the necessity for auto- grafting
InductOs [®] (INN: Dibotermin alfa)	Medicinal product for human use: July 1 st , 2002	Implant kit for periosseous use containing rhBMP-2 soaked on a matrix after reconstitution	adjunct treatment of acute, open tibia fractures in adults in combination with SOC (open fracture reduc- tion, intramedullary nail fixation)
OP-1 Putty	HDE: April 7, 2004	mixture of genetically engineered OP-1 with bovine collagen, sterile saline water and a thickening agent for- ming a putty-like material	posterolateral spinal fusion in patients who are not able to provide autograft material and failed a previous spinal fusion surgery
Infuse [®] Bone Graft	PMA: April 30, 2004	absorbable collagen sponge (bovine origin) soaked with rhBMP-2	aiding the healing of fresh, open fractures of the lower leg bone (ti- bia) in combination with internal stabilization

² Humanitarian Device Exemption: An application approved under HDE must demonstrate that the device does not pose an unreasonable or significant risk of illness or injury, and that the probable benefit to health outweighs the risk of injury or illness from its use; results of scientifically valid clinical investigations are not required (<http://www.fda.gov/>).

³ Premarket Approval: The application submission must provide valid scientific evidence collected from human clinical trials showing the device is safe and effective for its intended use ([Bauer et al., 2002]; <http://www.fda.gov/>).

1.1.5.2 Use of rhBMP in the Treatment of Non-unions

Another successful application for BMP is its use in supporting or accelerating fracture repair. A series of studies evaluated the potential of genetically engineered BMPs in humans for the treatment of large segmental bone defects [Cook et al., 1994, Geesink et al., 1999]. The crucial study leading to FDA approval for treatment of non-unions of the tibia was performed from Friedlaender et al. enrolling 122 patients. They demonstrated the safety of rhOP-1 supplied in conjunction with type I bovine bone-derived collagen and its equivalence to the SOC, the treatment with autograft, without the disadvantage of the latter of an additional harvesting operation site [Friedlaender et al., 2001]. Even superiority of an adjuvant treatment with an rhBMP-2 soaked collagen sponge in combination with SOC to SOC alone was demonstrated in the BESTT (BMP-2 Evaluation in Surgery for Tibia Trauma) study enrolling 450 patients. A significant increase in the rate of fracture-healing, measured by radiographic assessment and decreased number of secondary intervention after 12 months, could be demonstrated in patients treated with 1.5 mg/ml rhBMP-2. The number of fracture site infections in the subset of patients with the most severe tibia fractures was significantly lower, and accelerated soft-tissue healing could be observed.

1.1.5.3 Further Potential Applications

The currently available products demonstrate the usefulness of rhBMPs as osteoinductive component in bone graft substitutes and as adjuvant to SOC to accelerate and support fracture healing of delayed and non-unions and emphasize their importance in the field of orthopedic surgery. Promising results in related fields of tissue engineering demonstrate that the full potential of BMPs is not yet tapped. However, a lot of work still has to be done to elucidate and optimize the ideal delivery strategy for the targeted indication.

Use in oral-maxillofacial surgery:

The successful augmentation of the alveolar ridge has been reported by Howell and coworkers [Howell et al., 1997]. The same carrier was tested by Boyne and colleagues for augmentation of the maxillary sinus floor [Boyne et al., 1997]. The feasibility of rhBMP-2 implanted with a collagen carrier to heal simulated critical-sized maxillofacial defects in subhuman primates has been demonstrated by Boyne and colleagues [Boyne, 2001]. Marukawa and coworkers succeeded in functional reconstruction of the mandible in non-human primates using rhBMP-2 [Marukawa et al., 2002]. Pivotal clinical trials for this indication are underway [Valentin-Opran et al., 2002]. The potential of some BMPs to induce new dentin could be demonstrated. The size, shape and kind of osteoinductive carrier greatly influence the outcome and needs further evaluation [Nakashima et al., 2003]. Therefore, the use of BMPs in periodontal and dental diseases is in its early states.

Tendon repair and cartilage regeneration:

In contrast to bone, cartilage has a limited capacity to heal after injury. The repair tissues achievable with currently available methods still differ from healthy articular cartilage in respect to stiffness, morphology and biochemical composition [Aigner et al., 2003]. A promising concept should cover three important aspects. First, due to the limited number of potential responsive cells available in the adult articular cartilage, the introduction of a new cell population seems to be advantageous. A second aspect is the delivery of cytokines and growth factors with the aim to increase the metabolic activity of the cells and to support the induction of the regenerative process. Finally, an appropriate carrier matrix is required for both the cells and the growth and differentiation factors. For success, the release kinetics of promising growth and differentiation factors are of mayor concern. As bone morphogenesis is a sequential cascade with a cartilagenous intermediate formed (endochondral ossification), BMPs are as well cartilage morphogenetic proteins. The chondro-inductive property of a single BMP-2 injection was demonstrated in murine knee joints [van Beuningen et al., 1998]. Application of BMP-2 via an adenoviral approach (vectors carrying complementary DNA of rhBMP) also resulted in the induction of new cartilage and extensive osteophyte formation [Gelse et al., 2001]. The repair of full thickness defects in the articular cartilage of rabbits can be improved with an rhBMP-2 impregnated collagen sponge, as demonstrated by Sellers and coworkers. One year after implantation, the histological appearance of the rhBMP-2 treated defects were significantly better than untreated defects [Sellers et al., 2000]. Forslund and co-workers evaluated the potential of tendon healing with cartilage derived morphogenetic proteins (CDMPs, Table 1-1) and OP-1 [Forslund et al., 2003]. A series of other members of the transforming growth factor superfamily showed effectiveness in chondrogenetic tissue induction. However, the incidence of undesired side effects was lower within the BMPs [Hunziker et al., 2001]. In the future, not only focal defects of articular cartilage, but also diseases affecting the joints more generally such as osteoarthritis or rheumatoid arthritis might benefit from a controlled delivery of BMPs [Kaps et al., 2002].

Osseointegration:

Improved adhesion and proliferation of BMP-2 pretreated osteoblastic cells on titanium alloy often used for orthopedic implants was demonstrated in cell culture [Shah et al., 1999]. Therefore, enhanced osseointegration of implants might be achieved by bonding BMPs to screws, pins, joint prosthesis or other implant surfaces [Kirker-Head, 2000]. Hartwig and coworkers demonstrate the positive effects on osseointegration of BMP coated composite titanium implants [Hartwig et al., 2003].

Metabolic bone diseases:

Apart from the indications requiring local BMP delivery, there are also indications that might benefit from a systemic application. Osteoporosis, a disease characterized by excess bone fragility due to a loss of bone mass and alterations in bone microarchitecture, is in part the result of a reduced number of osteoprogenitor cells and reduced differentiation into osteoblasts [Fromigue et al., 2004] – events BMPs have proven to be effective. Depressed BMP levels are reported in patients with osteoporosis [Kirker-Head, 2000]. BMP-2 and BMP-7 have shown to up-regulate modulators within the bone responsible for bone density increase [Nemec et al., 2001]. Further evidence is provided by the bone anabolic effect of statins, which are known to be BMP-2 inducers [Koida et al., 2004]. Simple systemic administration of soluble BMP is not feasible due to the rapid clearance in the liver, resulting in a short serum half life. An injectable sustained releasing formulation might overcome the obstacle of short serum half life. However, the question of side effects still needs to be addressed. Intraosseous injection of a sustained releasing formulation might be another thinkable scenario. Morbus paget, characterized by accelerated bone remodeling due to increased bone katabolic processes, might also benefit from the osteoinductive properties of BMPs [Nemec et al., 2001].

Actions beyond bone:

The discovery of BMP as modulators in bone formation has attracted the attention of research on potential applications in the field of skeletal surgery. With the elucidation of BMPs molecular genetics, their expression pattern and gene depletion experiments, a more fundamental role of the BMPs became apparent. BMPs have demonstrated to be also involved as differentiation factors and physiological regulators in a series of soft tissues, including the skin, the nervous system, the eye, the urogenital system, the kidney, and the cardiovascular system [Martinovic et al., 2002 Reddi, 2001]. Within wealthy skin, BMPs are involved in the regulation of hair follicle growth, melanogenesis and innervation and in the differentiation and proliferation of the epidermis, making them attractive candidates for applications in the field of wound healing, proliferative skin disorders and corrections of hair growth disorders [Botchkarev, 2003]. The observation that BMP-7 reduces the severity of injury after renal failure might also gain clinical relevance [Martinovic et al., 2002]. Multiple uses in a variety of clinical indications are foreseeable, and it was even suggested to re-name them ‘body morphogenetic proteins’ to measure up to their wide-ranging role.

The possible benefit from immobilized BMP, (i) the importance of sustained release for osteoinduction, (ii) the desire for an injectable formulation to overcome the necessity of “open” surgical approaches required for the implantation of rigid carriers (see 1.1.4) and (iii) to serve as formulation for new emerging

indications (see 1.1.5.2) mark the key requirements for an innovative formulation. A particulate rhBMP-2 formulation can cover the desired features.

1.2 Formation of Protein Particles by Precipitation

A particulate protein formulation offers a series of advantages. It provides a carrier free sustained releasing delivery system that can be injected as a suspension. In addition, it has the potential to be used in alternative administration routes, such as pulmonal delivery, or as a component in more complex controlled release formulations, e.g. incorporation in implants or microspheres. According to the concept of improved stability in the solid-state [Maa et al., 2000], a particulate formulation might be superior to a liquid formulation. Furthermore, large amounts of protein can be administered in a small volume. In some cases, an increased therapeutic effect may arise from the presentation of immobilized protein to the target cells. A number of techniques are currently available to prepare relatively pure, dry protein particles.

1.2.1 Formation of Dry Particles by Standard Methods

a) Freeze-Drying and Pulverization

Freeze drying is the method of choice to transfer a protein solution in the solid state. The lyophilization process can be divided into three steps: At first, the protein solution along with adequate excipients is frozen. During primary drying, the main amount of frozen water is removed by sublimation. In the following secondary drying associated water is removed to the desired residual moisture content under increased vacuum and elevated temperatures [Jennings, 1999]. The obtained lyophilisat, a dry and ideally fluffy cake, is then subjected to a milling or grinding process to obtain protein particles. Among the variety of mills, the jet-mill (fluid-energy mill) seems to be most suitable for size reduction of protein particles and aggregates [Maa et al., 2000]. In dependence of inlet fluid pressure, powder feed rate, bulk powder morphology, material hardness and starting size distribution, particles smaller than 5 μm can be achieved. As a rule of thumb, the smaller the desired particle size, the more energy is required for its pulverization. The energy input is partially transformed into heat. Stability problems may arise both from the thermal and mechanical stress during the milling process. Electrostatic charging of the processed particles is another problem. The main disadvantage of freeze drying lies in its expensiveness, as it is a time and energy consuming process. A broad size distribution with irregular shaped particles and poor particle size control further limit its rational application for particle formation. A novel approach based on co-lyophilization with PEG directly leads to the formation of spherical fine particles without the need of pulverization (see 1.2.3.5). The major disadvantage of this approach is the need of organic solvents for particle separation [Morita et al., 2000].

b) Spray (Freeze) Drying

A well-established method for the preparation of particulate solids is spray drying [Lee, 2002]. Atomizing a liquid feed into a hot drying medium generates particles. The water of the feed fluid evaporates at once due to the tremendous surface increase by the atomizing process and the elevated temperatures of the drying medium, leaving alone the dried particle. Spray freeze drying combines the principles of classic spray drying and lyophilization. The protein solution is atomized in liquid nitrogen, where the formed droplets were frozen immediately. Subsequent lyophilization leads to dry particles. The rationale is to circumvent any possible thermal stress for the protein caused by accelerated drying temperatures in the classic spray drying procedure. Problematic in spray drying is the risk of surface denaturation. Spray freeze drying is a complex process, and the particle density control is poor.

c) Supercritical Fluids (SCF)

Above a critical temperature and a critical pressure, a fluid features unique physical properties [Winters et al., 1996]. Minor changes in the pressure can then be utilized to modulate these properties within the extremes of its liquid-like solvent power and its gas-like transport characteristics. For biopharmaceutical applications, CO₂ is advantageous due to its mild critical temperature of 31.1°C, relative moderate critical pressure of 73.8 bars, non-toxicity and non-flammability [Subramaniam et al., 1997]. In dependence of the solubility of the biomolecule in the SCF, it serves as an antisolvent or as a solvent. In the latter, rapid expansion of a supercritical fluid utilizing a nozzle or a capillary leads to supersaturation of the solute and subsequent to precipitation of pure solute particles. In the antisolvent technology, two process scenarios are thinkable: A classic solvent is required that serves as solvent for the protein and is miscible with the supercritical solvent. By simple mixing the solution with the supercritical phase, its solvation power is reduced and the protein is forced to precipitate or crystallize. Another possibility to generate particles with SCF is spraying the protein solution into supercritical carbon dioxide, a process termed ASES (Aerosol Solvent Extraction System). The handling of processes dealing with SCF is technically demanding. In addition, biomolecules generally feature limited solubility in SCF, and the process often requires organic solvents.

The above-discussed methods all deliver dry particles, so that the development of an aqueous protein suspension will need additional operations. Difficulties may arise from undesired dissolution processes of the particles in the dispersion fluid. Furthermore, the above-mentioned techniques either mean stress to the biomolecule (heat denaturation, shear stress, surface denaturation, use of organic solvents), or the process is costly (requires expensive equipment, time, energy). Therefore, the development of a cheap, easy performable procedure that does not harm the protein is challenging. Based on the limited

solubility of rhBMP-2 in water, classic precipitation in an aqueous environment might meet the criteria.

1.2.2 Protein Precipitation: Definition and Principles

In a comprehensive definition, precipitation can be described as a reduction of the solute solubility so that most of the solute molecules can no longer stay in solution [Maa et al., 2000]. Solubility of a protein in a solvent is determined by the complex interactions between the surface of a protein with a given solvent, the interactions between protein molecules as well as interactions between the solvent molecules [Rothstein, 1994]. The surface characteristics of a given protein are mainly determined by the properties of the amino acids building up the protein backbone and their distribution at the solvent accessible surface. Depending on the chemical structure of the amino acid side chain, they can be classified as hydrophobic (apolar aliphatic, heterocyclic or aromatic residues, e.g. Gly, Ala, Val, Leu, Ile, Met), hydrophilic (polar aliphatic residues, e.g. Ser, Thr, Cys, Asn, Gln) or ionisable (Asp, Glu, His, Lys, Arg) [Simpson, 2004a]. According to simplified basic thermodynamics, each system is seeking for minimal energy and a maximum of chaos. Therefore, a protein is soluble in a given solvent if the solvent-solute interactions are attractive, indicated by a negative free energy change, that more than compensates the sum of the free energy decrease caused by solvent-solvent and protein-protein interactions. Positive, i.e. repulsive protein-protein interactions further favor increased solubility. Otherwise, the protein is insoluble, resulting in crystallization or precipitation.

1.2.3 Precipitation Methods

Protein precipitation methods can be divided in physical methods (e.g. changes in temperature; changes in pressure (see 1.2.1); evaporation of solution) and methods based on the addition of reagents, either directly interacting with the solute or indirectly influencing its solubility by changing the characteristics of the solvent without dramatic changes in temperature and in the solute/solvent ratio [Fornasiero et al., 1999]. In principle, reversible and irreversible precipitation can be distinguished. In the latter, the protein structure is damaged or lost and cannot be restored. A lot of stresses can cause irreversible precipitation, the most prominent being temperature, pH and organic solvents [Scopes, 1995]. In this work, focus is laid on the methods leading to reversible precipitation by chemicals, although it must be pointed out that there is a smooth transition from reversible to irreversible precipitation in dependence of the applied conditions. One should consider that our knowledge about precipitation is still very empirical and the described theories and mechanisms are simplifications and serve as models to support our understanding of the complex process of precipitation. In reality, the itemized methods might influence and interact with

each other, and the adjustable parameters needed to be orchestrated for an optimized precipitation process.

1.2.3.1 Crystallization

Crystallization can be classified as a special form of precipitation. In simplified terms, protein crystals are generated from a concentrated protein solution under very specific conditions. Detrimental are the creation of a gradual supersaturated solution and the maintenance of this non-equilibrium state during the crystallization process (Figure 1-5).

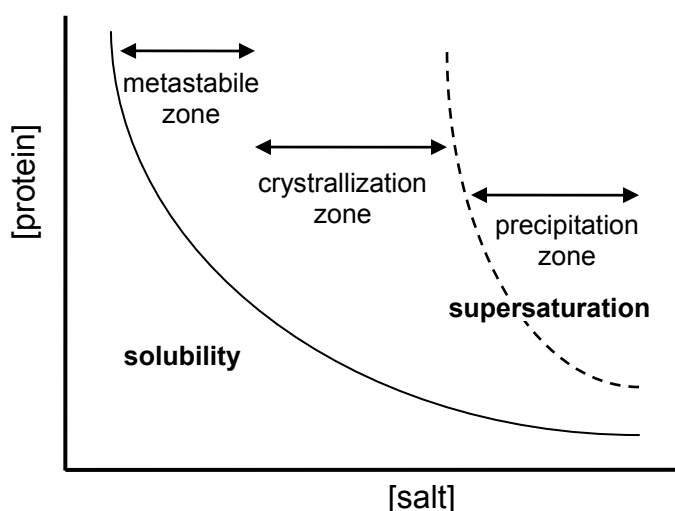


Figure 1-5: Crystallization window of a hypothetical protein (adapted from Ducruix et al., 1990)

Initially spontaneous formed nuclei act as crystallization centers for an ordered addition of macromolecules, thus forming new intermolecular contacts resulting in the crystal [Feher et al., 1985]. Insulin suspensions provide the most prominent example [Brange, 2000]. Also based on the concept of crystallization is the Crystalomics™ technology from Altus. In principle, a concentrated crystallization buffer is allowed to slowly equilibrate with the protein of interest by dialysis. Over time, the concentration of both the protein solution and the crystallization buffer rises, forcing the protein to crystallize or precipitate [Yakovlevsky et al., 2002]. Crystallization is a complex, time consuming and sensitive process, and scaling up might be difficult.

1.2.3.2 Isoelectric Precipitation

Protein solubility can be easily influenced by variation of the solution pH. A classic pH-solubility profile mimics the form of an asymmetric U. Therefore, by addition of either acid or base, a point can be adjusted where the solubility possesses a minimum (Figure 1-6).

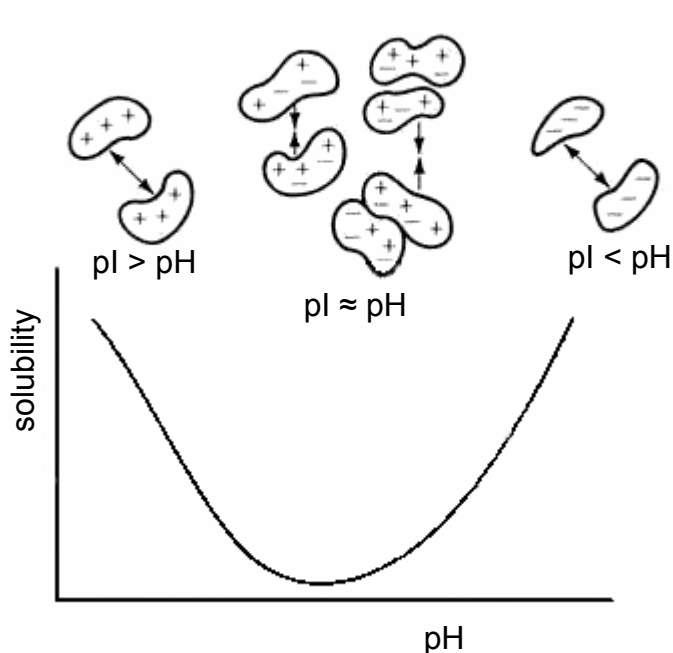


Figure 1-6: *pH-solubility profile and model illustration of isoelectric precipitation (adapted from Scopes, 1995)*

Due to its titratable groups, derived from the side chains of the amino acids and potentially associated sugars, biomolecules are polyampholytes, i.e. they carry both positive and negative charges in dependence of the solution pH. The pH at which the net charge of a given protein is zero defines its isoelectric point (pI). At this pH, electrostatic repulsive forces are minimized, the number of thermodynamically favored interactions of charged entities with water as dipole is diminished, and hydrophobic forces dominate the solubility behavior. Hydrophobic patches on the surface of the protein coming in contact with water molecules force them to order. This process is termed hydrophobic hydration. The ordering is accompanied by a large decrease of entropy. This decrease, which is proportional to the surface area of the apolar entity, is correlated with a reduced solubility in water [Privalov et al., 1989]. Thus, apolar entities tend to avoid or at least minimize contact with water by reducing the exposed surface by self association. Additional charges can be introduced into a protein by salt specific ion binding. Anion binding can shift the pI of proteins to more acid values and therefore might increase the minimum solubility (salting-in). The binding of cations shifts the pI to higher pH values. Extremes of pH can have great impact on the charge distribution within a biomolecule, thus creating destructive repulsive forces or diminish initially stabilizing interactions within the protein structure. Such processes finally lead to irreversible precipitation.

1.2.3.3 Salt-induced Precipitation: Salting-out

The phenomenon of salting-out can be observed by the addition of high amounts of neutral salts to protein solutions. The nature of the salt has great

influence on its ability to precipitate proteins. Hofmeister, the name generator of the famous lyotropic series, first elucidated the relative effectiveness of neutral salts in salting-out proteins. For some common anions, the potency to salt-out proteins increases in the order thiocyanat < chlorate < nitrate < bromide < chloride < acetate < sulphate < phosphate < citrate. A minor contribution derives from the cations, with ammonium being most effective, followed by potassium and sodium [Hofmeister, 1888, Von Hippel et al., 1969]. Interestingly, the potential of the ions to stabilize the structure of a macromolecule parallels this series, with ions favoring precipitation act as stabilizers. The most frequently used and therefore the most prominent reagent for salting-out is ammonium sulphate. It unites a series of advantages (modified from England et al., 1990):

- saturated solutions pose sufficiently high molarity to precipitate most proteins
- marginal heat of solution allows addition to protein solution without the need to cool it
- even saturated solutions pose a sufficiently low density not to interfere with precipitate recovery by centrifugation
- preservative properties of concentrated solutions
- protects most proteins from denaturation

The required salting-out concentration depends on the nature of the salt and on characteristics of the protein. Size and shape of the protein are critical parameters. Irregular shaped proteins and proteins of higher molecular weight and otherwise similar features require smaller amounts for precipitation.

The effect of salting-out is empirically linked to the ionic strength by the equation of Cohn [Edsall, 1947]. On a semi-logarithmic scale the solubility decreases linearly with increasing ionic strength of a concentrated salt solution:

$$\log S = \beta - K_s I$$

S solubility

I ionic strength

β , K_s constants

The salting out constant K_s is specific for the protein and the salt employed. The constant β marks the hypothetical solubility at zero ionic strength (Figure 1-7) and is a function of temperature and pH, with a minimum at the isoelectric point [Bell et al., 1983]. This empirically found relationship is only true for concentrated salt solutions. Low concentrations of salts have a solubilizing effect for most proteins at and above its isoelectrical point [Rothstein, 1994], a process termed salting-in.

Melander and Horwarth provide a theoretical approach explaining the dual role of salt on the solubility of macromolecules [Melander et al., 1977]. It is based on the cavity model, which assumes that in a first step work is required to form a cavity in the solvent in which the solute can be introduced (ΔG_{cavity}) before the solute can interact with the solvent ($\Delta G_{\text{interaction}}$). The model also considers the decrease in entropy by the solute free volume change. According to their work, the observed solubility is the net result of both electrostatic and hydrophobic interactions (Figure 1-7). Salting-in, mainly determined by surface charge distribution and polar interactions, dominates at low ionic strength. At sufficient high salt concentrations, the specific interactions between electrolytes and proteins are masked, and the macromolecule effectively behaves as a neutral dipole. Then, the overall salting-out curve is dominated by hydrophobic interactions that now superimpose the still present solubilizing influence of electrostatic repulsion [Scopes, 1995].

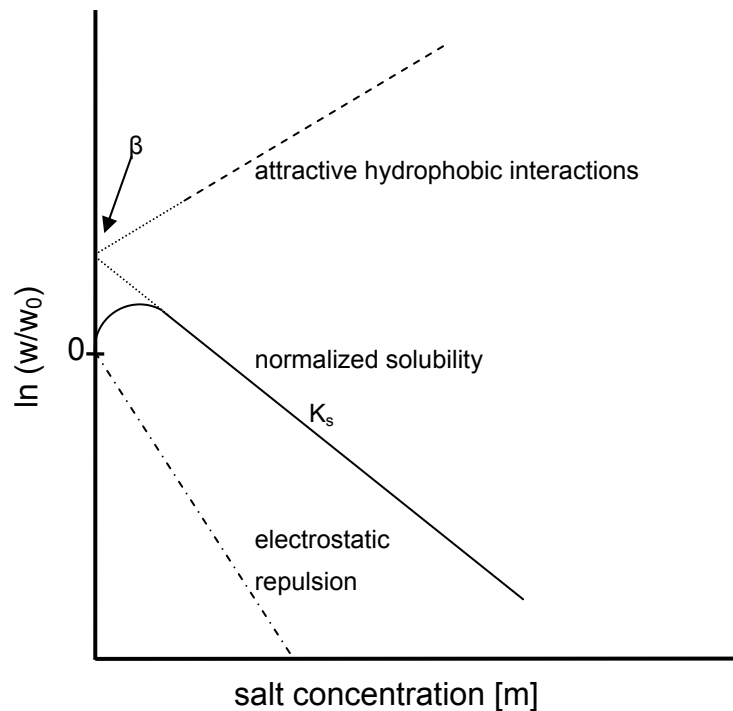


Figure 1-7: Schematic illustration of the overall salting out curve (solid) as the net result of electrostatic (dash dot) and hydrophobic (dashed) interactions (modified from Melander et al., 1977)

The model character of this approach becomes apparent, as it fails to describe salt specific effects at low ionic strength. Up to now, a comprehensive theory is lacking.

1.2.3.4 Miscible Organic Solvent Precipitation

With the exception of the prolamines, most proteins become rapidly insoluble with rising concentrations of organic solvents [Kistler et al., 1980]. A lot of different solvents have been utilized. Practical importance gained methanol, diethyl ether, acetone and ethanol, with the later being the reagent of choice due to a number of advantages:

- melting point depression enables fractionation at subzero temperatures, thus minimizing denaturation
- no generation of explosive gas mixtures under usual working conditions
- low molecular weight
- highly volatile
- chemically relative inert
- low toxicity
- inexpensive and easily available
- inhibition of bacterial growth

The most prominent example utilizing ethanol is the fractionated precipitation of plasma proteins. Basically developed by Cohn and co-workers in the middle of the last century (1946), the procedure is still the basis for the production of the main plasma proteins [P.Kistler et al., 1980]. Plasma fractionation is performed according to the “five parameter system”: pH, ionic strength, protein concentration, organic solvent concentration and temperature. The latter should be held well below 0°C to minimize the denaturing effect of the alcohol. At higher temperatures, the flexibility of a protein might be sufficient for small molecules entering the “interior”, interacting with hydrophobic residues usually buried within the molecule and therefore destabilizing it.

The free energy of electrostatic interactions is linked to the inverse of the solvent dielectric constant. Therefore, the high dielectric constant of water is used to explain its solvating power for hydrophilic, charged proteins, with the free energy being minimal between the dipole water and the polar protein. Additional, hydrophilic solvation occurs in this system: water molecules form a hydration shell by the formation of a structured layer around the polar protein. The electric field of the ionic entity also affects the properties of water molecules beyond this layer ‘deeper’ in solution, building up the hydration zone. In a mechanical view, the hydration layer(s) acts as a physical spacer between the surrounded protein molecules, thus preventing them to come into contact and improving its solubility. The addition of an organic cosolvent to water decreases its solvation power, accompanied by a decrease of the dielectric constant. Another approach suggests a competitive process for the water molecules between the protein and the added alcohol to be responsible, leading to protein

dehydration at sufficiently high 'cosolvent' concentration (Figure 1-8). Electrostatic and dipolar forces are thought to be mainly responsible for subsequent aggregation. Hydrophobic forces seem to be less relevant due to the solubilizing influence of organic solvent on the hydrophobic patches. The removal of ordered structures of water molecules from such protein surfaces (hydrophobic hydration) and their replacement by the organic solvent provides an explanation for the increased solubility of hydrophobic proteins such as the prolamins in organic water mixtures [Kistler et al., 1980].

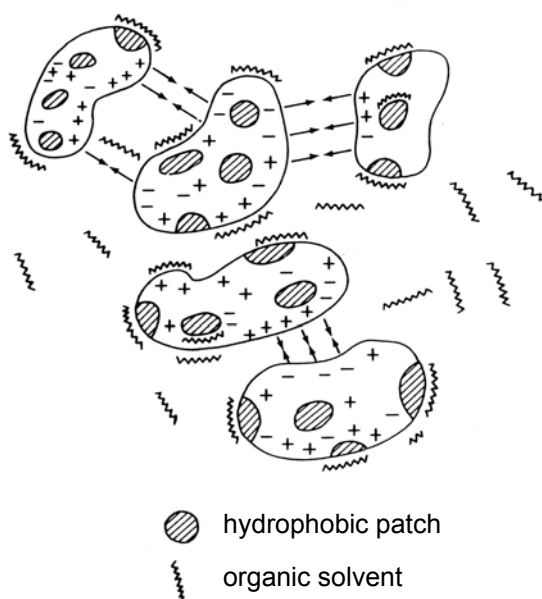


Figure 1-8: Simplified illustration of the precipitation mechanism by organic solvents (modified from Scopes, 1995)

Based on the precipitation power of organic solvents is the PCMC[®] technology (Protein-coated Microcystal) from XstalBio. Drop wise addition of an aqueous solution containing the biomolecule and an inert crystal-forming coprecipitant into an organic solvent leads to non-covalently immobilization of the protein on the surface of the support material [Bechthold-Peters, 2003, Moore et al., 2000].

1.2.3.5 Precipitation by Non-ionic Polymers

Dextrans, polyvinyl pyrrolidone, polypropylene glycol and polyethylene glycol (PEG) have found applications as non-ionic polymeric precipitating agents. PEG is most widely used due to the following advantageous properties (modified from Hao et al., 1980):

- no interaction with proteins and no denaturing potential even at high concentrations
- acceptable viscosity in solutions up to 20 % (w/v) with respect to recovery by centrifugation, compared to other non-ionic polymers

- low heat of solution
- precipitation behavior relative insensitive to minor changes in temperature
- shorter equilibration time, compared with ethanol or ammonium sulphate

It is generally accepted that non-ionic polymer induced protein precipitation is based on the concept of steric exclusion: in the three-component system water-protein-PEG, the polymer is sterically excluded from the protein domain and therefore the protein is preferentially hydrated. By continuous addition of a polymer to a protein solution, the polymer occupies more and more volume of the solution. This forces the protein to concentrate in the extrapolymer space, and finally to precipitate [Atha et al., 1981]. As PEG is a polymer, different types varying in their molecular weight are available. Up to a limit of 6000 Da, the higher the molecular weight, the larger is the protein displacement. Species with higher molecular weight are considered to undergo chain folding and therefore did not further increase the excluded volume, but increase the viscosity. Consequently, PEG species in the range of 4000 - 6000 Da are preferred. A theoretical expression describing the precipitation of proteins by non-ionic polymers is provided by Juckes [Juckes, 1971]:

$$\log S = \log S_0 - K_P [\text{PEG}]$$

S solubility of protein

S_0 solubility of protein in absence of PEG

K_P constant

[PEG] polyethylene glycol concentration

K_P is a linear function of the Stokes radius of the protein and the size of PEG up to 6000 Da, but relative independent from the solution conditions pH and ionic strength, which influences S_0 . The use of the term is limited to dilute protein concentrations, as it does not account for specific protein-protein interactions that occur at higher concentrations. The analogy of the equation to the expression used for salting-out should be mentioned (see 1.2.3.3).

1.2.3.6 Precipitation by Metal Ions

A number of polyvalent heavy metal ions have affinities to certain structures present in proteins and therefore can be used for protein precipitation (Table 1-3). The great advantage of these reagents is that millimolar concentrations are sufficient. It is important to point out that minimal solubility is obtained at slightly higher pH-values than pI, however, basic milieu should be avoided to prevent formation of metal hydroxides [Rothstein, 1994].

Table 1-3: Affinities of cationic metal ions to certain structures (modified from Bell et al., 1983)

cation	preferred interaction with
Ca ²⁺ , Pb ²⁺ , Ba ²⁺ , Mg ²⁺	carboxyl groups
Zn ²⁺ , Cu ²⁺ , Cd ²⁺ , Mn ²⁺ , Fe ²⁺ Co ²⁺ , Ni ²⁺	nitrogenous compounds: hererocycles, amines
Hg ²⁺ , Ag ⁺ , Pb ²⁺	sulfhydryl groups

In general, two kinds of binding are suggested: the formation of a simple ion-ion complex and the combination of the metal ion with two or more ligands, building up a coordination complex [Gurd, 1954],[Bertini et al., 1995]. Dimer and hexamer formation by self association of insulin monomers in the presence of zink probably provides the most significant example in the pharmaceutical field [Brange, 2000]. It should be mentioned here that specific ion binding can be advantageous in combination with other precipitation techniques, e.g. Ca²⁺, Ba²⁺ and Zn²⁺ in ethanolic precipitation [Bell et al., 1983].

1.2.3.7 Protein Binding Dyes

One example of this class has gained major attention for the fractionation of plasma proteins: the organic base rivanol (2-ethoxy-6,9-diamino acridine lactate) [Steinbuch, 1980]. The electrostatic rivanol-protein complex, which is formed at pH slightly above pI of the protein, is hydrophobic and precipitates. Other dyes with high binding capacities, used for selective protein purification from crude mixtures are described elsewhere [Niederauer et al., 1992].

1.2.3.8 Precipitation by Ionic (Poly)-Electrolytes

Compared to the already described precipitation agents, ionic polyelectrolytes have received little attention, probably due to their tendency to damage protein structures [Simpson, 2004b]. Nevertheless, single candidates have shown to be useful and effective for specific separation tasks. Their advantage is cheapness and the lack of waste disposal problems, making them attractive in industrial applications. In addition, only concentrations between 0.05 and 0.1 % (w/v) are required. A classification with selected examples is given in Table 1-4. Also included are some acid precipitants which do not fit into the polyelectrolyte category, but were noteworthy to mention. Polyelectrolytes precipitate proteins with an opposite charge by complex formation, preferring molecules of higher charge density [Niederauer et al., 1992]. Suffice to say that variables that influence the charge, especially pH and ionic strength, greatly influence their precipitation behavior. In addition, the type, molecular weight and concentration of the polyelectrolyte on the one hand and size and surface characteristics of the target protein on the other are critical parameters.

Table 1-4: Selective polyionic precipitation agents (extracted and modified from Rothstein, 1994)

	precipitation agents	target protein(s)	references
Cationic precipitants			
natural and synthetic poly-electrolytes	protamines	fibrinogen from plasma	Mylon, 1942
	polyvinylamine	bovine albumin	Morawetz and Hughes, 1952
	polyethylenimines	isolation of enzymes	Boeringer Mannheim, 1972
Anionic precipitants			
acids [small anions]	short chain fatty acids: caprylic acid	IgG	Steinbruch et al., 1965
	TCA (trichloroacetic acid)	large scale separation from human albumin from placental blood	Liautaud, 1974
	perchloric acid, sulfosalicylic acid	isolation of highly glycosylated, very soluble glycoprotein from plasma	Winzler et al., 1948
natural anionic polymers	sulfosalicylate, tungstate, metaphosphates, linear polyphosphates	differential precipitation of serum proteins, plasma fractionation	Astrup et al., 1954, Berry et al., 1956, Nitschmann et al., 1959
	tannic acids	isolation of glucose dehydrogenase from bacterial cultures	Coulthard, 1945
	heparin (in presence of MgCl ₂)	lipoproteins (VLDL; LDL)	Burnstein, 1970
	chondroitin sulphate	fibrinogen, beta- lipoproteins	Anderson, 1963
synthetic anionic poly-electrolytes	polyacrylic acid	protein fractionation	Weiland et. al., 1953
	carboxymethyl cellulose	egg white protein	Clark and Glatz, 1987
	polystyrene sulfonates	albumin-gama globulin separation	Isliker, 1957
	polysaccharides: polysulfuric acid	fibrinogen from plasma	Astrup and Piper, 1946
	dextran sulfates (of higher molecular weight)	fibrinogen from plasma	Walton, 1952
	sulphated amylopectin	low-density lipoprotein precipitation	Day, 1975

1.2.3.9 Affinity Precipitation

This highly specific binding is based on the concept of complementary antigen-antibody interaction between a target protein and a ligand. Complex formation will result in aggregation and precipitation. The affinity of lectins to glycol-moieties of glycoproteins provides an example [Latner et al., 1980]. For a comprehensive review, see Hilbrig [Hilbrig et al., 2003]. The formation of insoluble protein-anion complexes at low ionic strength at pH values acid to the proteins isoelectric point is also considered to be an affinity precipitation mechanism.

Particle stabilization by Cross-linking

Cross-linking is a well known procedure for the stabilization of nanoparticles [Langer et al., 2003]. Woizwillo suggested cross-linking for the production and stabilization of precipitated macromolecules [Woizwillo, 1994]. However, the covalent linkage of biomolecules is considered to be problematic with respect to bioactivity, immunogenicity and antigenicity.

1.2.4 Precipitate Formation

For the preparation of particles by precipitation, it is helpful to understand the underlying principles. Precipitate formation can be divided into 4 stages (modified from Rothstein, 1994 and Bell et al., 1983):

Stage I: Nucleation and perikinetic growth

Fundamental for precipitation is an initial supersaturated and therefore metastable state as driving force for nucleation and growth. These are energy consuming processes, as a more ordered structure of associated molecules compared to their random distribution in solution is created. Initially, submicron sized associations are generated on a molecular level based on diffusion, referred to as nucleation, and condensation of additional molecules to stable associates further increases their size.

Stage II: Perikinetic association and aggregation

Collisions of nuclei by diffusion and consequent adhesion to each other result in the formation of stable primary particles of colloidal size.

Stage III: Orthokinetic growth

Orthokinetic growth describes the growth and formation of a macroscopic visible precipitate composed of primary particles and nuclei condensed after collision caused by bulk movement (convective transport). In this stage, larger particles can also be subjected to breakup and erosion as a consequence of fluid shear forces.

StageIV: Protein aging

During this phase, effects of overprecipitation are partially reversed by redissolution of proteins which are usually soluble under the given solution conditions. Furthermore, under appropriate shear, aggregates 'mature' in respect to size, strength, shape and density.

1.2.5 Precipitation Process Conditions

With the knowledge of the basics in precipitate formation, the influence of process parameters on the physical properties of the precipitate characteristics might become clear. The major concern in adjusting the system and operation variables is the avoidance of local excess concentrations of the precipitating agent in the protein solution, as this can cause overprecipitation, damage to the protein and the formation of highly solvated, small precipitates. For the conduction of a precipitation experiment, three components are required: a protein solution, a precipitating reagent and a reactor system:

A parameter that is critical for all precipitation procedures is the initial protein concentration in the bulk solution. To achieve precipitation, a sufficiently high starting concentration is required which exceeds the benchmark of protein solubility under the chosen precipitation conditions. For the purification of protein mixtures, higher selectivity could be achieved from more diluted solutions, with an increased amount of required precipitation agent as consequence.

The choice of an appropriate reagent, its physical stage (solid vs. liquid), its concentration in stock solution, the rate of addition to the protein solution and the final concentration are important factors.

The mode of operation (batch vs. continuous), the subsequent reactor design (tank geometry, agitator design and geometry, sparger design and geometry, use of static mixers) and the mixing mode (turbulent vs. laminar) have a great influence on the shear profile and therefore on the characteristics of the precipitate. It should be noted that turbulent mixing is advantageous to quickly achieve a homogeneous distribution, but bears the risk of particle breakage due to the shear stress. Some precipitation methods require the possibility to adjust and control the temperature (e.g. low temperatures required for ethanolic precipitation; removal of excess heat of dissolution caused by a precipitant).

2 Objectives of the Work

The aim of the thesis was the development of an injectable, sustained release rhBMP-2 formulation, based on the concept of controlled precipitation to create protein particles. Furthermore, the potential of precipitation to generate highly concentrated formulations and the feasibility of precipitated protein as alternative storage form was to be evaluated. In this context, several aspects had to be addressed.

- Development of a controlled precipitation process leading to an aqueous protein suspension of highly pure rhBMP-2 microparticles. The influence of process parameters on particle formation and distribution had to be evaluated. The parameters that allow controlling the particle size should be elucidated. The feasibility of the process for scaling-up should be investigated.
- Optimization of the formulation composition. The influence of the formulation composition on particle size and the potential of selected excipients to control size and stability had to be tested.
- For characterization of the formed microparticles, a suitable tool had to be established that allows sizing of small volumes of highly concentrated protein suspensions, and a method for visualization should be implemented.
- The influence of precipitation on the native conformation of rhBMP-2 should be analyzed, and the secondary structure in the precipitated state had to be elucidated. Bioactivity testing of precipitated material should be performed in cell culture.
- The potential of precipitation to prevent chemical and physical instabilities had to be evaluated and compared with the commercial available formulation, and storage conditions had to be defined allowing sufficient shelf life.
- Establishment of an in vitro release assay for the microparticle suspension using serum and evaluation of the release profile. The feasibility of the formulation to accelerate bone formation had to be tested in vivo in an animal model.

3 Materials and Methods

3.1 Materials

3.1.1 rhBMP-2

Recombinant human bone morphogenetic protein-2 (rhBMP-2), expressed in a genetically engineered Chinese hamster ovary cell line was provided by Wyeth BioPharma, Andover MA, U.S.A. The protein was delivered in a bulk concentration of 4-6 mg/ml, formulated in a buffer pH 4.5 containing 5 mM L-glutamic acid, 2.5 % L-glycine, 0.5 % sucrose, 5 mM NaCl and 0.01 % polysorbate 80 (referred to formulation buffer) and was stored frozen at -80°C until use.

3.1.2 Reagents and Substances

reagent	description	supplier
acetonitrile	HPLC gradient grade	Merck (Darmstadt, Germany)
purified water	freshly prepared with a PureLab Plus™ purification system	ELGA LabWater (High Wycombe, Buckings, UK)
CaCl ₂ * 2 H ₂ O	p.a.	Merck (Darmstadt, Germany)
Collodial Blue staining kit	composed of stainer A and B	Invitrogen GmbH (Karlsruhe, Germany)
chondroitinsulfate		Symatase Biomatériaux (Chaponost, France)
dithiothreitol (DTT)		Aldrich-Chemie (Steinheim, Germany)
EDTA * 2 H ₂ O, disodium salt	≥ 99.9 %	Sigma (Steinheim, Germany)
Endoproteinase Asp-N	sequencing grade	Roche Diagnostics (Mannheim, Germany)
ethylene glycol	purissimum	Fluka (Buchs, Switzerland)
gelatin	type B, from bovine	Sigma

reagent	description	supplier
	skin, 75 bloom	(Steinheim, Germany)
glacial acetic acid	pure	in-house supply
glycine	≥ 99 %	Sigma (Steinheim, Germany)
guanidine * HCl	≥ 98 %	Fluka (Buchs, Switzerland)
HCl	1 N solution p. a.	Merck (Darmstadt, Germany)
heptafluorobutyric acid	purris. p.a.	Fluka (Buchs, Switzerland)
hyaluronic acid	1 % solution	Fidia (Munich, Germany)
iodoacetic acid, sodium salt	99 %	Aldrich-Chemie (Steinheim, Germany)
KCl	p.a.	Merck (Darmstadt, Germany)
KH ₂ PO ₄	p.a.	Fluka (Buchs, Switzerland)
KOH	0.1 N solution	Merck (Darmstadt, Germany)
KOH	flakes, p.a.	Merck (Darmstadt, Germany)
L-arginine * HCl	extra pure	Merck (Darmstadt, Germany)
L-glutamic acid	99-100 %	Sigma (Steinheim, Germany)
L-glycine	p.a.	Sigma (Steinheim, Germany)
L-histidine	98 %	Aldrich-Chemie (Steinheim, Germany)
Mark12™	unstained markers (2.5 – 200 kDa)	Invitrogen (Karlsruhe, Germany)
methanol	gradient grade	Merck (Darmstadt, Germany)
Na ₂ HPO ₄ * 2 H ₂ O	p. a.	Fluka (Buchs, Switzerland)
Na ₂ SO ₃	anhydrous, p.a.	Sigma (Steinheim, Germany)

reagent	description	supplier
NaCl	p.a.	Fluka (Buchs, Switzerland)
NaOH	1 N solution p. a.	Merck (Darmstadt, Germany)
NuPAGE [®] LDS Sample Buffer	containing glycerol, Tris Base, Tris HCl, LDS, EDTA, Serva Blue 250, Phenol Red, ultrapure water	Invitrogen (Karlsruhe, Germany)
NuPage [®] MOPS SDS running buffer	containing MOPS, Tris Base, SDS, EDTA	Invitrogen (Karlsruhe, Germany)
NuPAGE [®] Reducing Agent	0.5 M DTT	Invitrogen (Karlsruhe, Germany)
poloxamer	Lutrol [®] F68	BASF (Ludwigshafen, Germany)
polysorbate 80	Crillet HP4, high purity	Croda (Nettetal, Germany)
Povidone K 90	Kollidon 90F, Ph. Eur, USP, JP	BASF (Ludwigshafen, Germany)
SilverExpress [®] staining kit	composed of sensitizer, stainer A/ B, developer, stopper	Invitrogen (Karlsruhe, Germany)
sodium alginate		Fluka (Buchs, Switzerland)
sodium azide	purum, p.a. >99 %	Fluka (Buchs, Switzerland)
sucrose	p.a.	Sigma (Steinheim, Germany)
trifluoroacetic acid	for spectroscopy	Merck (Darmstadt, Germany)
Trizma [®] base	reagent grade	Sigma (Steinheim, Germany)
urea	> 99.5 %	Fluka (Buchs, Switzerland)
CaCl ₂	p.a.	Merck (Darmstadt, Germany)

Serum was prepared from fresh human blood (3*50 ml) which was allowed to coagulate for approx. 1 hour at room temperature. The tubes were centrifuged for 40 minutes at 4410 RPM with a Universal 16R centrifuge (Hettich GmbH, Tuttlingen, Germany). The supernatant was collected and frozen at -20°C. For the in vitro release studies, the serum was preserved with 0.02 % sodium azide.

3.2 Methods

3.2.1 Focus on the Protein

3.2.1.1 Dialysis of Bulk Formulation

For buffer exchange, rhBMP-2 was dialyzed against 1 mM HCl using a Spectra/Por[®]7 membrane with a molecular weight cut-off (MWCO) of 3.000 (Spectrum Medical Industries Inc., Los Angeles, CA, U.S.A.). After intense rinsing of the membrane with demineralized water, up to 10 ml rhBMP-2 were loaded into the membrane tube of appropriate length, closed with clamps and placed into the dialyse fluid, with a bulk to buffer ratio of 1:100-200. For the first 4h dialysis was performed at room temperature, than at 2-8°C, with buffer exchange after 4 and 12 hours. After 24 hours under gentle stirring, the dialyzed protein solution was recovered, sterile filtrated through a 0.22 µm Minisart[®] filter (Sartorius AG, Goettingen, Germany) and aliquots were frozen at -80°C until use.

For protein preparation of the microparticles used in the animal study, dialysis was performed in a sterile, ready to use Slide-A-Lyzer[®] (Pierce, Rockford, IL, U.S.A.) with a MWCO of 10.000 and a dialysis volume capacity of 3-12 ml. The dialysis fluid was exchanged for three times within a period of 42 hours at 2-8°C under gentle stirring.

3.2.1.2 Ultrafiltration

For concentration of diluted samples (for ATR-FTIR) or for buffer exchange of small sample volumes (<500 µl, for DSC measurements), centrifugation was employed, using Biomax Ultrafree[®] 0.5 centrifugal filters and tubes (10.000 MWCO, Millipore Corporation, Bredford, MA, U.S.A.). Repeated runs at 4°C at 10.000 G for 5 minutes were performed until the desired residual volume was achieved. For buffer exchange, 500 µl sample were centrifuged for 15 min (10.000 G/4°C), the retentate was diluted with the appropriate buffer to 500 µl and the procedure was repeated twice.

3.2.1.3 Concentration Determination

3.2.1.3.1 UV

For quantitative analysis of rhBMP-2, samples were measured spectroscopically at 280 nm in a Thermo Spectronic UV1 (Thermo Spectronic, Rochester, NY, U.S.A.). Results were corrected for basic absorbance of the solution at 320 nm. Protein concentrations [mg/ml] were calculated via the following equation:

$$[\text{rhBMP-2}] = \frac{[(\text{Absorbance sample}_{280/320 \text{ nm}}) - (\text{Absorbance buffer}_{280/320 \text{ nm}})]}{1.43}$$

3.2.1.3.2 RP-HPLC

Separation from other components and quantification of rhBMP-2 by reversed phase high performance liquid chromatography was performed on a VYDAC protein C4 column (4.6 mm x 50 mm, 300 Å, 5 µm particle size; VYDAC, Hesperia, CA, USA). The standard run used a water-acetonitril gradient containing 0.1 % trifluoroacetic acid from 0 to 80 % acetonitril. At a flow rate of 3 ml/min, an injection volume of 50 µl was analyzed within 5 minutes. For improved separation from serum, the gradient was modified, ranging from 0-100 % acetonitrile, and the flow rate was reduced to 2 ml/min. Detection of rhBMP-2 was performed at 214 and 280 nm [Duggirala 1996]. The analysis was carried out on a Hewlett-Packard HP Series 1100 instrument, comprising a degasser, a quaternary pump, a thermostatted autosampler and a diode array detector. The system was operated with ChemStation V6.0 software.

3.2.1.4 High Molecular Weight Species and Aggregation

3.2.1.4.1 SEC

SEC was performed on a Spectra HPLC system consisting of a P 4000 quaternary pump, AS 1000 autosampler and FL 3000 fluorescence detector (Thermo Separation Products GmbH, Darmstadt, Germany) or a Hitachi-Merck L-6200/L-4000 HPLC system equipped with fluorescence detector and a D 2500 manual integrator (Hitachi Ltd, Tokyo, Japan). Samples were analyzed with a TSK-Gel®2000WXL column (7.8 mm x 30.0 cm, 5 µm particle size; Toso Haas, Japan) and isocratic elution with a 0.4 M L-arginine*HCl/5 mM glutamic acid buffer pH 4.5 at a flow rate of 0.6 ml/min. Controlling of the Spectra HPLC System and subsequent analysis was performed with ChromQuest® software.

3.2.1.4.2 SDS-PAGE

Gel electrophoresis was carried out in a XCell SureLock Mini-Cell electrophoresis chamber on NuPAGE® Novex Bis-Tris pre-cast gels (12 %, 10 wells, 1 mm) and NuPAGE® MOPS SDS running buffer (Invitrogen GmbH, Karlsruhe,

Germany). According to the vendors instructions, non-reduced samples were prepared with 25 % of the NuPAGE[®] LDS sample buffer; reduced samples additionally contained 10 % NuPAGE[®] reducing agent. After heating for 10 minutes at approx. 90°C and centrifugation, 20 µl typically containing 1 µg rhBMP-2 were loaded per lane. The loading volume of the Mark12[™] unstained marker (1:10 diluted for silver stained gels) was 10 µl. Gels were run with a constant current of 0.04 A per gel for 2-3 hours. Silver staining was performed with the SilverExpress[®] staining kit according to the vendor's protocol: Fixation in a methanol/acetic acid/water mixture, followed by the steps sensitizing, washing, staining, washing, developing, stopping and final washing. Coomassie staining (Collodial Blue staining kit) was carried out in two steps. Staining in a methanol/water/stainer mixture (55 % water, 20 % methanol, 5 % stainer A and 20 ml stainer B) for 3 to 12 hours was followed by a de-staining and washing step in deionised water for at least 7 hours. After drying, analysis of the stained gels was performed by densitometry, using an Epson GT 9600 scanner and ScanPack 3.0 software (Biometra GmbH, Göttingen, Germany).

3.2.1.5 Monitoring of Oxidation and Isomerization

3.2.1.6 Peptide Mapping

Samples were desalted on two 5 ml HiTrap[™] desalting columns operated in series (Amersham Biosciences Europe GmbH, Freiburg, Germany), connected to a Merck-Hitachi L-6200/L-4000 HPLC system equipped with a D 2500 integrator (Hitachi Ltd, Tokyo, Japan). Samples containing 50 µg protein were digested with 0.5 µg Endoproteinase Asp-N for 1.5 h at 37°C. Separation was achieved with a TSK Super-ODS 4.6 mm ID x 10.0 cm (Toso Haas, Japan) on a Agilent HP1100 HPLC system (Agilent Technologies Deutschland GmbH, Waldbronn, Germany) with UV detection at 214 nm. Met³⁷¹ oxidation and the amount of isomerized Asp³³⁵ were calculated according to the following equations (Figure 3-1):

$$\text{Met}^{371}_{\text{ox}} = \text{peak } A_{\text{ox}} * 100 / (\text{peak A} + \text{peak } A_{\text{ox}}) [\%]$$

$$\text{Asp}^{335}_{\text{iso}} = \text{peak } AB_{\text{iso}} * 100 / (\text{peak } AB_{\text{iso}} + \text{peak A} + \text{peak B} + \text{peak } A_{\text{ox}}) [\%]$$

peak A = peak area of peak A

peak A_{ox} = peak area of peak A_{ox}

peak B = peak area of peak B

peak AB_{iso} = peak area of peak AB_{iso}

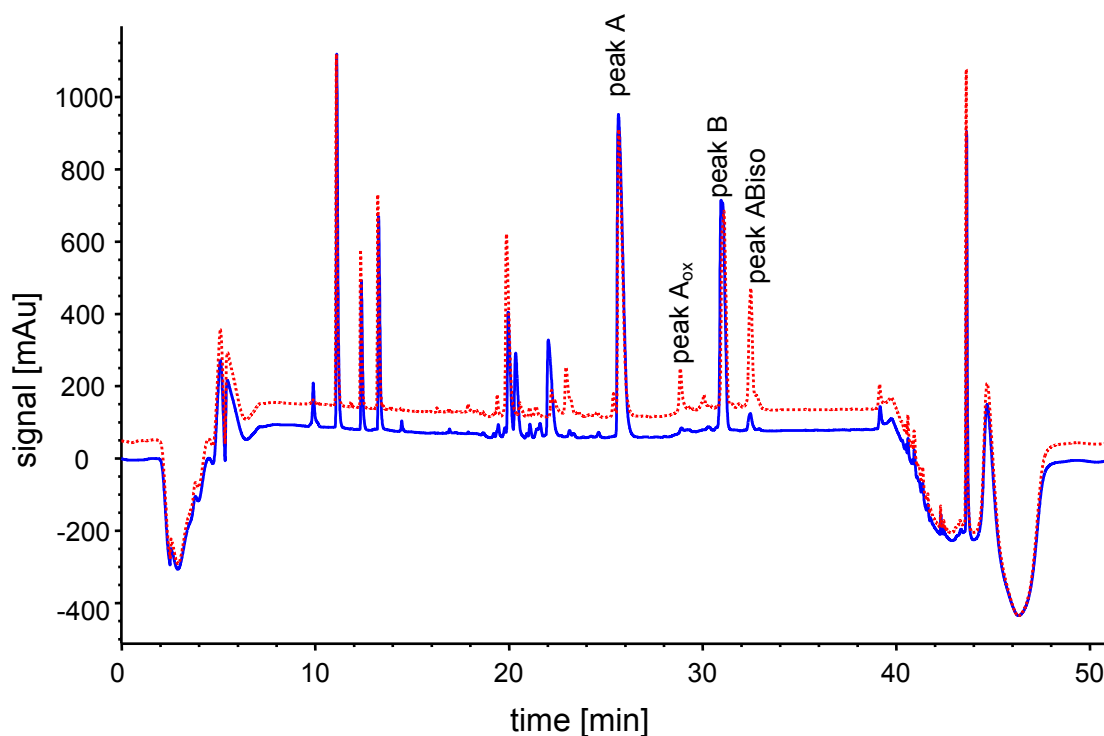


Figure 3-1: representative peptide map chromatograms of native standard (solid) and a degraded (dotted) sample

3.2.1.7 Proteins' Secondary Structure Integrity

3.2.1.8 Differential Scanning Calorimetry

Measurements were conducted with the Nano II Differential Scanning Calorimeter 6100 (Calorimetry Sciences Corp; Lindon, UT, USA). Data acquisition was performed from 25 to 110°C with a heating/cooling rate of 1°C/min ($n = 2$). Analysis was performed utilizing the Cp_{convert} program of the instruments analysis software, assuming a two state process for the transition. Samples and background solutions were prepared either by dialysis or centrifugal filter devices. The concentrations were adjusted to 2.0 mg/ml by dilution with the appropriate buffer. The buffer exchange medium of the last dialysis step serves as background.

3.2.1.9 (ATR) FT-IR Measurements

Measurements were conducted with the Confocheck™ (Bruker Optik GmbH, Ettlingen, Germany) at a constant temperature of 25°C, an acquisition time of 30 seconds and a resolution of 4 cm⁻¹. For transmission measurements the Confocheck™ was equipped with the AquaSpec™ flowthrough transmission cell (6 μm path length, 1 μl sample volume), for ATR measurements the BioATR II™ cell (with silicon crystal, 10 μl sample volume) was used. Temperature dependent spectra were acquired from 25 - 94°C in steps of 3°C at an effective heating rate of approx. 0.7°C/min. Data were analyzed with the

OPUS™ software. Quantification of secondary structure elements was performed by comparison of the native transmission protein spectra with a protein transmission spectra library, using a partial least squares algorithm. Origin®7.0 software was used to obtain the point of inflection (applying a sigmoid fit according to the Boltzmann model and subsequent differentiation of the fitted curve). The concentrations of the samples vary within 10 - 20 mg/ml. Protein-free reference material was obtained by ultrafiltration.

3.2.2 Focus on the Formulation

3.2.2.1 Preparation Methods

3.2.2.1.1 Turbulent Mixing: Vortex

Precipitation was achieved by adding the precipitating reagent(s) in form of a solution, the so called precipitation solution, to the protein solution. Mixing of the precipitation solution with the protein solution was performed with the help of a Vortex Genie®2 (Scientific Industries, Bohemia, NY, U.S.A.) tuned on half-maximum. In general, the test tube was filled with the appropriate volume of protein solution and the adequate volume of the precipitation solution was added with a manual pipette. Employed mixing ratios were 10+1, 9+1 to 1+1, and final suspension volumes of 1 to 33 ml were targeted. The standard procedure for microparticle preparation has turned out to be the combination of equal volumes of rhBMP-2 ($c = 2 \text{ mg/ml}$ in 1 mM HCl) with $2 \times$ phosphate buffer pH 7.4 ($2 \times 50 \text{ mM}$, ionic strength $2 \times 154 \text{ mM}$, adjusted with KCl).

For the evaluation of excipients, 1+1 mixtures were performed with a final sample volume of $500 \mu\text{l}$ and a protein concentration of 1 mg/ml . The excipient was added together with the precipitation solution to the protein solution.

For the incorporation of the microparticles in gel-like formulation, gels were prepared by mixing adequate amounts (w/v) of PVP with phosphate buffer (pH 7.4, 50 mM) and allowed to swell overnight. Microparticles were prepared according to the standard procedure (see above), concentrated by removal of the half supernatant volume and combined with the prepared gels in 1.5 ml glass vials with the help of a stir bar.

3.2.2.1.2 Laminar Mixing: Micromixer

The micromixer® (Institut für Microtechnik Mainz GmbH, Mainz-Hechtsheim, Germany) was equipped with a nickel on copper inlay ($10 \mu\text{m}$ channel width, $25 \mu\text{m}$ channel depth) or a silizium inlay ($30 \mu\text{m} \times 100 \mu\text{m}$). Feeding of the micromixer® was either performed with two syringe drivers (Perfusor®, Braun Medicare GmbH & Co KG, Melsungen, Germany) connected to the device with plastic tubes or two HPLC pumps (Hitachi-Merck L 6200, Waters type 590

(Waters Corporation, Milford MA, U.S.A.). In the HPLC approach, a rheodyne[®] valve (Rheodyne Europe GmbH, Bensheim, Germany) in combination with a 500 μ l sample loop was used to introduce small volumes of protein solution into the mixing process.

3.2.2.1.3 Storage Stability Sample Preparation

The reference formulations were prepared by dilution of protein bulk solution with appropriate volumes of formulation buffer (see 3.1.1) to a target concentration of 2.5 mg/ml. The reference formulations intended to stay liquid were additionally preserved with 0.2 % sodium azide. 400 μ l were filled into 2R vials. Precipitation was performed in 50 ml tubes by adding 10 x 1 ml dialyzed protein solution ($c = 2.0$ mg/ml) to (i) 10 ml preserved and (ii) 10 ml unpreserved phosphate buffer solution pH 4.5 (composed of 1.833 g KCl, 6.805 g KH_2PO_4 , titrated with KOH to a pH of 7.4 and filled up to a volume of 500 ml). The 50 ml tube was vortexed before, during and after the addition. After an equilibration time of one hour, the microparticles were resuspended, and 1 ml aliquots were filled in 2R vials. Subsequently, the precipitate was concentrated at the bottom of the vial by centrifugation at 2550 RPM for 10 minutes, and 900 μ l supernatant was removed. All vials containing no preservative were freeze-dried according to 3.2.2.2.2. The preserved formulations, both precipitated and liquid were directly closed with stoppers, flanged and placed into storage.

3.2.2.2 Additional Operations

3.2.2.2.1 Centrifugation

For concentration of the microparticle suspension, for preparation of storage stability samples and for the ultrafiltration experiments with centrifugal filter devices, either a Universal 16R centrifuge (Hettich GmbH, Tuttlingen, Germany) or a Sigma 4K15 (Christ, Osterode, Germany) was used.

3.2.2.2.2 Lyophilization

Already frozen samples (pre-treated with liquid nitrogen) were lyophilized with the program given in Table 3-1, performed with a Delta 1-24 KD Model freeze-dryer (Christ, Osterode, Germany).

Table 3-1: Lyophilization cycle for already frozen samples

step and time	temperature [°C]	vacuum [mbar]
start	0	-
ramp within 20 min	-30	1
hold for 40 h	-30	1
ramp within 2 h	20	0.04
hold for 5 h	20	0.04

For the samples of the stability study, lyophilization was performed with a Christ LPC-16/NT Epsilon 2-12 D (Christ GmbH, Osterode, Germany) according to the program given in Table 3-2:

Table 3-2: Lyophilization cycle for samples of stability study

step and time	temperature [°C]	vacuum [mbar]
start	20	-
ramp within 45 min	-45	-
hold for 90 min	-45	-
ramp within 16 min	-30	0.1
hold for 20 h	-30	0.1
ramp within 2 h	20	0.001
hold for 4 h	20	0.001

3.2.2.2.3 Viscosity Determination

Viscosity was measured with a PaarPhysica MCR 100 (PaarPhysica; Ostfildern, Germany) equipped with a cone plate CP 50-1 at 25°C. The shear rate was modified according to the following program to reveal structural behavior of the gel: Within 3 min from 0-500 sec⁻¹, holding at 500 sec⁻¹ for 3 min, decreasing the shear rate from 500-0 sec⁻¹ in 3 min. The viscosity at a shear rate of 141 sec⁻¹ was taken to characterize the gels.

3.2.3 Particle Characterization

3.2.3.1 Photon Correlation Spectroscopy

PCS, also referred to as dynamic light scattering utilizes the random movement due to Brownian Motion of suspended particles to characterize them. As the

pace of the movement is inversely proportional to particle size, the analysis of the time dependency of the light intensity fluctuations scattered from the illuminated particles can be used to determine the size. Measurements were conducted with the ZetaPlus® Bi-MAS (Brookhaven Instruments Corporation, Holtsville, NY, U.S.A.). All solutions were filtrated through a 0.22 µm Minisart® (Sartorius AG, Goettingen, Germany) prior use for sample preparation.

3.2.3.2 Laser Light Diffraction

Measurements were conducted with a Mastersizer® X (Malvern Instruments Ltd, Worcestershire, UK) in a modified sample cell. The required sample volume was minimized by omitting the dispersion unit typically used for measurements. To further reduce the dead volume within the sample cell, inert teflon inlays were prepared and inserted, allowing measurements of sample volumes < 5 ml. After background alignment with protein free buffer, the protein suspension was measured. Therefore, it was directly filled into the modified sample cell, the whole cell was shaken manually, installed and the measurement was started after a delay of one minute to allow air bubbles to pass off. Laser light intensity was evaluated by Fraunhofer analysis underlying a polydisperse model.

3.2.3.3 Light Microscopy

Microparticles were visualized with a binocular microscope (Axiovert 25, Zeiss, Goettingen, Germany) under phase contrast, using a Ph1-0.4 filter. 3-5 µl were dropped on an object holder covered with a slip and examined under 20 fold magnification. Digital imaging of microparticles was done with a Sony Cyber-shot DSC S75 (Sony GmbH, Cologne, Germany) connected to the microscope.

3.2.3.4 Laser Light Blockade

Laser light blockade measurements were performed with a Pamas®SVSS (Pamas, Rutesheim, Germany). Measurements were performed in triplicate and consumed a total suspension volume of 900 µl. Results were presented in number distributions.

3.2.3.5 Environmental Scanning Electron Microscopy

Environmental scanning electron microscopy (ESEM) was conducted at the FAU-Erlangen/Nuremberg, Department of Material Science, Glass and Ceramics with a Philips XL30 ESEM equipped with a gaseous secondary electron detector and operated in the low vacuum mode.

For SEM, samples were carbon-coated by burning up a graphite-twine with a BAL-TEC MED 020 (Baltec AG, Balzers, Liechtenstein) with a maximum current of 125A, and examined with a JEOL Field Emission Scanning Electronic Microscope JSM-6500F (JEOL USA, Peabody MA, U.S.A.).

3.2.4 In-vitro Release

In-vitro release of rhBMP-2 from microparticles was tested in serum containing 0.02 % sodium azide. The microparticle suspension was combined with the serum in 2 ml plastic test tubes and placed in a Julabo SW21 shaking water bath (Labortechnik GmbH, Seelbach, Germany) at 37°C/50 RPM. At designated time points, either serum exchange was performed or the tube was finally sampled.

3.2.5 Bioactivity Testing

3.2.5.1 Determination of Bioactivity in Cell Culture

The bioassay was performed at Wyeth BioPharma (Andover MA, U.S.A.). The target cell line W-20 clone 17, a bone marrow derived stromal cell line of the mouse, exhibits increased alkaline phosphatase activity in response to rhBMP2. Cells were grown in DME (Dulbecco's modified Eagle's medium) supplemented with FBS (fetal bovine serum) in flasks until a confluent cell layer developed. After harvesting, cells were seeded in a 96-well, flat-bottomed plate and incubated at 37°C overnight in a fully humidified 0.5 % CO₂ incubator. Samples and controls, diluted with assay medium to encompass the working range of the standard, were added. Each plate includes all the standard curve points, media controls, internal controls and test samples. After a second incubation of the treated cells for 24 hours, the assay medium was removed from the plates and the target enzyme alkaline phosphatase was liberated by lysis of the cells by a repeated freeze-thaw cycle. The substrate, p-nitrophenyl phosphate, was added to the well plate and developed while shaken gently. Absorbance values were read at 405 nm after stopping the reaction with diluted NaOH. Bioactivity was calculated from the reference standard curve using a four-parameter logistical fit.

3.2.5.2 Efficacy Study in an Animal Model

Surgical Procedure

The efficacy study was conducted at Wyeth Research (Cambridge MA, U.S.A.). It involves four skeletally mature New Zealand White rabbits, treated in a unilaterally regimen with the precipitated microparticle suspension. The animals were pre-treated with an antibiotic and an analgesic (Table 3-3). Approximately twenty minutes before anesthetic induction, the animals received medication for muscle relaxation and general anesthesia. Corneal dryness was prevented by application of a bland ophthalmic ointment to both eyes. After shaving, the skin was disinfected with betadine solution and 70 % ethanol. After sedation and preparation, general anesthesia by halothane was administered via face mask. Intraosseous injection of the microparticle suspension was performed with a 18-gauge needle under fluoroscopic guidance. The needle was positioned and

inserted into the distal femur through the lateral cortex with a slow rotation until the end was visualized in the region of interest in the intercondylar region of the epiphysis. After flushing the needle with 0.1 to 0.2 ml sterile saline, 300 μ l rhBMP-2 microparticles were injected. To minimize leakage out of the bone, the needle was held in place for at least one minute after the injection and pressure was applied to the injection site before the needle was taken out. For fluorescence labeling, tetracycline and calcein were administered as given in Table 3-3. After four weeks, the animals were sacrificed and examined.

Table 3-3: Medication administered by injection

time of application	substance	dose [mg/kg]	route
before surgery, after 1d	cefazolin	10	SQ
before surgery, after 1d	buprenorphine	0.03	SQ
before surgery	ketamine	35	IM
before surgery	xylazine	5	IM
10 and 25d post surgery	tetracycline	25	SQ
15 and 25d post surgery	calcein	5	SQ

Evaluation

Radiographs were taken post-op and every two weeks in lateral position. For histology, the distal femur was isolated and undecalcified specimens were dehydrated with gradients of ethanol (70-100 %) and cleared in xylene using the LX120 Automatic Tissue Processor. Infiltration and embedding was done in methyl metacrylate which was allowed to polymerize for 3-5 days at room temperature. Blocks were cut at 10 μ m using a Riechert-Jung Polycut or a Lecia 2065 Supercut. Sections were stretched and pressed on gelatin-coated slides and tissue adherence to the slides was ensured by overnight storage at approx. 50°C. After equilibration to room temperature, standard VonKossa staining was performed, followed by quantitative histomorphometry with a digitizing image analysis system (NIH Image software).

4 Results and Discussion

4.1 Formulation Development

Researchers developing formulations for rhBMP-2 were often confronted with the phenomenon of macroscopic precipitation [Friess, 2000]. As this is usually considered to be an undesired instability criterion [Wang, 1999] efforts were made to avoid this. The rationale of this formulation approach is to utilize the high tendency of rhBMP-2 to precipitate for the generation of highly pure rhBMP-2 microparticles. In general, protein precipitates feature broad particle distributions with poor uniformity [Maa et al., 2000], and therefore are usually intermediate products during purification or concentration. In this work, a precipitation method should be developed leading to uniform microparticles, and the parameters determining particle size and distribution should be evaluated.

4.1.1 Initial Precipitation Process Development

4.1.1.1 Considerations and Setup

As described in the theoretical part, three main categories - process technology, precipitation solution and protein solution - are the determining variables in a precipitation experiment. To keep the process quite simple, the combination of a precipitation solution with the protein solution is initially performed in a batch mode, using a manual pipette for liquid addition and a classic vortex for rapid and homogenous mixing of the two fluids (Figure 4-1). The batch volume is set to be 5.5 ml, adapted to the requirements of a modified particle size measurement setup (see 3.2.3.2). A mixing ratio of 10 + 1 is chosen, leading to a total of 5 ml protein solution pH 4.5 and 0.5 ml precipitation solution.

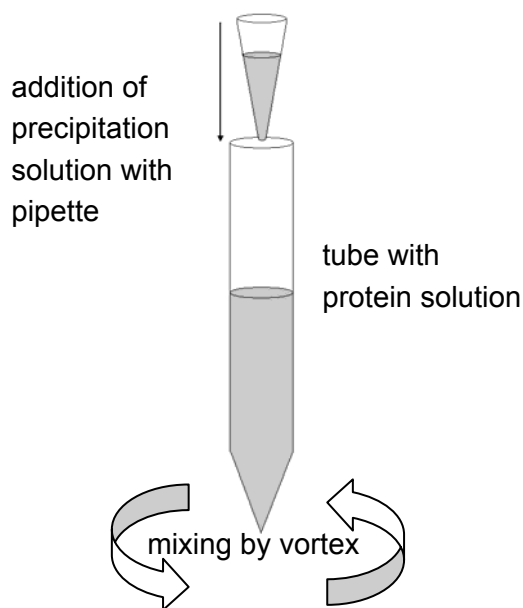


Figure 4-1: Scheme of initial process setup: the precipitation solution is quickly added to the already turbulent protein solution, and vortexing is continued for 10 seconds

The idea for the novel formulation is to utilize the low solubility of BMP under physiologic conditions [Abbatiello et al., 1997] for its controlled precipitation. Consequently, blood fluid serves as a template (Table 4-1) [Thews et al., 2004], with focus on the anion composition to mimic physiologic properties. The amount of base to adjust the pH to 7.4 is determined experimentally by titration (Figure 4-2). Finally, the precipitation solution contains the adequate salt concentrations (275 μl of a 20x stock solution), the desired amount of sodium hydroxide to achieve physiologic pH of 7.4 (20 μl 1M NaOH) and purified water (to adjust the precipitation solution volume to 500 μl). Based on a 10 + 1 mixing ratio and a final volume of 5.5 ml after mixing, a final protein concentration of 0.18 mg/ml has proven to be suitable to allow direct laser light diffraction measurements of the precipitate without the need to dilute or concentrate the protein suspension altering the environmental conditions.

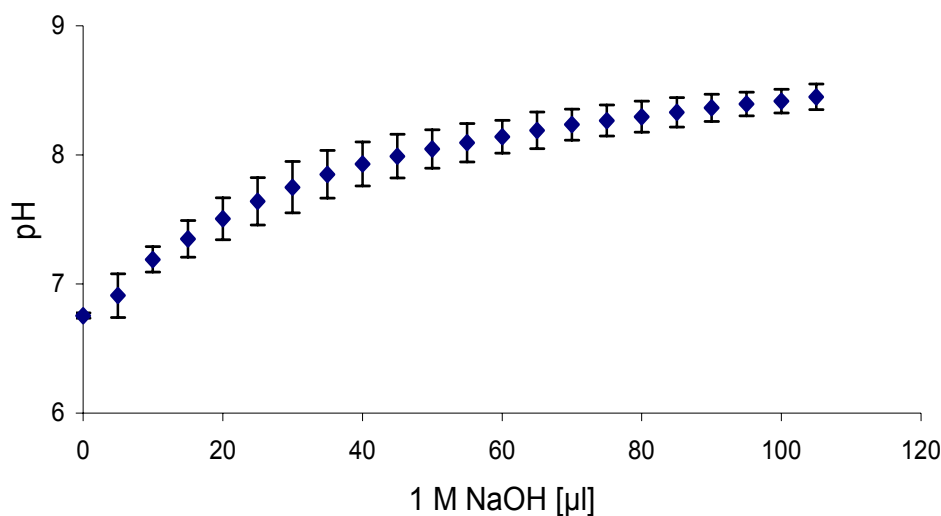


Figure 4-2: Titration of a mixture of 5 ml pure protein formulation buffer, 275 μ l salt stock solution (20 x) and 225 μ l purified water with 1 M NaOH

Table 4-1: Electrolyte-concentrations in blood fluid: the precipitation solution contains the grey underlined anions as sodium salts, resulting in the listed concentrations after mixing with the protein solution

ion	concentration [mmol/l]
sodium	142
potassium	5
calcium	2.5
magnesium	1
chloride	102
bicarbonate	27
phosphate	1
sulphate	0.5
organic acids and proteins	7

4.1.1.2 Particle Size Distribution of Initial Formulation

Particle formation is a time dependent process. Initially, broad monomodal distributions are found, with maxima between 5 – 10 μ m (Figure 4-3). In some experiments, an additional, very small population with a particle size below 1 μ m is present.

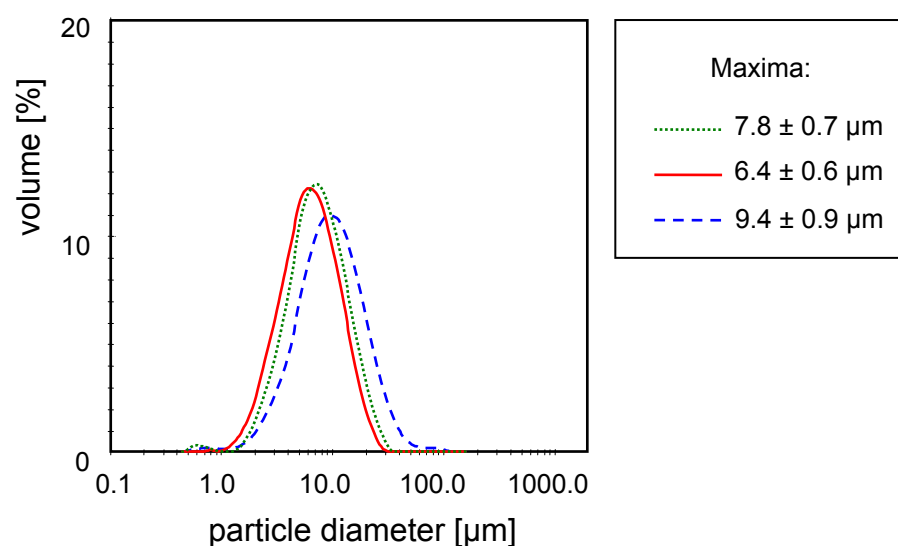


Figure 4-3: Initial particle size distributions of three different batches

Over time, a second population develops leading to a bimodal distribution with two maxima at approx. 7 and 35 μm at equilibrium (Figure 4-4). In some batches, the small population below 1 μm is still present. The ratio of the two dominating maxima slightly varies in dependence of the shear force applied by the manual shaking procedure preceding each measurement.

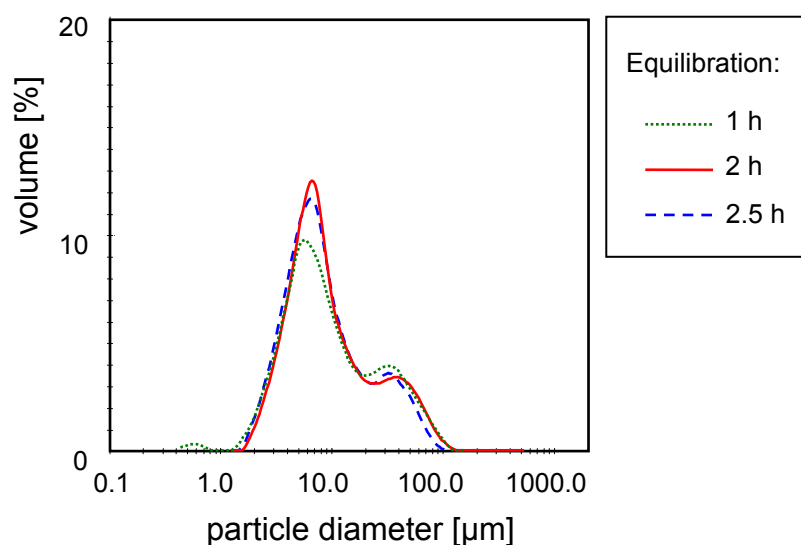


Figure 4-4: Particle size distributions of three batches after turbulent mixing and equilibration at room temperature

The results demonstrate that the precipitation conditions are suitable to create microparticles. The distributions are in good agreement with theory. The small particle fraction at approx. 0.5 μm reflects the remnants of the primary particles formed in the perikinetic association and aggregation phase. Glatz postulates a primary particle size of 0.1 to 0.2 μm to be typical for proteins and sizes of 10 to

20 μm after flocculation [Glatz, 1992]. Isoelectric precipitated soy protein and casein led to basic particles of approximately 1 μm [Hoare, 1982, Bell et al., 1982], being in good correlation to our findings. Further association of these submicron-sized particles can be classed to the ortokinetic growth phase, leading to microparticles with a preferred average size of approx. 7 μm . The transition from the ortokinetic growth phase to the protein aging phase is reflected by the formation of the second maximum, resulting in the bimodal equilibrium distribution. The observation of an equilibrium balance within the bimodal distribution and its sensitivity to shear forces suggests that the microparticle fraction of 35 μm consists of microparticles which are loosely associated with each other. With a residual solubility of $39 \pm 3 \mu\text{g/ml}$ ($n=3$) and a final protein concentration of 0.18 mg/ml after mixing, almost 80 % of the deployed protein form microparticles.

4.1.1.3 Effect of Centrifugation

As centrifugation is the method of choice to concentrate the microparticles, its influence on particle size distribution was analyzed. Moderate centrifugation is reversible, and the underlying bimodal distribution can be restored after vortexing (Figure 4-5).

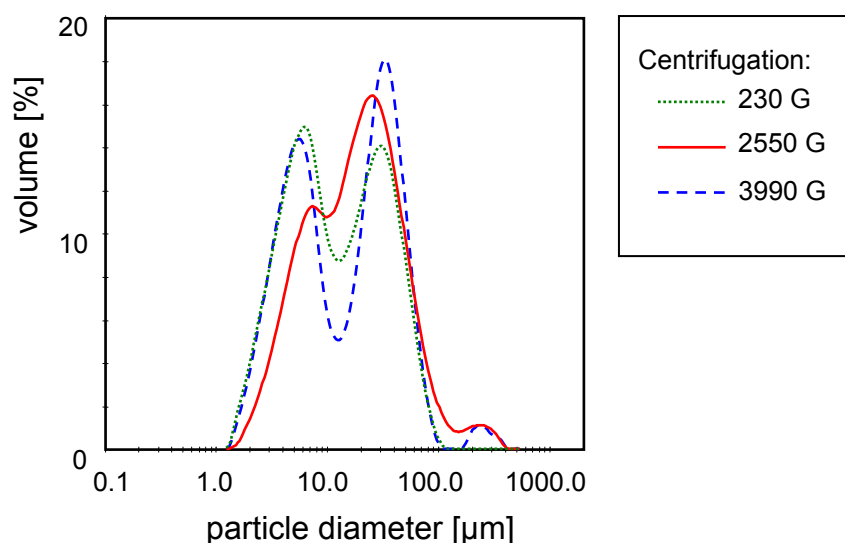


Figure 4-5: Particle size after centrifugation and resuspension

4.1.1.4 Influence of Lyophilization

The feasibility of lyophilization to create dry microparticles was tested. Dried particles might be desired to circumvent classic formulation instabilities of suspensions such as caking after sedimentation during storage [Defelippis et al., 2000]. Furthermore, protein stability might be further improved in the dry solid state, compared to protein particles in an aqueous environment. Finally, dry microparticles might serve as starting material for other formulation

approaches, e.g. incorporation in implants. Microparticles were first concentrated by moderate centrifugation, frozen in liquid nitrogen and then subjected to a lyophilization process. After subsequent dispersion, the larger population around 35 μm is favoured, although the smaller fraction is still present as a shoulder (Figure 4-6). For images of lyophilized microparticles see Figure 4-23.

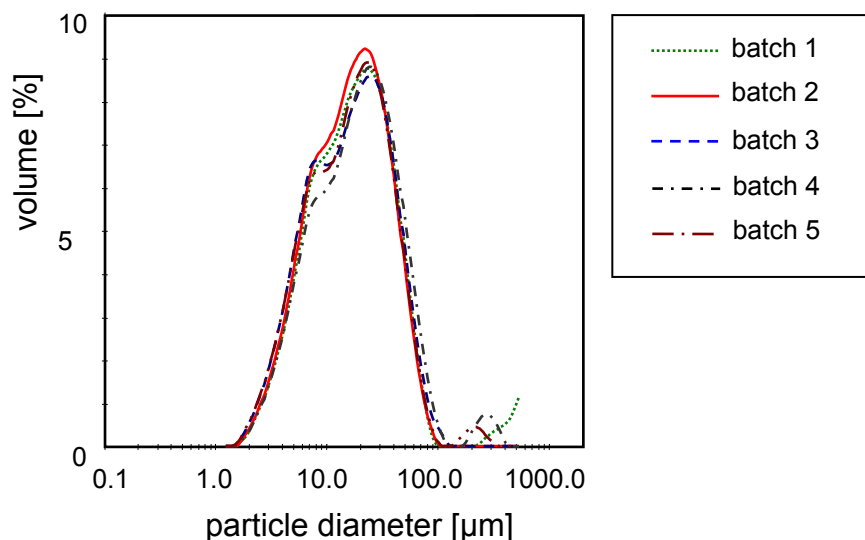


Figure 4-6: Particle size distribution of different batches after lyophilization

The process is feasible to create dry microparticles. The underlying particle distribution can be preserved, emphasizing the importance of initial particle formation within the precipitation step. However, in some batches formation of associates larger than 100 μm is observed after lyophilization. This might be caused by the high protein concentration, forcing individual protein particles to close contact with each other during freezing and drying. Removal of water enables the particles to build up interparticular connections. As the result is given in volume%, the total number of these large aggregates is small.

4.1.1.5 Influence of Protein Concentration and Batch Volume

For the production of larger amounts of microparticles, a scaled-up procedure, combining microparticles of 12 batches with a total volume of 360 ml and an initial protein concentration of 2 mg/ml was performed and analyzed with respect to the particle size distribution (Figure 4-7).

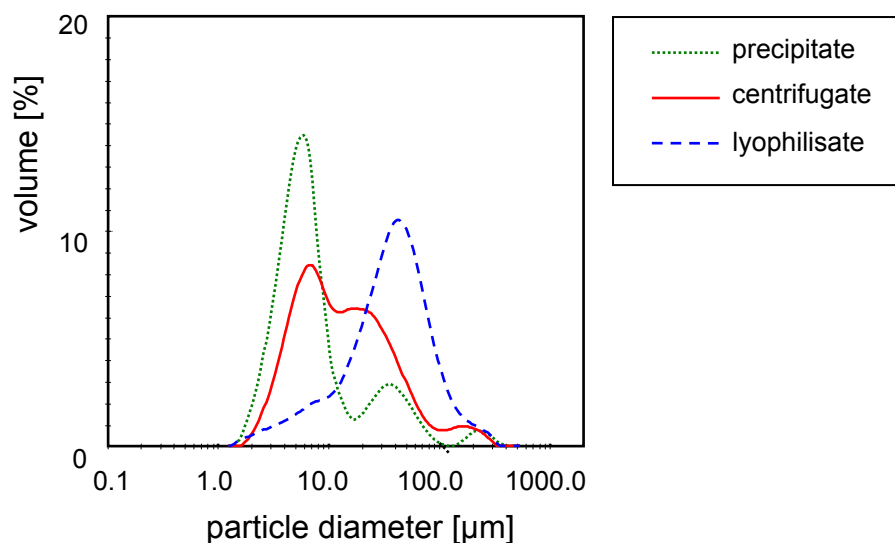


Figure 4-7: Particle size distributions of a 30 ml batch after equilibration, centrifugation and pooling (2550G for 15 minutes, combination of 12 batches), and lyophilization

The higher protein concentration and the larger batch volume did not alter the preferred particle sizes after equilibration. However, a tendency to form larger associates, with average sizes of approx. 250 µm becomes apparent, creating a third maximum. The particle fraction with a maximum at 5.8 ± 0.6 µm covers 81.3 % of the total particle volume, the intermediate fraction 16.3 % and the large associates 2.4 %. Subsequent concentration by centrifugation and pooling to approx. 50 mg/ml increases the amount of medium sized associates on cost of the small ones. Lyophilization further pushes the balance towards this population, with mean sizes of 41.9 ± 4.2 µm at maximum. For the process steps precipitation and concentration by centrifugation, the particle size distributions from the scaled-up procedure differ only marginally from smaller scaled batches. After freeze drying and redispersion, the microparticle size slightly increases. Thus, higher initial protein concentrations and larger batch volumes are general feasible for scaling-up, keeping in mind that lyophilization alters the distribution.

4.1.1.6 Variations of Mixing Technique and Protein Concentration

The micromixer[®] enables laminar mixing of two liquids, the protein and the precipitation solution [Hessel et al., 2001] (Figure 4-8). The mixing process can be performed continuously, and the technique allows precise adjustment and variation of a number of parameters, e.g. the mixing speed by manipulation of the feed rate or by exchanging the inlays differing in the channel size. Furthermore, by parallel operation of multiple devices, this approach possesses unique scaling-up properties. To adapt the experimental design of the batch precipitation process to the setup and the dimensions of the device, identical

volumes of precipitation solution and protein solution are used (mixing ratio 1 + 1).



Figure 4-8: Experimental setup with micromixer[®]: two syringe pumps feed the micromixer[®] with a constant, pulsation-free flow of the protein and the precipitation solution, laminar mixing and precipitation is performed within the device, thus forming the microparticles.

Again, precipitation is a time dependent process. After equilibration, similar particle distributions were found as in the precipitation experiments conducted with the vortex mixing technique. Both mixing techniques result in particle formation in the range of 0.5 to approx. 200 μm with a preferred size of approx. 7 μm . Whereas precipitation via vortex results in a second peak with sizes around 30 μm , micromixing delivers larger particles in the 60 μm range after equilibration. The variation of the total inlet flow within 0.32 and 1.66 ml/min did not markedly affect the resulting particle size. Higher protein concentrations increase the volume fraction of the small microparticles, being well above 85 % (volume based) at a final precipitation concentration of 2.5 mg/ml (Figure 4-9).

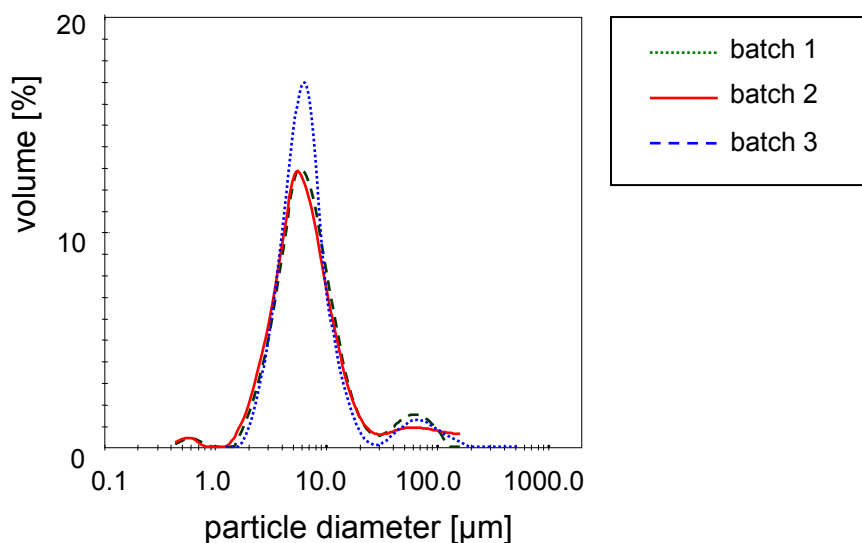


Figure 4-9: Particle size distribution after laminar mixing and equilibration: bimodal, with preferred maxima at 7 and 60 μm

The major disadvantage of the formulation is the difficulty to keep the pH constant. Repeated measurements over time indicate a shift by approx. 0.3 units within 24 hours (Figure 4-10).

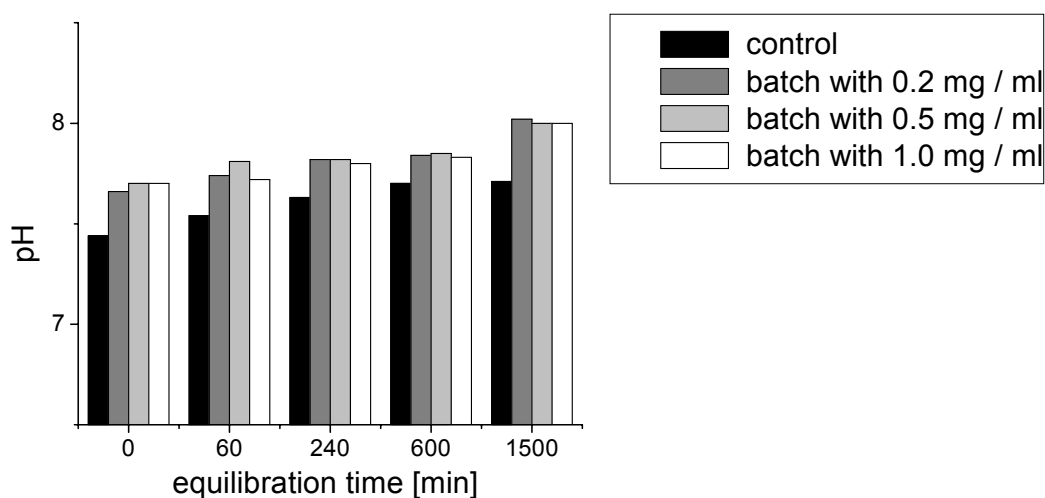


Figure 4-10: pH-shift of the formulation to more basic values over time: control and samples containing different amounts of precipitated microparticles.

In contrast to physiologic blood fluid, which features diverse mechanisms to balance and maintain the pH, the artificial physiologic formulation lacks sufficient buffer capacity. With a concentration of 1 mM, the contribution of phosphate to the buffer capacity is minimal. With a maximal buffer capacity of bicarbonate being around pH 6.1, the contribution of 27 mM of this salt to the

buffer capacity is marginal at the target pH of 7.4, [Martin et al., 1987]. The observed pH increase might be the result of a CO₂ loss to the environment

Overall, controlled precipitation in the batch mode leads to the formation of protein microparticles suspended in an artificial physiologic environment. Scaling up is feasible by utilizing the continuous laminar mixing approach provided by the micromixer[®]. Dry microparticles can be obtained by concentrating (moderate centrifugation of the suspension) and subsequent lyophilization.

4.1.2 Optimization of Formulation Composition

To keep the pH constant, a sufficient buffer capacity should be introduced. Furthermore, the number of excipients present in the final microparticulate suspension should be reduced. At first, residual excipients derived from the protein bulk formulation, which was initially optimized for lyophilization (glutamic acid as buffer, sucrose and glycine as cryo/lyoprotectant and amorphous cake former) should be removed and replaced by an adequate buffer. Especially the surfactant (polysorbate) might interfere with the formation of particles and should therefore be eliminated. Secondly, the precipitation solution should be optimized by omitting bicarbonate and focusing on a single buffer system and adjusting to physiologic ionic strength with a single type of salt. This is legitimate, as the solubility of rhBMP-2 is mainly dependent on the ionic strength and not salt specific [Abbatiello et al., 1997].

4.1.2.1 Solubility in Different Phosphate Buffer Systems

An ideal candidate useful to optimize both the precipitation and the protein solution is phosphate buffer. It can serve as protein formulation buffer to support solubility in the acid milieu ($pK_1 = 2.16$) and as precipitate stabilizing buffer after shift to physiological pH ($pK_2 = 7.21$) and salt content. Therefore, the solubility of different phosphate buffer systems was tested. Figure 4-11A shows the residual protein solubility in dependence of the ionic strength at different pH values and phosphate buffer molarities. Salting-in of rhBMP-2 is observed over the entire observed ionic strength, ranging from 22 – 280 mM. Thus, an increase in buffer molarity is accompanied by an increase in solubility of the protein. The differences in solubility of equimolar buffers of different pH values are also a direct consequence of the altered ionic strength, with formulations of higher pH values featuring higher ionic strengths. The solubility profile is in good correlation with the literature (see Introduction). Extrapolation at the target ionic strength of 154 mM delivers protein solubility in the range of 0.03 to 0.04 mg/ml.

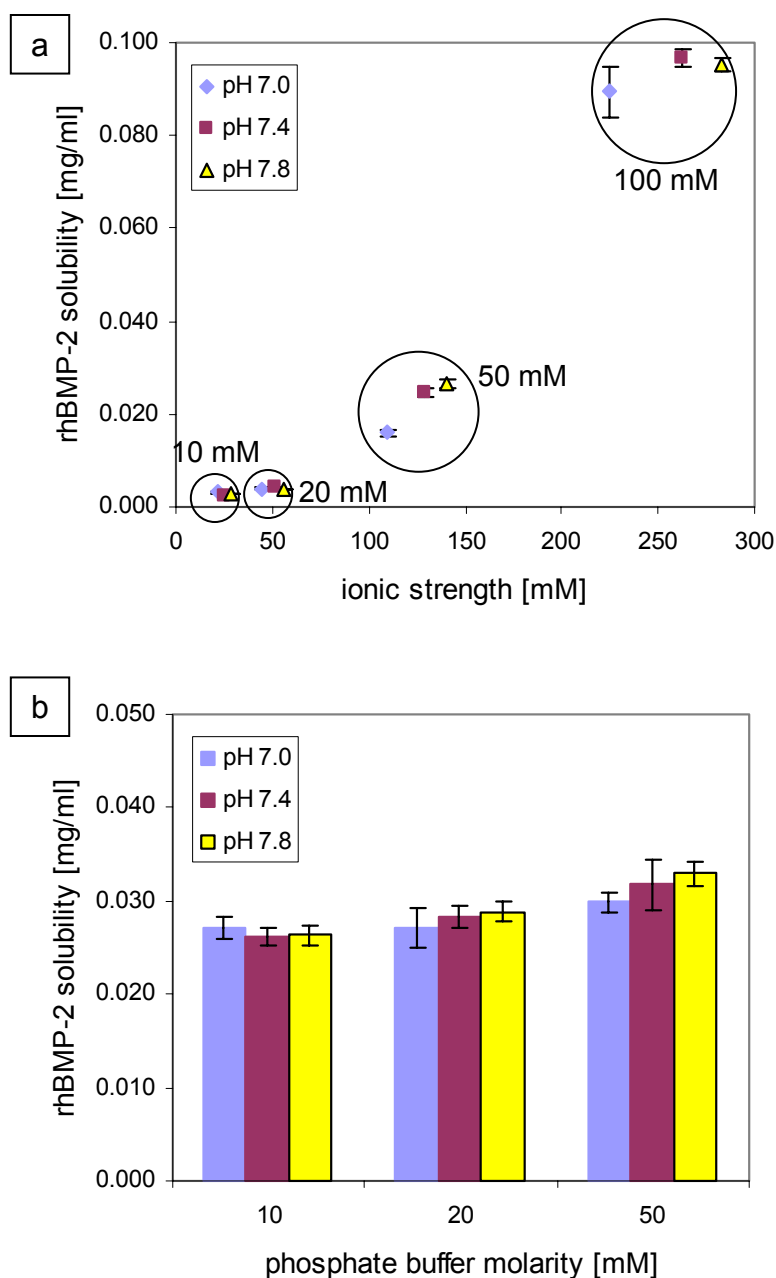


Figure 4-11: Residual solubility of rhBMP-2 in dependence of the ionic strength and pH (a), at constant final ionic strength of 154 mM (adjusted with KCl) and different buffer molarity and pH (b)

Figure 4-11B shows the residual solubility of rhBMP-2 in phosphate buffer formulations with different pH values and buffer molarities, adapted with KCl to a final ionic strength of 154 mM to mimic physiological conditions. Within the accuracy of the measurement, similar solubility's are obtained at different pH values, but equimolar ionic strengths, confirming the finding that solubility of rhBMP-2 is mainly dependent on the ionic strength. The 50 mM buffer with a pH of 7.4 is selected for the novel formulation, as it features the highest buffer

capacity and requires the fewest amount of KCl to adapt the ionic strength to 154 mM. These conditions are optimal because the administration of a protein suspension with a higher ionic strength is expected to result in uncontrolled precipitation of residual soluble protein at the injection site, whereas in solutions with lower ionic strength microparticles are thought to be subjected to rapid redissolution.

4.1.2.2 Particle Size Distribution of Optimized Formulation

Microparticles were prepared according to the optimized formulation composition: the protein formulation was buffer exchanged into 50 mM phosphate, and the composition of the precipitation solution was reduced to the excipients KCl and KOH to increase the pH and the ionic strength to induce precipitation. In order to be able to use laser light diffraction measurements (Malvern® Mastersizer) for the analytics without the need to dilute the sample, initially low final protein concentrations were used. Turbulent mixing of the protein solution ($c = 0.2 \text{ mg/ml}$) with the precipitation solution in a 9 + 1 ratio results in a final protein concentration of approx. 0.18 mg/ml .

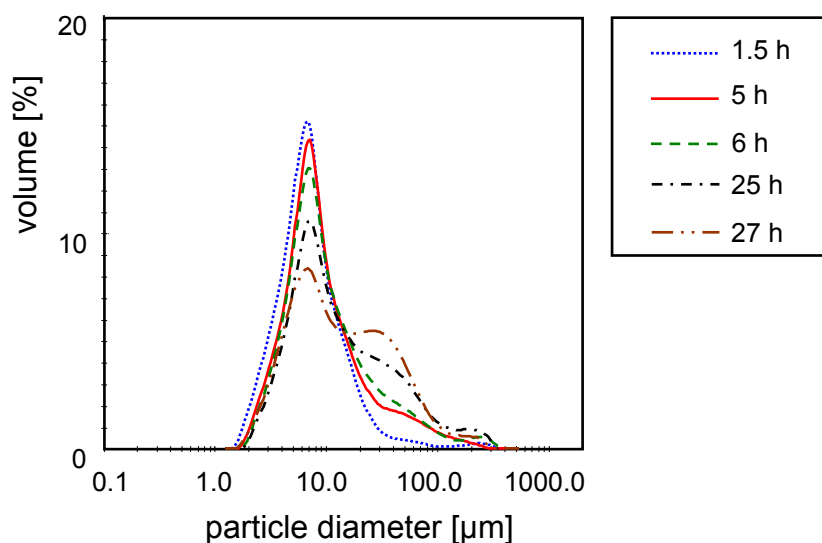


Figure 4-12: Time dependent particle formation and equilibration distribution of optimized formulation: maxima at $7.1 \pm 0.7 \mu\text{m}$, $34.4 \pm 3.4 \mu\text{m}$ and 203.5 ± 20.0 .

Figure 4-12 depicts the course of particle growth on cost of an initially formed, almost monomodal particle population. At equilibrium, the same two maxima are obtained as in the previous, more complex formulation (Figure 4-3). However, a slight tendency to form associates of approx. $200 \mu\text{m}$ can be observed.

With a residual solubility of approx. 0.03 mg/ml (Figure 4-11), higher final precipitation concentrations than the initially tested 0.18 mg/ml are desired to increase the ratio of immobilized to soluble protein and thus the precipitation efficacy. However, at higher protein concentrations the phosphate buffered protein solution shows premature precipitation already before the precipitation solution is added. Consequently, the protein solution is reformulated without phosphate at an acidic pH of 3.0 to ensure solubility (1 mM HCl), and the phosphate buffer component is added with the precipitation buffer.

Figure 4-13 compares the equilibrium distributions of the formulation with phosphate in the protein solution (mixing ratio of 9 + 1, final protein concentration 0.18 mg/ml), and the modified formulation with the phosphate salt in the precipitation solution (mixing ratio of 1 + 1, final protein concentration 0.18 mg/ml and 1.0 mg/ml). Apart from a slightly broader peak for the small particle fraction and a shoulder instead of a discrete maximum for the particle fraction around 30 μm of the low concentrated formulation, essentially the same distribution patterns are obtained independent of the mixing ratio.

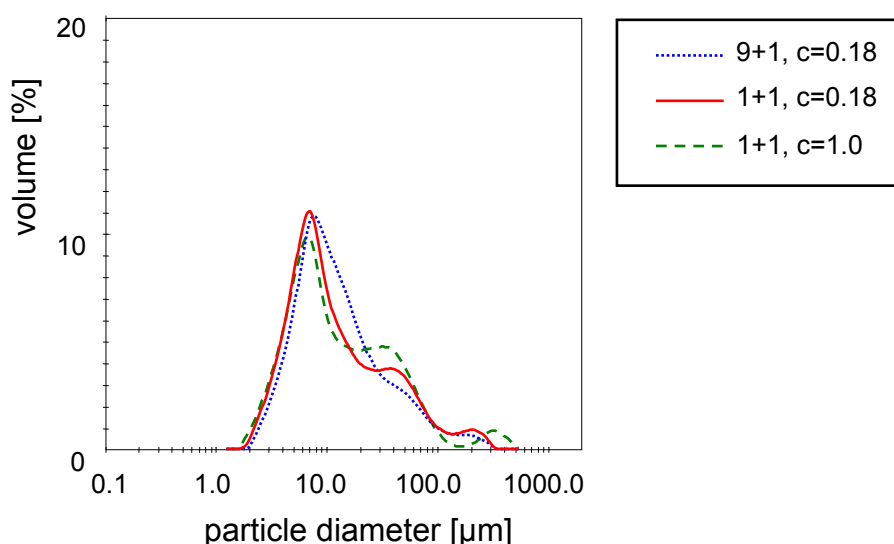


Figure 4-13: Equilibrium distributions of optimized formulations after turbulent mixing basically show the same distribution pattern: prominent maxima at $7.1 \pm 0.7 \mu\text{m}$ and $34.4 \pm 3.4 \mu\text{m}$.

To elucidate scaling-up properties of the optimized formulation, microparticles were generated by laminar mixing of equal volume flows of precipitation solution and protein solution, resulting in a high final protein concentration of 1 mg/ml. Figure 4-14 shows the course of particle formation. In analogy to previous results, an almost monomodal population with maximum around 7 μm can initially be detected, which gives way to a bimodal distribution after equilibration for one hour.

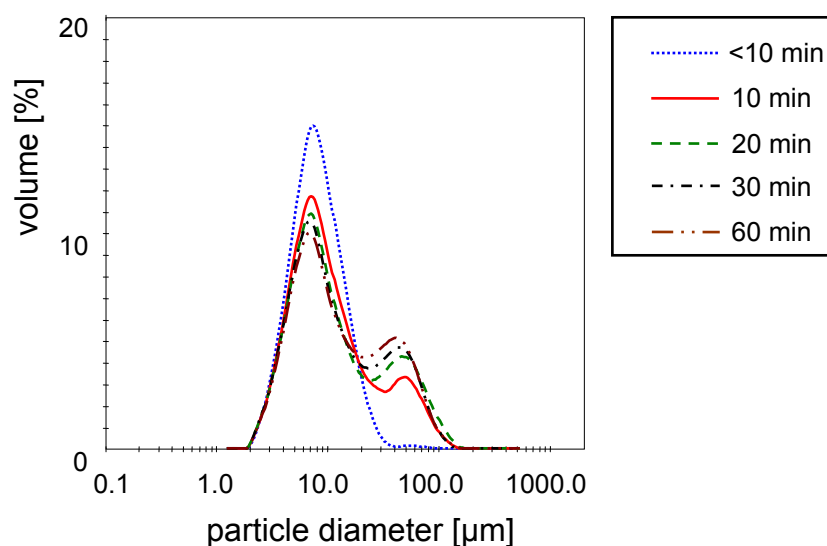


Figure 4-14: Time dependent particle formation of optimized formulation after laminar mixing: maxima at $7.1 \pm 0.7 \mu\text{m}$ and $41.9 \pm 4.1 \mu\text{m}$

Further proof of the robustness and the high scaling-up potential of the method can be concluded from Figure 4-15. It shows essentially the same distributions of three batches prepared with different feeding rates and confirms the independence of particle size from this parameter.

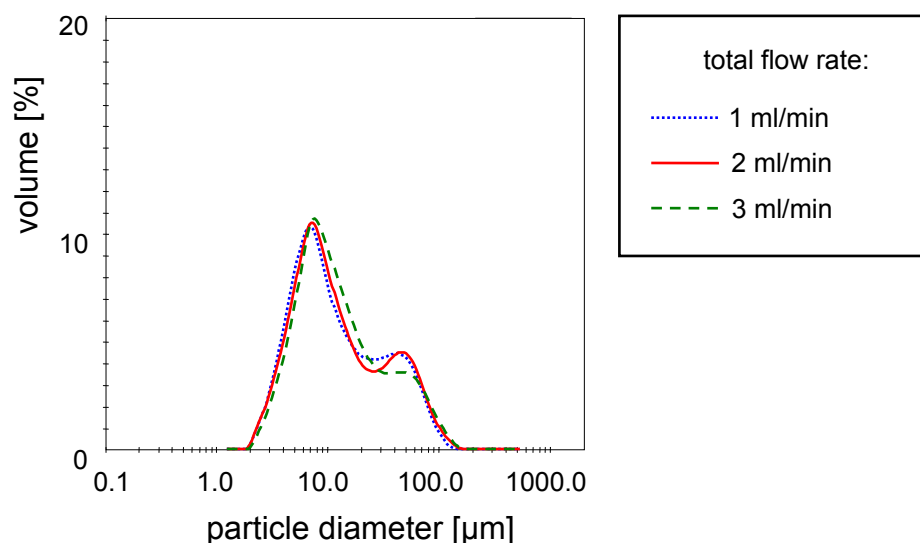


Figure 4-15: Particle distribution after laminar mixing with different flow rates and a high final protein concentration of 1.0 mg/ml after equilibration for one hour.

4.1.2.3 Phase Contrast Microscopic Imaging of Microparticles

The presence of large aggregates as they were detected by laser light diffraction measurements (Figure 4-12) cannot be confirmed by visual inspection. In the non-stirred diffraction measuring cell, the highly hydrated microparticles interact with each other, forming a network-like structure.

Consequently, two originally individual particles might appear to be a single, large one for the measuring system. With phase contrast microscopy, it is possible to visualize the microparticles. Figure 4-16 clearly demonstrates that the microparticles measure far less than 100 μm . Individual irregular shaped particles sizing approx. 1 to 30 μm can be seen, and larger microparticles appear to be loose agglomerates of smaller ones. Contrary to laser light diffraction measurements, the average size of initially formed particles remains essentially the same over time. Consequently, the large particle population measured with laser light diffraction is an artifact, caused by weakly associated small particles. In analogy to laser light diffraction results, the microscopic images also do not reveal a fundamental difference between samples prepared by turbulent and laminar mixing.

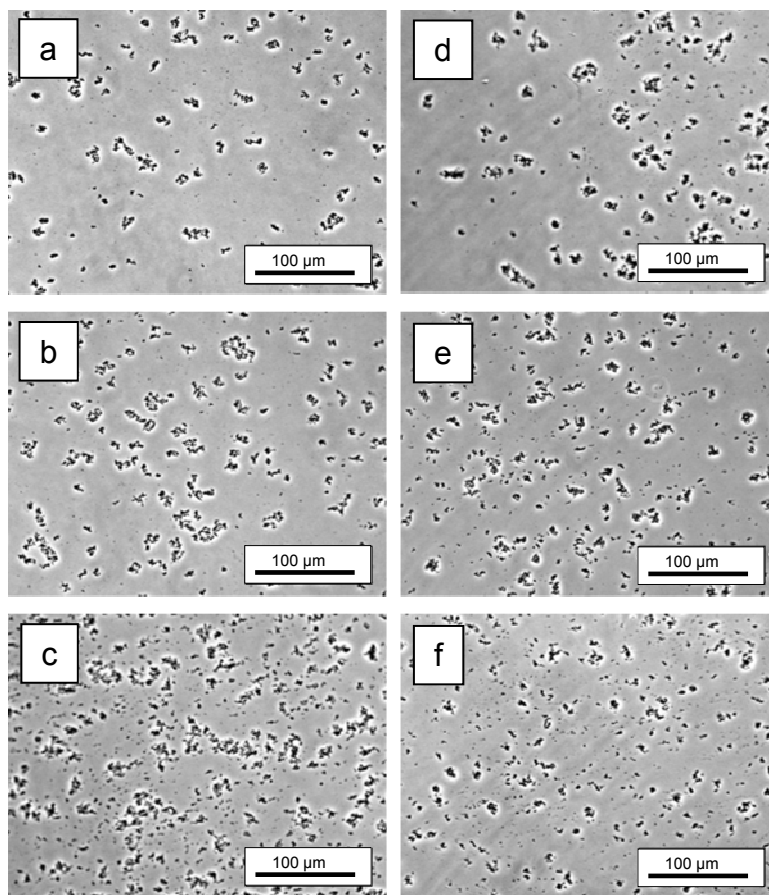


Figure 4-16: Images of microparticles with phase contrast microscopy prepared by different mixing techniques: turbulent mixing and equilibration for 10 min (a), 1 h (b), 64 h (c); laminar mixing and equilibration for 10 min (d), 1 h (e), 24 h (f)

The microscopic images show collectives of particles which seem to be individual ones. Minimal liquid streams caused by covering the suspension drop with the slit during sample preparation initiate the particles to move and come to

rest side by side, so that they appear to form large particles in the microscopic image (Figure 4-17a,b). Marginal shear forces, caused by a slight push of the cover slit, singles the particles out (Figure 4-17c,d). This observation further supports the assumption that larger microparticles are loose associates of compact, small ones.

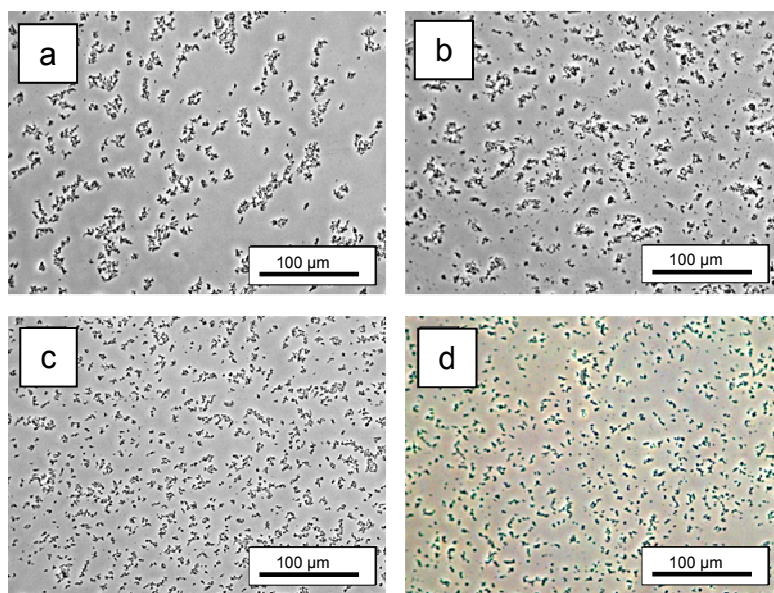


Figure 4-17: Particle size distributions before (a, b) and after manipulation of the cover-slit (c, d)

4.1.2.4 Laser Light Blockade Measurements

To support the hypothesis that large particles consist of loosely associated small particles, laser light blockade experiments were performed. This setup allows the measurement of the suspension on the move, as the sample is pumped to the optical system, thus separating loose associates due to shear forces. The data confirm that the optimized formulations do not contain any particle larger than $48.7\ \mu\text{m}$, and the percentage number of particles larger than $8.3\ \mu\text{m}$ is below 1%. Over 30% of the particles fall in the size category of $1.4\ \mu\text{m}$ (Figure 4-18). Comparison of the data acquired with LLD with the results of laser blockade measurements must be done with care, as the first technique delivers volume distributions, whereas the latter is based on particle numbers.

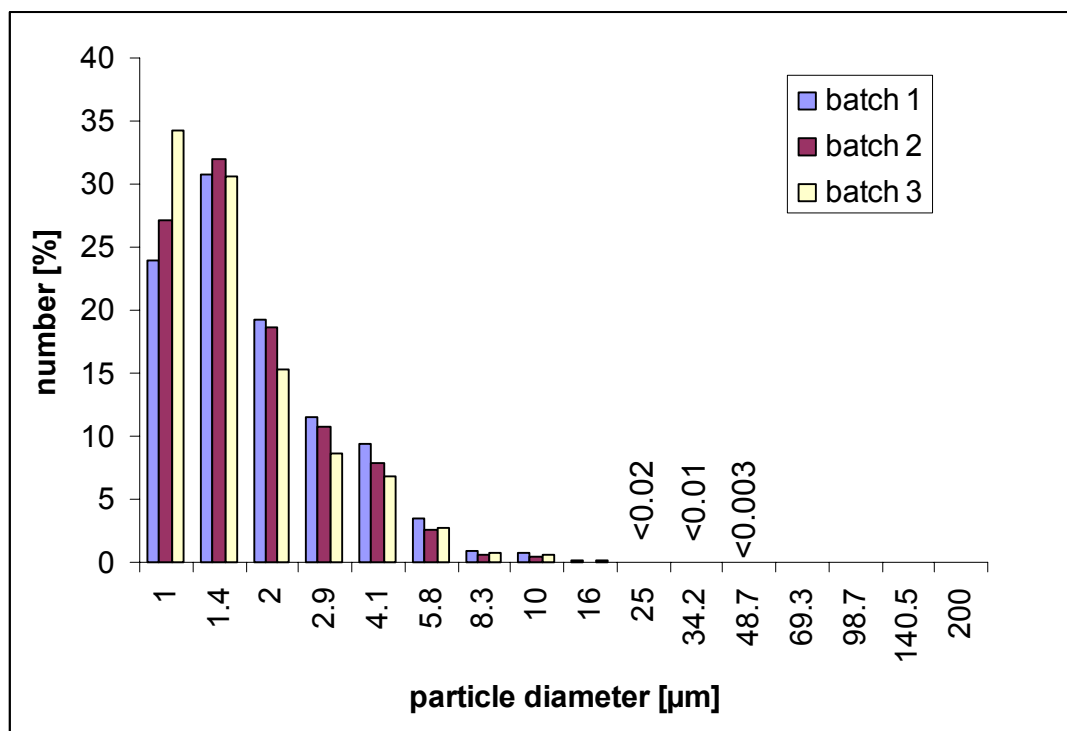


Figure 4-18: Particle number distributions of optimized formulation, measured with laser light blockage (PAMAS®)

4.1.2.5 Effect of Polymers and Surfactants

The variation of process parameters and the modification of the formulation did not allow the adjustment of a predetermined uniform particle size. The optimized formulation delivers small particles in the range of 1-2 µm, which tend to form larger collectives of loosely associated small particles. Two approaches are followed to gain tighter control over the particle size: (i) stabilization of these individual small particles and prevention of additional particle growth and (ii) formation of a homogeneous population of large and robust particles. In a small set of experiments, the effect of some selected additives on the particle size distribution was tested and evaluated by microscopic imaging (Figure 4-19). As BMP carries a positive net charge below its pI of 8.2, coprecipitation with polyanionic excipients is a promising approach to achieve larger particles [Dumitriu et al., 1998]. The polyanionic mucopolysaccharide hyaluronic acid is a major component of connective tissues such as the synovial fluid of joints, the scaffold within the cartilage and the vitreous fluid of the eye [Segura et al., 2005]. It is involved in a number of physiologic processes, such as cell hydration and differentiation, proteoglycan organization and wound healing (Kim 2001), and its safety is demonstrated by a number of commercially available products (e.g. Hyalart® for injection, DuoVisc® eye drops, HYA Ophtal® solution for intraocular use; <http://www.rote-liste.de>). Furthermore, derivatives based on hyaluronic acid were evaluated for their use as biomaterials due to their well

established biocompatibility [Hyun, 2004]. Another biopolymer with polyanionic properties at physiologic pH is sodium alginate. It is a well known agent in the food industry, and alginate matrixes are widely used for encapsulation of proteins [Gombotz et al., 1998]. Coppi et al. demonstrated complex formation between alginate and BSA at pH values below the isoelectic point of the protein [Coppi et al., 2002]. Finally, acidic gelatin (type B) was tested as polyanionic counterpart to build insoluble complexes with the basic rhBMP-2. The safety of gelatin, a decomposition product of collagen, is proved by its long clinical usage as plasma expander, in surgical materials and as ingredient in drugs [Tabata et al., 1998]. The natural occurrence of hyaluronic acid and gelatin in cartilage and bone related tissues make them particularly suitable for formulations targeting these areas. For the same reason, chondroitinsulfate was included. None of the polymeric excipients resulted in a tighter control over the microparticle size (Figure 4-19). The formulations containing chondroitinsulfate and gelatin seem to favor larger aggregates, but again a uniform distribution cannot be achieved.

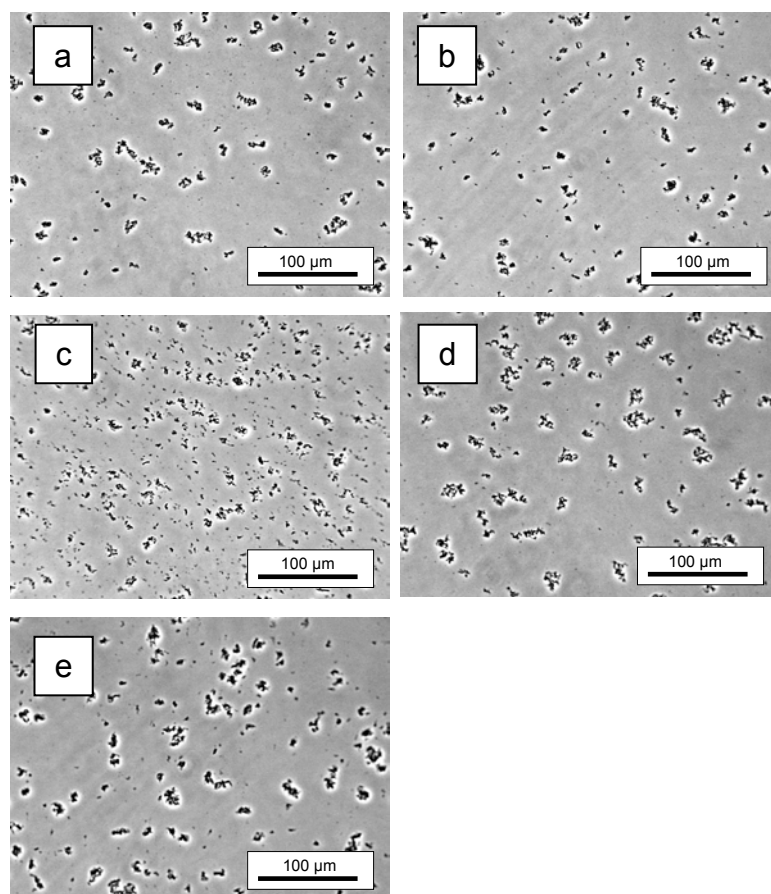


Figure 4-19: Phase contrast microscopic images of microparticles prepared with different concentrations of polyanionic biopolymeric additives: control (a), 0.1 % sodium alginate (b), 0.25 % hyaluronic acid (c), 1 % chondroitin-sulfate (d), 0.1 % gelatin (type B 175 bloom) (e)

The use of the two surfactants polysorbate 80 (polyoxyethylenesorbitan monooleat, Tween[®] 80) and poloxamer (Lutrol[®]F68) is based on the observation that larger associates are formed from an initial monomodal microparticle population (see 4.1.1.2). The surfactants might cover the hydrophobic surfaces of the primary particles, leading to minimization of attractive forces between individual microparticles, thus keeping them separated. Compared to the control and the polysorbate 80 formulation, the poloxamer tends to prevent association among microparticles. However, the overall distribution is not uniform, and larger associates are still present (Figure 4-20).

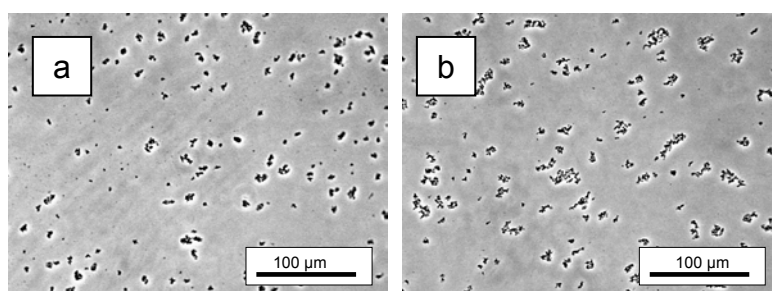


Figure 4-20: Influence of surfactants on particle separation: 1 % poloxamer (a), 1 % polyoxyethylenesorbitan monooleat (b)

To summarize, the addition of the tested excipients has only minor influence on the appearance of the microparticles and do not allow a tighter control of the particle distribution.

4.1.2.6 Gel Formulations

The observation that the large particle fraction consists of loosely associated smaller ones led to the idea to separate them by slight shear forces and to prevent reassembling of single microparticles by increasing the viscosity of the dispersant. As Povidon K17, a low molecular weight polyvinyl pyrrolidone with approval for injectable products, only marginally increases the viscosity even at high concentrations of 40 % (w/v), its high molecular derivate Kollidon[®] 90 was chosen as a model thickening agent. Figure 4-21 shows microscopic images of formulations containing different amounts of Kollidon[®] 90. Up to 10 % (w/v) gelling agent, the images of the formulations still show distinct agglomerates. 12.5 % are sufficient to keep the microparticles separated. The highest tested concentration of 15 % did not show further improvement (Figure 4-21). Viscosity measurements suggest Newton-like behavior, with 24 mPa s for 5 %, 129 mPa s for 10 %, 244 mPa s for 12.5 % and 443 mPa s for the 15 % gels.

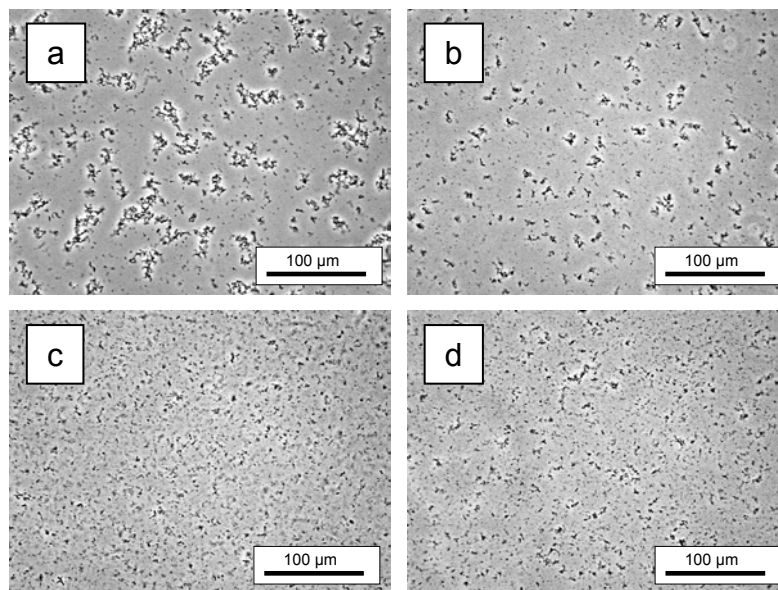


Figure 4-21: *rhBMP-2 microparticles suspended in formulations with different concentrations of Kollidon® 90: 5 % (a), 10 % (b), 12.5 % (c), 15 % (d)*

Due to the increased viscosity, laser light diffraction measurements were difficult to perform, as air bubbles were introduced during sample preparation which would be falsely considered to be particles. For the same reason, laser light blockade measurements are not suitable. By visual inspection, the formed microparticle suspension appears to be homogeneous. It could be shown that the approach of marginal shear forces caused by simple mixing in combination with increase of viscosity is suitable to separate and stabilize the primary particles. Furthermore, the release of rhBMP-2 from microparticles incorporated in a gel might be further prolonged, which would be advantageous. The high molecular weight polymer Kollidon®90 only serves as a model thickening agent. For a commercial product other biodegradable and approved biopolymers e.g. cellulose derivatives might be preferable. With a viscosity of 224 mPa s for the 12.5 % gel, syringeability should still be given.

4.1.3 Scanning Electronic Microscopy

Imaging of suspended rhBMP-2 microparticles has proven to be afflicted with a number of difficulties. Standard microscopy fails probably due to the marginal differences in the diffraction index between the highly hydrated protein particles and the dispersant water. For the same reason, techniques based on laser light reflection are considered to be unsuitable. With phase contrast microscopy, the hurdle of low diffraction index differences can be overcome. However, this technique is critical as shear forces during the sample preparation disturb the original particle size and geometry (Figure 4-17). AFM is not suitable, since the high resolution is thought to deliver macroscopic details of the particle surface rather than an overview of the whole microparticle. Consequently, the

microparticles were investigated with Environmental SEM, a modified SEM technique which allows the imaging of samples under adjustable conditions of relative humidity without previous blending of the sample with gold. As this technique can only visualize solid surfaces which are not submersed in water, a highly concentrated microparticle suspension was prepared and by the reduction of the pressure at constant temperature the water was removed, uncovering the microparticles. The removal of the liquid causes the microparticles to build up a dense layer of particles sticking together (Figure 4-22a). Furthermore, a spontaneous formation of spheres can be observed. Apart from this artifact formation, an initial particle size of approx. 1-5 μm , with an almost spherical particle size might be guessed from the images (Figure 4-22a,b).

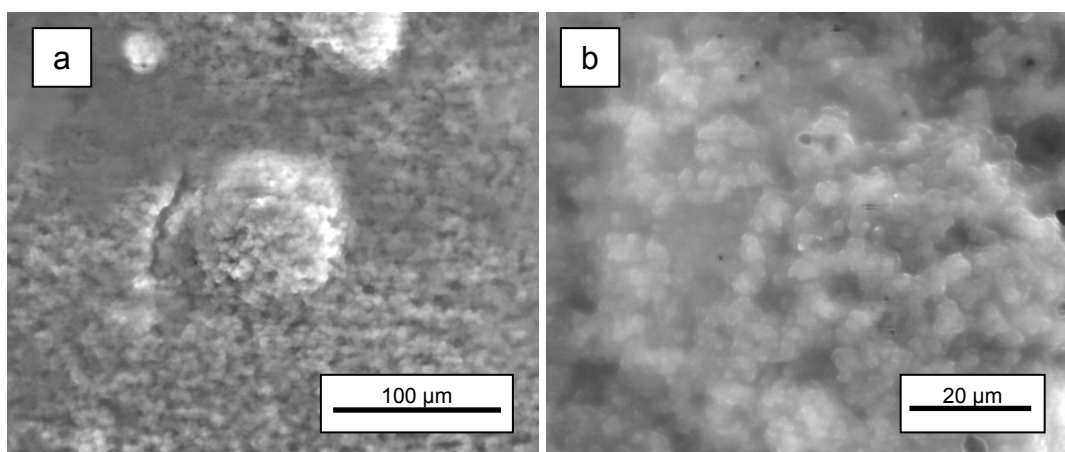


Figure 4-22: ESEM images of formulation at 800 (a) and 3000 (b) magnification

Overall, ESEM is not suitable to visualize the microparticles in the aqueous environment. However, the spontaneous formation of spherical particles, which is observed as a consequence of the water removal, might also occur during lyophilization of highly concentrated suspensions, thus explaining the shift in particle size. Furthermore, it underlines the tendency of the microparticles to stick together and form larger aggregates.

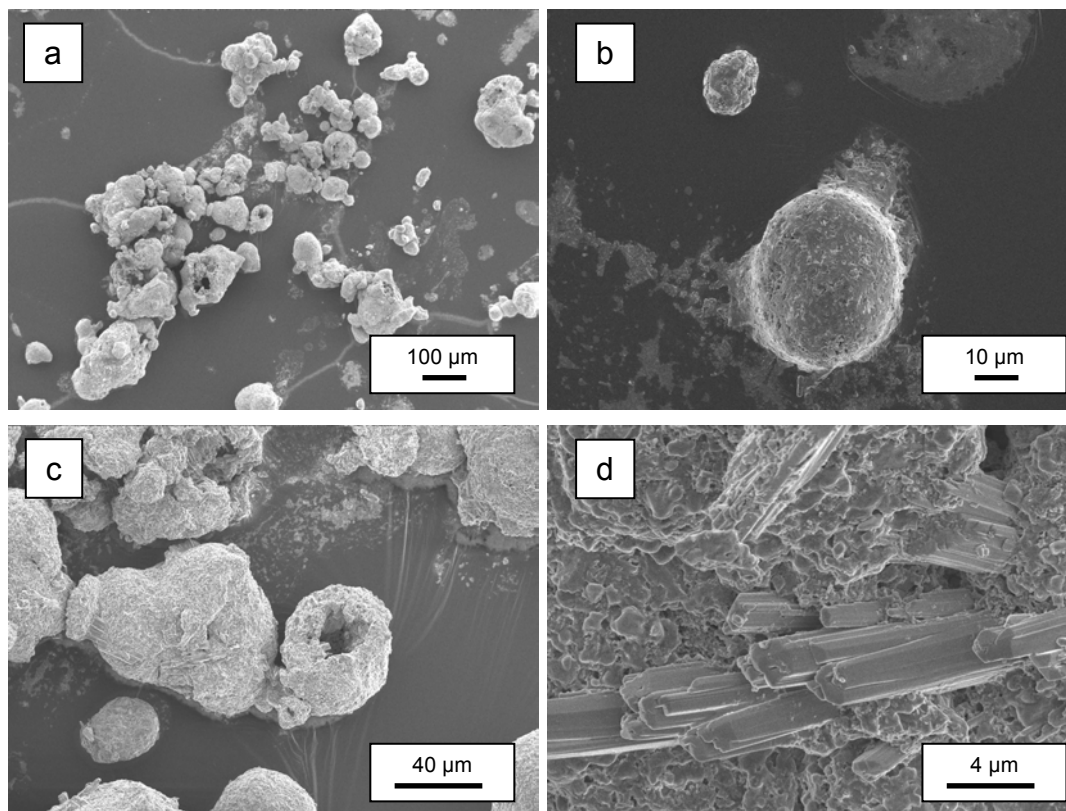


Figure 4-23: SEM images of precipitated microparticles after lyophilization at increasing magnification (a-d)

Images of freeze dried microparticles visualized with classic SEM are given in Figure 4-23. They show a rather heterogeneous particle distribution, with sizes partially exceeding 100 μm. Although care was taken to preserve the distribution present in the aqueous protein suspension (shock-freezing by submersing into liquid nitrogen) the large particles are supposed to be the consequence of the drying process (Figure 4-23a), as already indicated in the ESEM images. Beside these artifacts, particles of approx. 10 μm and 30-40 μm are visible, which is in good correlation to the results of laser light diffraction measurements (Figure 4-23b). Higher magnification uncovers a rough surface of the associates (Figure 4-23c). The crystalline structures seen at the highest magnification in Figure 4-23d are supposed to be inorganic salt, whereas the amorphous structures dominating the large particles were build up by small individual primary protein particles with sizes of approx. 1 μm.

4.1.4 Mechanistic Studies on Particle Formation with PCS

To gain insight further into the initial particle formation process during precipitation and the underlying mechanism, PCS measurements were performed. Standard formulations could not be directly measured as the suspensions were too concentrated to be measured without further dilution and the sizes of the formed microparticles exceed the measuring range. During the

precipitation process of rhBMP-2, both the pH and the ionic strength are shifted. Consequently, particle formation can be induced (i) by the pH shift, which would suggest an isoelectric precipitation mechanism, (ii) by the increase of the ionic strength, correlated to a salt induced precipitation mechanism, or (iii) by a combination of both. To differentiate between these mechanisms, experiments were performed analyzing both the precipitation behavior caused by solely shifting the pH under otherwise constant ionic strength and by an increase of the ionic strength at constant pH.

The ionic strength of an acidic protein solution (pH = 3.0) was increased by stepwise addition of KCl and monitored with PCS for aggregates. At a high protein concentration of 5.0 mg/ml, up to an ionic strength of approx. 25 mM, an effective diameter of 5.8 nm can be obtained. At 91 mM, an increase of the effective diameter to 11 nm indicates the beginning of molecule association. A further increase in ionic strength to 200 mM led to the formation of insoluble particles with sizes exceeding the resolution power of PCS (Table 4-2). After reduction of the protein concentration to 2.0 mg/ml (the starting concentration of the protein stock solution for precipitation experiments) no hints for precipitation can be detected with PCS over the tested ionic strength range, even at values exceeding the target of 154 mM (data not shown). Consequently, no precipitation would be expected at even lower concentrations, e.g. the usually employed precipitation concentration of 1 mg/ml and pH 3.0.

Table 4-2: Influence of ionic strength on particle formation at pH 3.0 and high protein concentration of 5.0 mg/ml

#	pH	ionic strength [mM]	effective diameter [nm]	polydispersity
1	3.0	24.3	5.8	0.187
2	3.0	91	11.0	0.237
3	3.0	200	3071.8	0.273

In general, a final protein concentration of 1 mg/ml was targeted for microparticle generation. Consequently, the influence of pH was analyzed at this concentration. The influence of the ionic strength was tested by measuring both low (without KCl) and at high levels (adjusted with KCl). The pH was increased by stepwise addition of a 0.1 M NaOH solution.

In the samples without KCl supplementation, pH ranges of 3.0 to 5.4 did not lead to detectable protein association. A very narrow monomodal distribution with an average size of 8.6 nm can be found. At pH 6.5, particle association occurs, leading to a substantial increase of the polydispersity index and a moderate increase of the effective diameter. Higher pH values lead to sizes exceeding the upper limit of the resolution of PCS (Table 4-3).

Table 4-3: *pH-shift at low Ionic strength and a protein concentration of 1.0 mg/ml rhBMP-2*

#	pH	ionic strength [mM]	effective diameter [nm]	polydispersity
1	5.33	0	8.6	0.094
2	6.49	0	11.6	0.245
3	8.54	0	1521.6	0.265

In the precipitation experiments supplemented with potassium chloride (I=130 mM) stable protein size data up to a pH of 4.2, and comparable parameters for the polydispersity index and the effective diameter to the approach without KCl were obtained. An additional minimal pH increase of approx. 0.4 units extremely pushes both the effective diameter and the polydispersity index to higher values. After a continued addition of NaOH to a pH value of 4.7, the particles formed exceed the valid detection range (Table 4-4).

Table 4-4: *pH-shift at high ionic strength and a protein concentration of 1.0 mg/ml rhBMP-2 in HCl (pH=3)*

#	pH	ionic strength [mM]	effective diameter [nm]	polydispersity
1	4.18	130	8.3	0.068
2	4.56	130	1293.7	0.207
3	4.72	130	2335.3	0.273

PCS measurements are suitable to determine the onset of particle formation, although it is was not possible to detect distinct intermediates reflecting a preferred aggregation pattern. At acidic pH values, protein concentrations below 2 mg/ml are not sufficient to cause precipitation by solely increasing the ionic strength up to a value of 334 mM. As compared to usually employed salting-out concentrations of several moles [Simpson, 2004b], the herein utilized amounts of KCl are quite low, suggesting an ion specific binding mechanism to be more likely than a classic salting-out process. This observation supports the finding of Abbatiello, who suggests an anion mediated bridging of rhBMP-2 molecules [Abbatiello et al., 1997]. Shifting the pH towards the isoelectric point already induces precipitation. Compared to samples without salt supplementation, the effect of the pH shift is more evident at an ionic strength of 130 mM, and particle formation is induced almost 2 units earlier. The results are in good agreement to the unusual solubility profile of rhBMP-2. In conclusion, both the pH and the salt contribute to the generation of microparticles by precipitation.

4.1.5 Summary

RhBMP-2 microparticles can be generated by controlled precipitation mimicking artificial physiological conditions. Particle formation is a time dependent process, and bimodal distributions are obtained after equilibration, with preferred sizes of 7 and 35 μm at maximum. Batch precipitation using turbulent mixing features good scaling-up properties. Both an increase of protein concentration and the batch volume have only minor effects on the particle distribution at equilibrium. Another helpful tool for scaling up is the micromixer[®], which allows laminar and continuous mixing of the precipitation solution with the protein solution. Similar bimodal distributions were obtained with this device compared to the turbulent batch approach, delivering particles in the range of 0.5 to 200 μm .

The recovery of microparticles after lyophilization of the microparticle suspension is generally possible. At final protein concentrations of 1 mg/ml, the underlying particle distribution can be preserved after resuspension. Freeze drying of highly concentrated suspensions shifts the particle size from approx. 35 μm to over 40 μm .

Optimization of the formulation leads to a reduction in the excipient number without an alteration of the particle distribution. Finally, the aqueous protein suspension is composed of rhBMP-2, phosphate buffer and potassium chloride. Three strategies were followed to gain a tighter control of the particle size, potentially leading to a monomodal distribution: (i) prevention of ongoing association of initially formed small particles by surfactants (ii) formation of larger particles by coprecipitation with polyionic macromolecules (III) separation of primary particles and prevention of particle growth by increasing the viscosity of the dispersant. Whereas the first two approaches did not lead to the desired result, the increase of the viscosity of the dispersant with a model thickener PVP has proven to be a potent tool to prevent the formation of larger associates, leading to a homogeneous particle suspension.

4.2 Protein Integrity

4.2.1 Process Stability of Precipitation

A major concern of a formulation based on precipitation is that the process may harm the protein. Alterations in the protein's secondary and tertiary structure, also referred to as denaturation, might be induced, which subsequently leads to instabilities such as adsorption to surfaces, aggregation or unwanted precipitation [Manning et al., 1989]. This might result in reduced bioactivity or increased immunogenicity [Wang, 1999]. Thus, even minimal amounts of aggregates can render a parenteral formulation unsuitable. Therefore, it should

be demonstrated weather precipitated microparticles can easily be redissolved, delivering the native, soluble and bioactive protein.

4.2.1.1 Aggregation

To show that the redissolved microparticle formulation does not show increased aggregate formation, microparticles were prepared by precipitation, equilibrated at 25°C and resolubilized after predetermined time intervals by adding the formulation buffer used for the lyophilized formulation. The aggregate content of the resolubilized samples was quantified by SEC and compared with the results of native, untreated rhBMP-2 reference material.

Redissolution resulted in clear solutions, with no turbidity indicating aggregates visible. SEC analysis did not reveal a significant increase in the high molecular weight species content as compared to unstressed rhBMP-2, even if the precipitate was allowed to age for 25 hours (Figure 4-24). Consequently, the coherence within the precipitated microparticles can be completely broken and the precipitation process did not induce the formation of aggregate-competent intermediates.

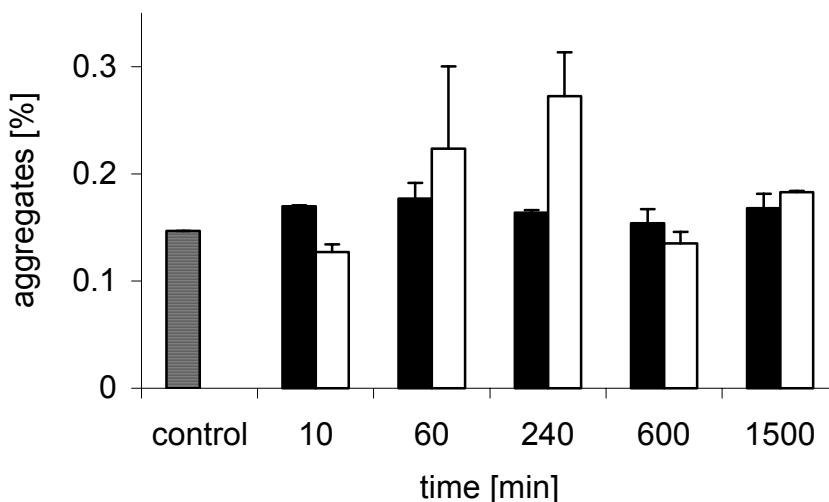


Figure 4-24: Soluble aggregates present before precipitation in the native soluble formulation (control) and after precipitation at 0.5 mg/ml rhBMP-2 (■) and 1.0 mg/ml rhBMP-2 (□) and subsequent resolubilization at denoted times in formulation buffer

4.2.1.2 Conformational Stability

FTIR provides a powerful tool to analyze the conformation of proteins. The amide I band is most commonly used to study protein structures since its band shape is very sensitive to the protein secondary structure. It is dominated by the signals of the carbonyl stretching vibration of the polypeptide backbone,

appearing in the spectral region between 1610 and 1700 cm^{-1} [Barth et al., 2002].

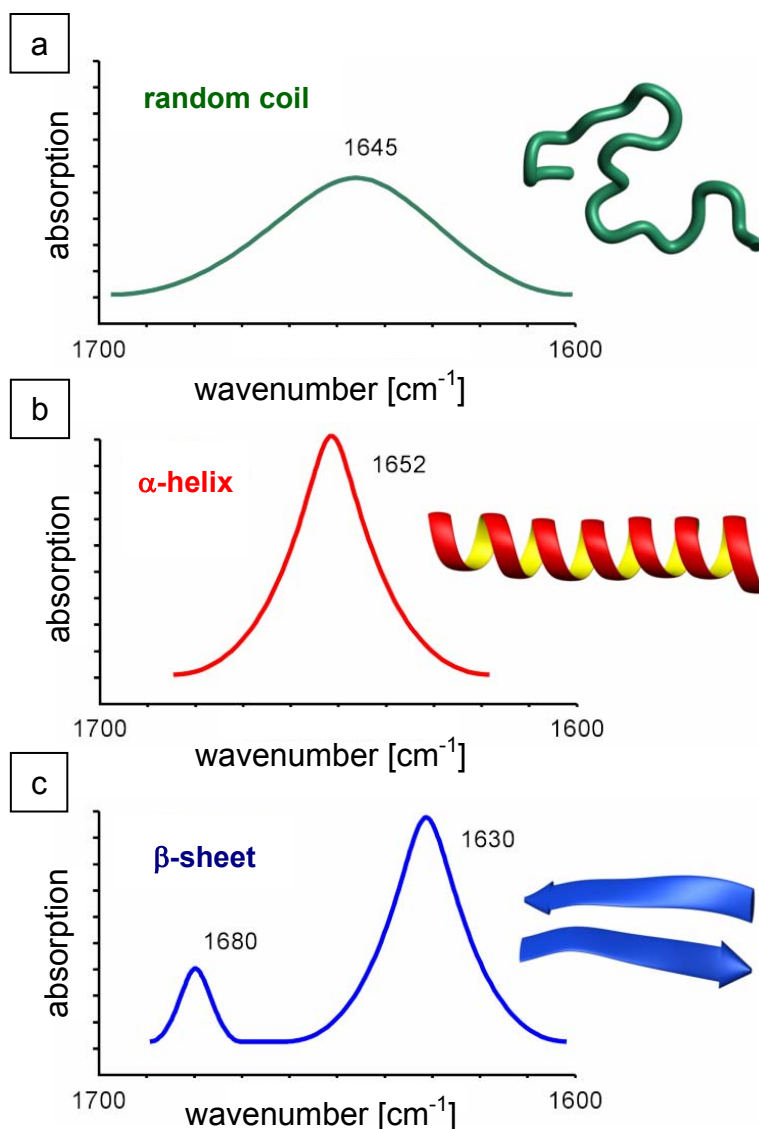


Figure 4-25: Idealized FTIR spectra of the amide I region of model proteins depicting (a) random coil structures, (b) α -helical structures, (c) β -sheet structures

The model spectra seen in Figure 4-25 depict band shapes of proteins solely featuring a single structure. In reality, proteins are more complex, and overlapping signals lead to a more or less broad and featureless amide I spectrum. This makes it difficult to identify discrete bands and to assign them to the adequate substructure. Therefore, resolution enhancement techniques are required. The advantage of second derivative calculation as compared to Fourier self-deconvolution as possible band-narrowing technique lies in the fact that there is no need to choose subjective parameters, and therefore is completely objective [Fabian et al., 2000]. Every band or shoulder in the original spectrum results in a negative band in the second derivative.

4.2.1.2.1 Analysis of Conformational Integrity

CD spectroscopy cannot be used to investigate the secondary structure of precipitated particles due to interfering light scattering [Kendrick et al., 1998]. In Raman spectroscopy, high fluorescence disturbs the measurement. The great advantage of FTIR lies in the fact that the physical state of the sample is less relevant, thus allowing insight into the secondary structure even in the precipitated state. To elucidate the influence of precipitation on the secondary structure of rhBMP-2, FTIR spectra before precipitation, in the precipitated state and after resolubilization were recorded and compared. Figure 4-26 shows normalized second derivative spectra of rhBMP-2 formulations featuring different sample histories: native rhBMP-2 (1 mM HCl), precipitated rhBMP-2 microparticles (physiological environment) and resolubilized microparticles (formulation buffer). The obtained spectra depict great overall similarity. All show the strong band at 1631 cm^{-1} , which can be assigned to β -sheet structure, and the weaker one at 1680 cm^{-1} , which is associated in the literature with β -turns. Furthermore, a band around 1658 cm^{-1} which is attributed to α -helical structure elements, and a band at 1646 cm^{-1} which reveals unordered structures can be identified [Barth et al., 2002, Dong et al., 1990, Susi et al., 1988]. As only minor differences in the intensities of some peaks are apparent, it can be concluded that no structural changes are induced by the precipitation process. The native secondary structure is maintained in the precipitated rhBMP-2 microparticles. Furthermore, precipitation is fully reversible, and the native structure is preserved after resolubilization. In the literature, additional proof for the integrity of proteins in the precipitated state can be found by Stratton and coworkers. They demonstrate for lactate dehydrogenase and α -chymotrypsin precipitated in a poloxamer gel that the native structure is maintained [Stratton et al., 1997]. Native-like secondary structure, measured by FTIR, was also found by Kendrick et al. for rhIFN- γ precipitated with PEG 8000. The authors outlined the difference between a destructive aggregation mainly caused by destabilizers directly influencing the conformation of the protein and salt induced precipitation based on the reduced solubility of the macromolecule due to the altered solvent [Kendrick et al., 1998]. The maintenance of the secondary structure in the precipitated state demarcates this kind of precipitation from non-native protein aggregation, where partly unfolded protein molecules (molten globules) are thought to be the reactive species responsible for protein assembly [Chi et al., 2003].

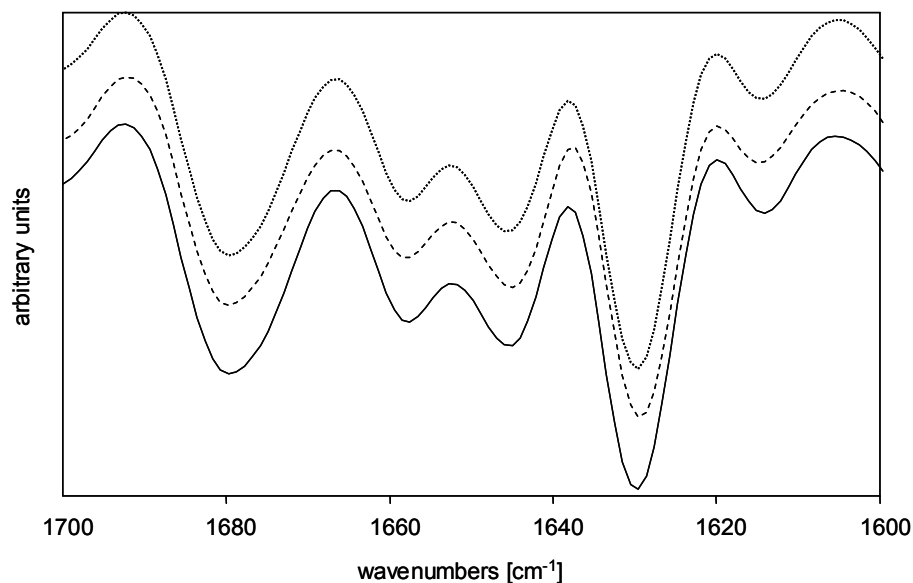


Figure 4-26: Area normalized, second derivative spectra of dialyzed (·····), precipitated (----) and resolubilized (—) rhBMP-2

4.2.1.2.2 Determination of Structural Composition via FTIR

Secondary structure element determination of native, liquid rhBMP-2 resulted in 9.5 % α -helix and 25 % β -sheet. Whereas the value for the α -helix is in good correlation to data from X-ray crystallography (9.5 vs. 8 % α -helix), the calculation for the β -sheet content varies considerably (25 % vs. 42 % β -sheet structure) [Scheufler et al., 1999]. This might be due to structural differences between the solved and the crystallized form of rhBMP-2 and the fundamental physicochemical differences between the techniques used.

4.2.1.2.3 Temperature Ramp of Precipitated and Redissolved Protein

Temperature ramps of both precipitated and resolubilized samples were performed and compared to address the question if possible variations in the secondary structure can be uncovered at higher temperatures. Figure 4-27 shows temperature induced changes in the secondary structure of precipitated microparticles. Up to 70°C, only continuous deviations in the intensities of the main bands compared to the previous temperature step appear, but significant changes in the curve patterns are absent. At 73°C, peak shifts that give evidence to a significant change in secondary structure become obvious. It is accompanied by clear losses of α -helical (1658 cm⁻¹) and β -turn structures (1680 cm⁻¹). Furthermore, a novel band at 1690 cm⁻¹, which can be assigned to intermolecular β -sheet structures, is formed [Dong et al., 1995]. At higher temperatures the band intensity at 1690 cm⁻¹ further increases and above 91°C the formation of an additional band at approx. 1622 cm⁻¹ is induced.

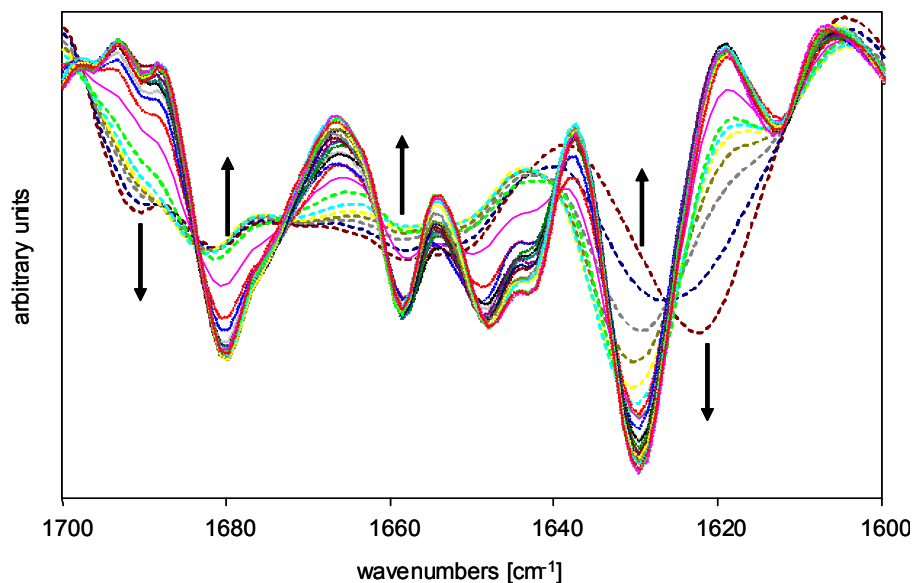


Figure 4-27: Second derivative, area normalized amide I spectra of temperature induced re/unfolding of precipitated rhBMP-2 microparticles; the arrows indicate the direction of intensity shift at wavenumbers of interest with rising temperatures from 25°C - 70°C (·····), 73°C (—), 76°C - 94°C (----).

Figure 4-28 illustrates temperature dependent re- and unfolding of resolubilized rhBMP-2 microparticles. In contrast to the precipitated material, the band contour between 1640 and 1680 cm^{-1} , which includes α -helical structures at 1658 cm^{-1} , is mainly preserved as the temperature is increased. However, the resolubilized sample also shows the formation of additional bands at 1690 and 1627 cm^{-1} .

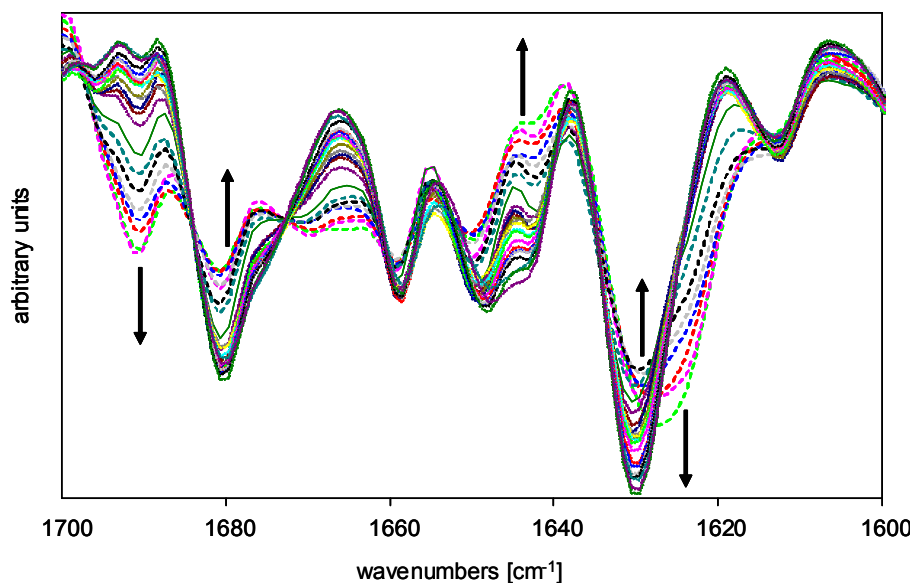


Figure 4-28: Second derivative, area normalized amide I spectra of temperature dependent re/unfolding of resolubilized rhBMP-2; the arrows indicate the direction of the intensity shift at wavenumbers of interest with rising temperatures from 25°C - 70°C (·····), 73°C (—), 76°C - 94°C (----).

The gradual intensity shift at 1642 cm^{-1} seen in both the precipitated (Figure 4-27) and the resolubilized (Figure 4-28) sample indicates a loss of β -sheet structures which are not completely resolved by band narrowing from the underlying unordered structures at 1645 cm^{-1} . Both samples show the formation of additional peaks at 1690 cm^{-1} and 1622 cm^{-1} (for the precipitated sample) and 1627 cm^{-1} (for the resolubilized sample) respectively. According to the literature, it is a common feature of thermally unfolded proteins to exhibit a low-frequency indicator band around 1620 cm^{-1} and a weaker high-frequency band around 1685 cm^{-1} , assigned to intermolecular antiparallel β -sheet structures. As these wavenumbers were determined in D_2O , slightly higher values will result in H_2O [Fabian et al., 2000]. Therefore, the change in band structure fits into the scheme of thermal unfolding. Interestingly, the observed structural losses were not accompanied with an increase in the peak at 1645 cm^{-1} representing unordered structures. The degree of loss of β -sheet structure (1630 cm^{-1}) in favour of antiparallel intermolecular β -sheet formation is more pronounced in the precipitated microparticles, and the α -helical structures are partially conserved in the resolubilized sample. The gradual overall shift of the intensities is explained by the conformational mobility of proteins and the assumption that not all protein molecules react to the altered conditions at the same time. Consequently, a loss of intensity at certain wavenumbers is caused by a structural loss of a certain population of protein molecules, whereas other molecules still exhibit the native conformation. With increasing temperatures, the balance between native and denatured protein molecules is further pushed into the direction of the denatured fraction.

To abstract, the alterations in the curve progressions of the amide I spectra are quite similar for both the precipitated and the resolubilized sample up to a temperature of 73°C and 76°C respectively. Up to these temperatures, no change in the secondary structure that could be attributed to the former precipitation process is detectable. At higher temperatures, heat-induced denaturation takes place. At these temperatures, the contribution of other parameters (e.g. the physical state of the samples: direct contact between protein molecules in the solid microparticles compared to soluble rhBMP-2 molecules) to the observed unfolding cannot be distinguished from the effect caused by potential structural changes. Even under the assumption that undetectable structural changes are induced during precipitation, the higher thermal resistance of the resolubilized sample at temperatures above 70°C as compared to the precipitated sample supports the hypothesis that these changes were completely offset after resolubilization.

4.2.1.2.4 Unfolding Temperatures Determined with ATR-FTIR

In the following, the transition temperature should be determined from the unfolding spectra. Chechin and co-workers use the intensity ratio decreasing to

increasing band (1618 cm^{-1} to 1650 cm^{-1}) to determine the transition temperature $T_{m(\text{spectroscopy})}$ from infrared spectroscopic measurements [Chechin et al., 1998]. In our studies, all bands with decreasing intensities show slight shifts in their maxima at higher temperatures, suggesting that they are not only due to structural losses. To estimate T_m from the temperature induced unfolding spectra, the intensity of the new arising band at 1690 cm^{-1} is plotted against temperature (Figure 4-29). Sigmoid curve fitting and differentiation deliver the point of inflection. The corresponding temperature at the inflection point is considered to be the transition temperature $T_{m(\text{spec.})}$. For the precipitated sample, $T_{m(\text{spec.})}$ was determined to be 75°C as compared to a slightly higher, but not significantly different transition temperature of 77.6°C for the resolubilized sample.

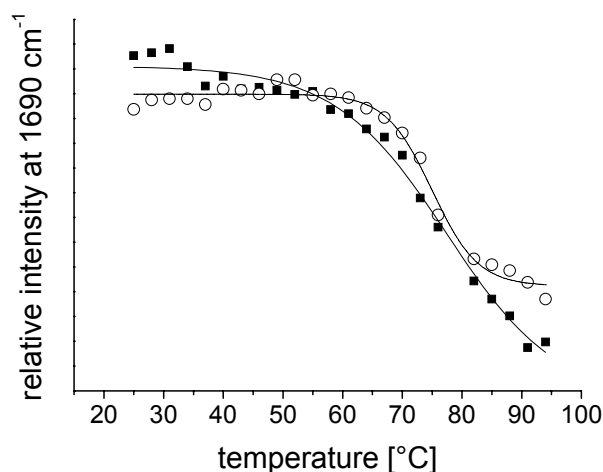


Figure 4-29: Transition temperatures of (O) precipitated and (■) resolubilized rhBMP-2 based on the intensity shift at 1690 cm^{-1} (sigmoid fit: $R2 = 0.990$ (—), $R2 = 0.988$ (·····))

To confirm the findings obtained with the spectroscopic approach, DSC measurements were performed to determine $T_{m(\text{cal.})}$ calorimetrically. It is well known from the literature that several factors such as formulation composition, pH, concentration and measuring conditions can affect $T_{m(\text{cal.})}$ of a given protein. At first, the influence of formulation, pH, and composition were investigated. It was demonstrated that samples containing between 1 and 5 mg/ml native rhBMP-2 in formulation buffer, $T_{m(\text{cal.})}$ is 64.3°C without statistically significant differences. Subsequently, all measurements were performed at 2 mg/ml to avoid any possible influence on $T_{m(\text{cal.})}$ due to concentration effects. As the controlled precipitation of rhBMP-2 to form microparticles is partly caused by an increase of pH to physiological values, the influence of pH on the transition temperature of rhBMP-2 is of special interest. With an increase of the pH from 3.0 to 5.5, the transition temperature rises from 48.1°C to 70.2°C

(Figure 4-30). In parallel to the T_m shift, the calorimetric enthalpy increases (Table 4-5).

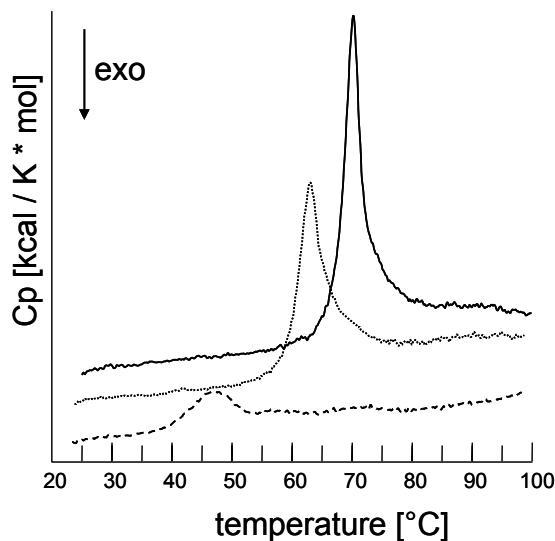


Figure 4-30: Thermograms of rhBMP-2 in formulation buffer at different pH values: 3.0 (----), 4.5 (.....), 5.5 (—).

The observed T_m shift can be explained based on repulsive forces present in the molecule. RhBMP-2 is a basic protein with an isoelectric point of 8.5. At low pH values, the carboxylic acid side chains are preferentially uncharged, whereas the dominating fraction of basic groups carries positive charges. This is energetically unfavorable due to repulsive forces. With increasing pH values, the net positive charge diminishes and so do the repulsive forces, leading to an increase in T_m .

Table 4-5: Transition temperatures and calorimetric enthalpies of different rhBMP-2 formulations

sample description	pH	T_m (calorimetry) [°C]	calorimetric enthalpy [kcal/mol]
soluble rhBMP-2 in 1 mM HCl	3.0	54.8 ± 0.05	107.2 ± 7.0
resolubilized microparticles in 1 mM HCl	3.0	54.6	103.4 ± 0.7
soluble rhBMP-2 in formulation buffer	4.5	64.3	107.0 ± 1.6
resolubilized microparticles in formulation buffer	4.5	63.9 ± 0.05	86.7 ± 1.3
precipitated microparticles in physiologic phosphate buffer	7.4	70.0 ± 0.05	165.1 ± 4.4
soluble rhBMP-2 in formulation buffer	3.0	48.5 ± 0.05	52.5 ± 1.9
soluble rhBMP-2 in formulation buffer	5.5	70.2	126.0 ± 4.5

The excipients also affect the transition temperature. For example, two different formulations of the same pH vary significantly in their unfolding behavior. Whereas rhBMP-2 in 1 mM HCl shows a T_m of 54.8°C, the T_m is more than 6°C lower in formulation buffer containing sucrose, glycine, glutamic acid sodium chloride and polysorbate 80 (both at pH 3.0). Sucrose is known to stabilize the native protein structure, and an increase in T_m is observed for lysozyme in the presence of sucrose in a concentration dependant manner [Cueto et al., 2003]. The effect of amino acids on T_m of a given protein is more sophisticated, and contradictory statements can be found in the literature. Whereas increased thermal stability is reported for lysozyme, no effect on the T_m of bovine α -lactalbumine is seen for a number of amino acids [Sabulal et al., 1997]. An increase of T_m by increasing the NaCl concentration is reported for Interleukin-1 receptor [Remmele, Jr. et al., 2000]. Thus, comparison and interpretation of T_m determined by DSC must take the pH and excipient conditions of the protein into consideration.

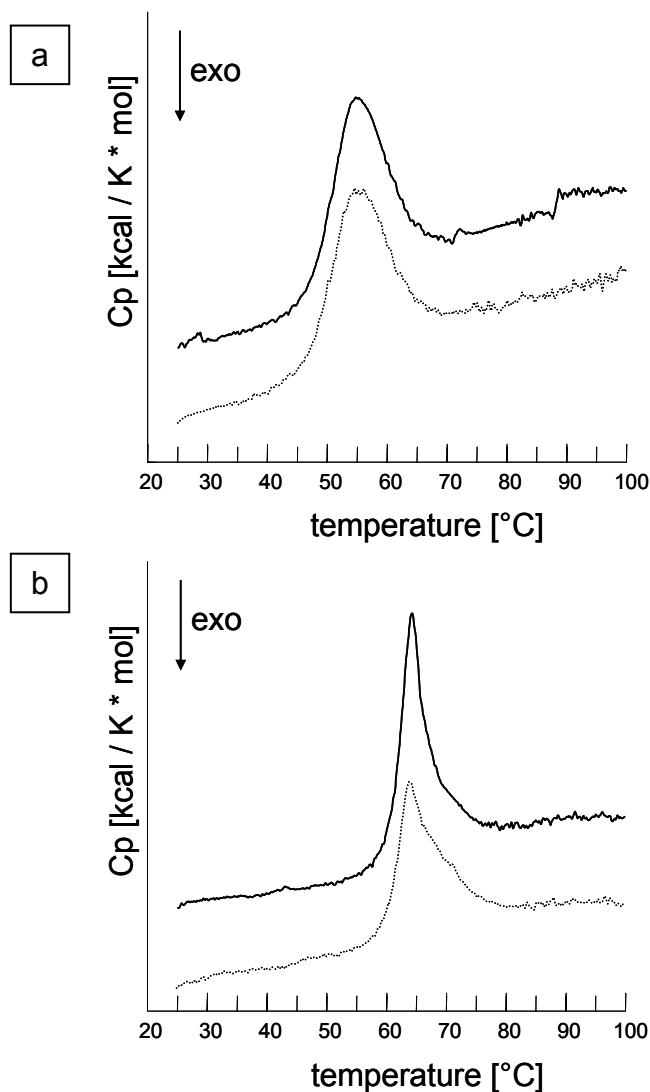


Figure 4-31: DSC curves of rhBMP-2 before precipitation (—) and after dissolution of the precipitate (·····) in 1 mM HCl (a) and in formulation buffer pH 4.5 (b)

The transition temperatures of rhBMP-2 before precipitation in aqueous HCl (pH 3.0) and after precipitation, solubilization and dialysis into the same formulation are nearly identical (54.8°C vs. 54.6°C, Figure 4-31a). In addition, rhBMP-2 precipitated, redissolved and dialyzed against formulation buffer results in the same T_m as the starting material in the same buffer (64.3°C vs. 63.9°C, see Figure 4-31b). These data strongly support the finding that the precipitation process itself does not induce any permanent changes and is fully reversible. Further increase of pH, phosphate and KCl concentration leads to rhBMP-2 precipitation and a further increase in the transition temperature to 70°C (Figure 4-30). Thus, the precipitated state of the protein goes hand in hand to improved thermal stability. In the precipitate, the associated protein molecules interact in a stabilizing manner with each other. To unfold their native structure, higher temperatures are necessary. A closer look at the calorimetric enthalpy further

supports the hypothesis that precipitation is reversible. Within the accuracy of the method, the calorimetric enthalpies of the 1 mM HCl samples are nearly identical (107.2 ± 7.0 kcal/mol vs. 103.4 ± 0.7 kcal/mol). For the rhBMP-2 samples analyzed in formulation buffer, the difference is more pronounced (107.0 ± 1.6 kcal/mol vs. 86.7 ± 1.3 kcal/mol). In general, calorimetric enthalpies below 100 kcal/mol indicate weak transitions, and results based on integration of such transitions were accompanied by higher errors. Therefore, interpretations should be done with care [Sanchez-Ruiz, 1995]. Nevertheless, the precipitated formulation exhibits the highest value in calorimetric enthalpy of all samples tested, arguing for its enhanced stability.

4.2.1.2.5 DSC vs. ATR-FTIR

The unfolding temperature of precipitated rhBMP-2 calculated from the intensity shift of the ATR-FTIR temperature ramp is slightly higher than the corresponding value determined by DSC (Table 4-6). In the resolubilized samples, the more pronounced difference is a consequence of the sample preparation. Excipients of the precipitation process (phosphate buffer salts and KCl) were not removed by dialysis in the resolubilized ATR-FTIR sample. Consequently, the higher pH and the presence of phosphate led to the higher $T_{m(\text{spec.})}$. Minor differences between T_m acquired with ATR-FTIR and DSC are expected, as there are fundamental differences between the techniques in the way of data analysis and the way of sample heating. In the spectroscopic approach, the sample is equilibrated at the measuring temperature and kept constant during the measurement with an effective heating rate of approx. $0.7^\circ\text{C}/\text{min}$, whereas the sample is heated continuously in the calorimeter. Furthermore, $T_{m(\text{spec.})}$ is calculated as the temperature where the rate of intermolecular β -sheet formation is maximal (inflection point of sigmoid fit, Figure 4-29), whereas the temperature of maximal heat flux (at peak maximum in the thermogram, Figure 4-30) is considered to be $T_{m(\text{calorimetry})}$.

Table 4-6: Comparison of unfolding temperatures of rhBMP-2 formulations determined with ATR-FTIR and DSC

	T_m (spectroscopy) [$^\circ\text{C}$]	T_m (calorimetry) [$^\circ\text{C}$]
precipitated rhBMP-2	75.0	70.0
resolubilized rhBMP-2	77.6	63.9

4.2.1.3 Bioactivity of Redissolved Microparticles in Cell Culture

Further evidence for the integrity of rhBMP-2 after redissolution of precipitated microparticles derives from cell culture experiments. The bone marrow stromal cell line W-20-17 shows increased alkaline phosphatase activity after incubation

with bioactive rhBMP-2 in a dose-responsive manner [Blum et al., 2000, Thies et al., 1992]. The inducible enzyme converts a non-colored substrate into the colored p-nitrophenol, which can be quantified by optical density reading at 405 nm. The OD reading is transferred into potency by the use of a reference with an assigned value. The specific activity is calculated from the potency by dividing by the rhBMP-2 sample concentration used for enzyme induction. Figure 4-32 shows the results for rhBMP-2 which was immediately redissolved after precipitation. With a specific activity of 5.02×10^5 Uwho/mg for the sample and 5.08×10^5 Uwho/mg for the control, full bioactivity of the sample is demonstrated.

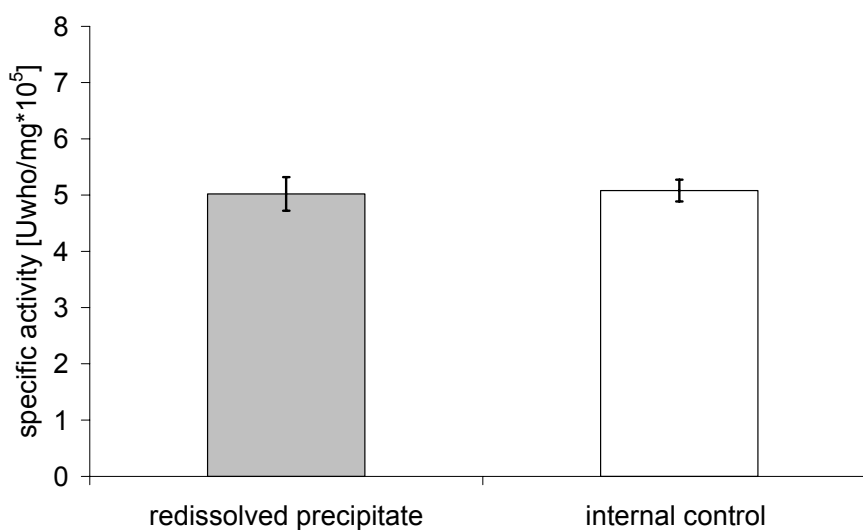


Figure 4-32: Specific activity of rhBMP-2 after precipitation and subsequent redissolution, compared to a native rhBMP-2 standard

4.2.1.4 Summary

Dissolution studies of precipitated microparticles demonstrate that the precipitation process did not induce the formation of higher amounts of aggregates. Furthermore, it could be shown by ATR-FTIR that the secondary structures of native liquid, precipitated and resolubilized rhBMP-2 are essentially identical. Analysis of thermal unfolding after precipitation and reolubilization did not reveal any conformational alteration induced by the precipitation process. DSC measurements further confirmed these findings. No change in the transition temperature and process could be observed after precipitation and redissolution. Further evidence for the proteins integrity is provided by cell culture experiments, as no loss in bioactivity can be observed in resolubilized rhBMP-2 microparticles. Consequently, a precipitation process mimicking physiological conditions did not harm rhBMP-2 and is fully reversible. Thus, controlled precipitation is suitable to generate microparticles which can deliver native, active and intact rhBMP-2.

4.2.2 Storage Stability of rhBMP-2 in Microparticles

4.2.2.1 Study Design

Besides the exploitation of precipitation for the generation of relatively pure microparticles, protein precipitates might also serve as a tool to prepare highly concentrated formulations and as alternative to frozen or lyophilized storage, provided that the formulation is sufficiently stable. To address this issue and to determine storage conditions at which stability can be maintained, the influence of time and temperature on precipitated rhBMP-2 was evaluated. Furthermore, the benefit of a supplementary freeze drying step on protein stability of the precipitated formulation should be determined. The formulation commercially available as a lyophilisate serves as “gold standard”, and the pre-lyophilized formulation was included as reference for the aqueous dispersion. The precipitated formulations contain 1 mg precipitated rhBMP-2 dispersed in 100 μ l aqueous, phosphate buffered solution (50 mM, pH 7.4), supplemented with KCl to physiologic ionic strength (154 mM). 1 ml reference formulation contains 2.5 mg rhBMP-2, 0.5 % sucrose, 2.5 % glycine, 5.0 mM L-glutamic acid, 5.0 mM sodium chloride and 0.01 % polysorbate 80 at a pH of 4.5. The samples were either freeze dried or preserved with 0.02 % sodium azide. A short overview of the study design, with images of the resulting formulations is given in Figure 4-33. The “liquid”, i.e. non-lyophilized aqueous precipitated dispersion delivers a thin, milky layer at the bottom of the vial, covered with residual liquid after centrifugation and removal of the supernatant. Subsequent lyophilization results in a dry and fragile flat disc. The “liquid” reference is a clear solution, and freeze drying of this formulation delivers a nice and fluffy lyophilization cake. Storage was carried out at -20, 4-8°C (in the following referred to 5°C), 25°C and 40°C for up to 10 months. The freeze dried samples were pre-closed with stoppers in the lyophilization chamber under vacuum. The liquid samples were prepared and closed at ambient conditions. After sealing, the sample vials were flanged and placed in storage.

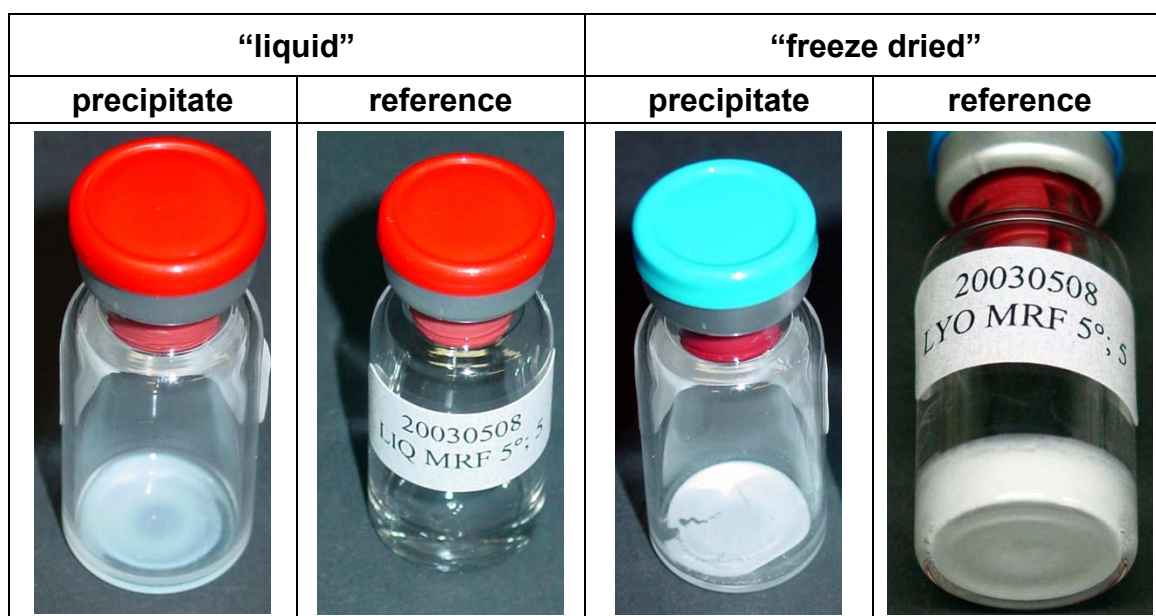


Figure 4-33: Study design with images of resulting formulations

4.2.2.2 Oxidation

Among the variety of chemical instabilities [Goolcharran et al., 2000], rhBMP-2 is known to be susceptible to oxidation and isomerization. Monitoring of these major degradation pathways was performed with peptide mapping, a method which has recently entered the European Pharmacopoeia.

Oxidation of amino acid side chains is a common degradation seen in protein pharmaceuticals during storage. This chemical modification can induce changes in the structure that might alter bioactivity. Among the potential points of attack (Met, Cys, His, Trp and Tyr), Met is most susceptible to oxidation, as it can even be oxidized by atmospheric oxygen. Under these mild conditions, Met sulfoxide is the resulting degradation product. More potent oxidants are required to obtain Met sulfone [Manning et al., 1989]. RhBMP features two Met amino acids, Met³⁷¹ and Met³⁸⁸, which are both subject to oxidation. By peptide map, oxidation of Met³⁷¹ can be monitored, and the sensitivity of the formulations listed in Figure 4-33 at this site was evaluated.

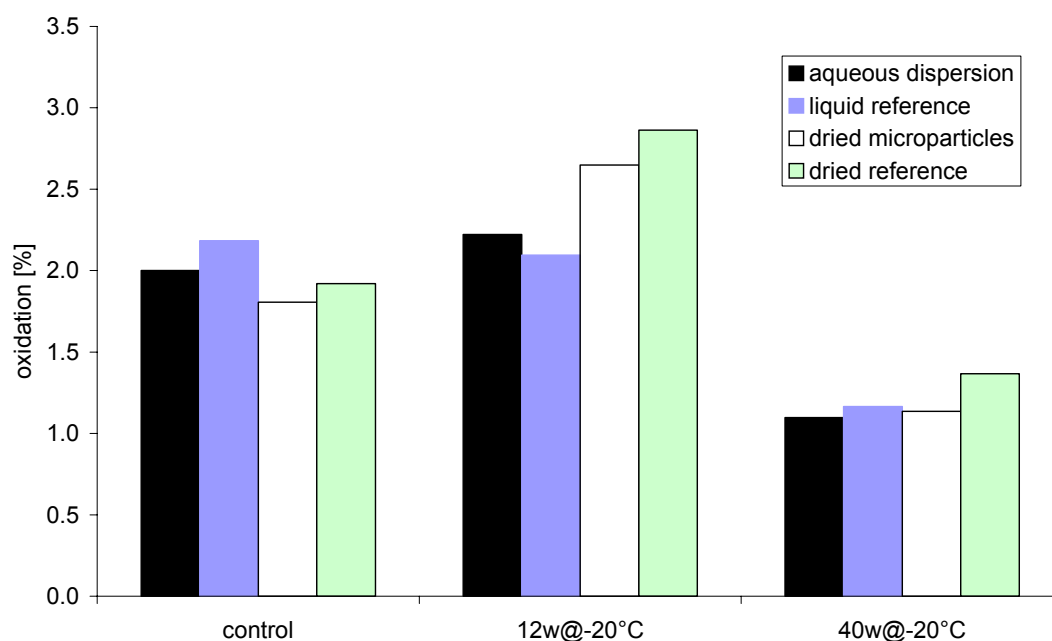


Figure 4-34: Oxidation of rhBMP-2 in different formulations after preparation (control), storage for 12 weeks and 40 weeks at -20°C

The effect of refrigeration and storage at -20°C to minimize oxidation was tested only with a limited number of samples. The results are depicted in Figure 4-34. The liquid reference prepared by simple dilution of protein bulk material already shows approx. 2 % oxidation, marking the starting level for oxidation in the bulk product. The controls show similar levels for oxidation, calling for the maintenance of protein stability during the preparation procedure. After a slight increase in the values measured for 12 weeks storage, the determined amounts for oxidation decrease in the samples stored for 40 weeks. This observed decline is thought to mirror the accuracy of the assay, with variations of 1 to 2 % to be taken into account for interpretation. All samples stay well below 3 % of Met³⁷¹ oxidation, suggesting that refrigeration at -20°C is suitable to prevent or at least minimize this degradation pathway. Within the accuracy of the measurement, no differences can be detected among the different freeze-dried and the liquid formulations.

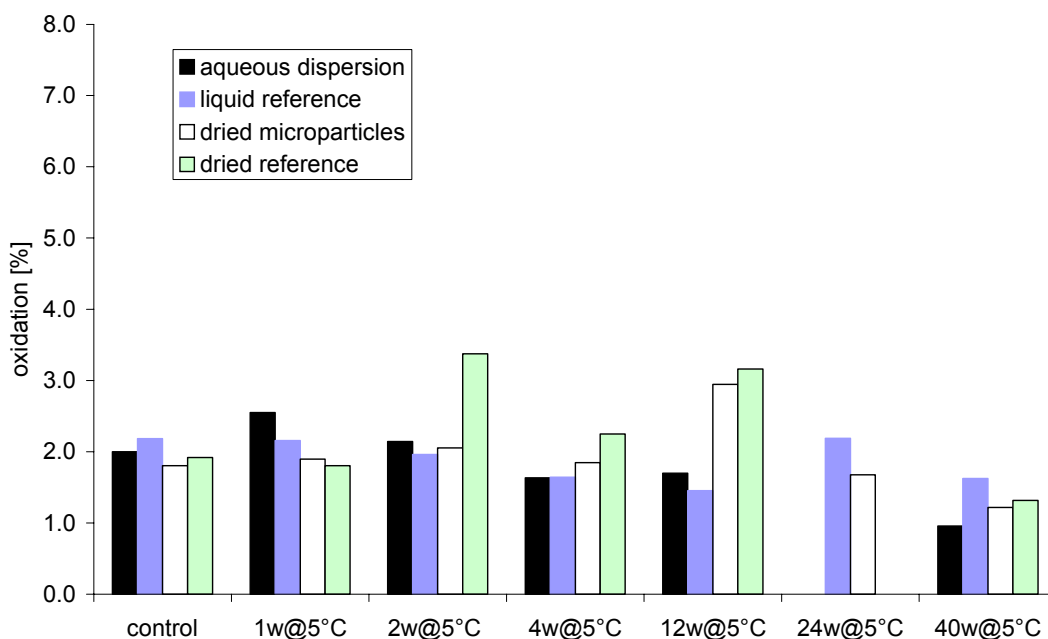


Figure 4-35: Oxidation over time in different rhBMP-2 formulations stored at 5°C

At 5°C storage, only minor differences in the oxidation levels were measured over time. However, the data do not reveal a clear trend, suggesting that the observed variations are inherent to the method. Consequently, no significant oxidation can be detected under the applied storage condition (Figure 4-35).

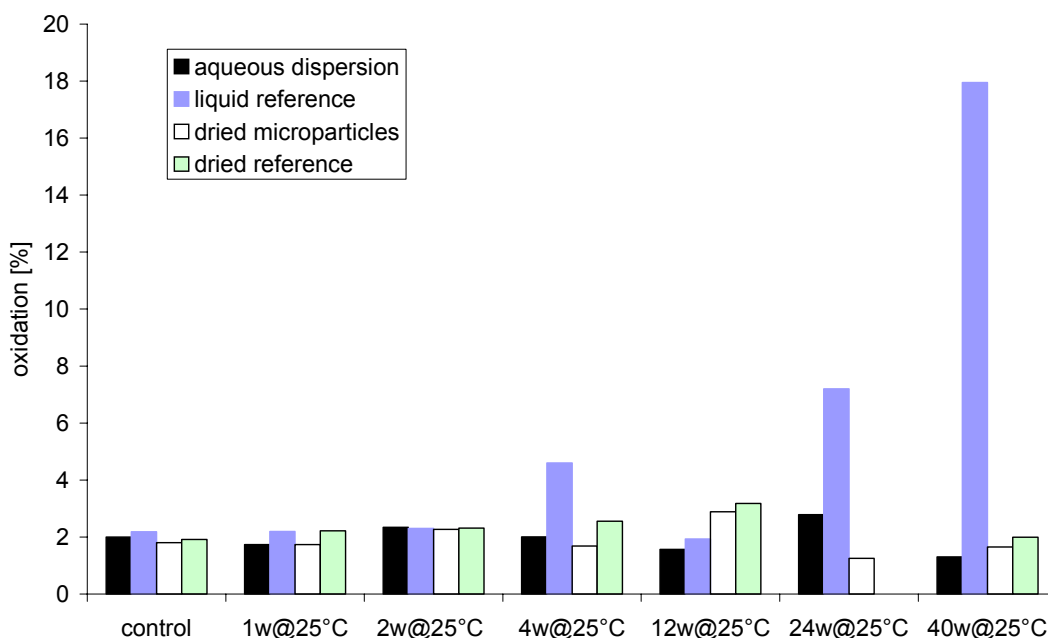


Figure 4-36: Oxidation over time in different rhBMP-2 formulations stored at 25°C

At 25°C, degradation due to oxidation was monitored over 10 months (Figure 4-36). Within the first two weeks, all formulations show acceptable low levels.

After storage for one month, the liquid reference clearly shows oxidation, and ongoing degradation led to a loss of almost 20 % within the observation period. In contrast, the “liquid”, precipitated formulation is stable, with oxidation levels comparable to the dried formulations, not exceeding 4 %. Within the dried formulations, no increase in oxidation can be observed over time.

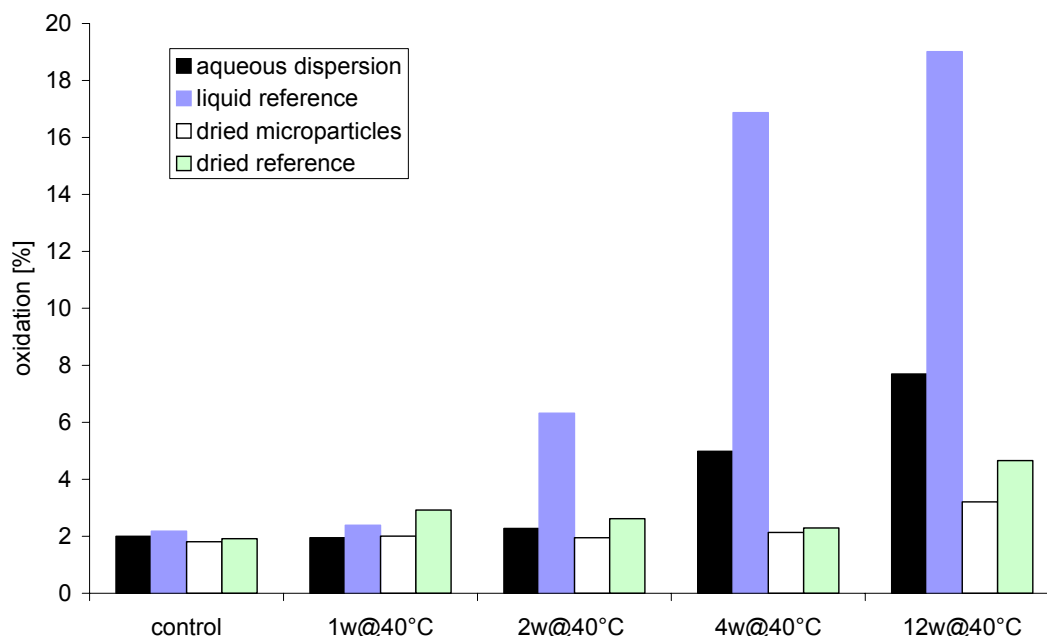


Figure 4-37: Oxidation over time of different rhBMP-2 formulations stored at 40°C

At 40°C, the ability of both liquid containing formulations to resist oxidation is considerably reduced, as depicted in Figure 4-37. Compared to the starting level and the levels for storage at lower temperatures, increased oxidation can be assumed in these formulations already after one week. A trend to higher resistance towards oxidation can be attributed to the aqueous dispersion as compared to the liquid reference. Superiority of the freeze dried formulations, both of the precipitated formulation and of the lyophilized reference compared to the aqueous dispersion becomes significant after 2 weeks. Whereas non-dried formulations hit the self-set specification of 5 % already at this time point, the freeze dried formulations stay below this level over the entire observation period. Among the dried systems, the approach based on precipitation shows slightly lower oxidation levels than the “gold standard”, the lyophilized product, affirming the trend already seen at 25°C.

Thus, the formulations show increasing resistance to oxidation in the order liquid reference < liquid precipitated < dried reference < dried precipitated. Within the liquid formulations, higher oxidation rates were found at increased storage temperatures. A storage temperature of 25°C is sufficient to gain acceptable low levels for oxidation in the precipitated formulation. The liquid

reference requires lower temperatures (5°C) to stay below a tolerable oxidation level over the entire observation period. The increased oxidation resistance of the precipitate might be a consequence of limited access of oxygen to the relevant methionine residue buried within the precipitate. As expected, removal of water by lyophilization further improves stability. Due to the closure of the lyophilized samples under a vacuum of 0.04 mbar, the headspace of the vials theoretically contains approx. 4 % of the oxygen present in the liquid formulations, which were closed at ambient atmospheric pressure. Thus, the lower oxygen content in the lyophilized samples might also contribute to this result. The dried samples can be considered to be stable over the whole observation period at all tested temperatures. A direct comparison between the lyophilized and the dried precipitated formulations at each sample point delivers lower amounts of oxidized Met for the latter, giving rise to the assumption that this approach is slightly more potent in preventing oxidative degradation.

4.2.2.3 Isomerization

Due to the double bond like character of the amide C-N bond, the neighboring C atoms can adopt cis and trans conformations, with the latter being energetically favored. In X-Proline (X-Pro) peptide bonds, however, this energetic difference is leveled by steric destabilization of the trans conformation, thus increasing the incidence of cis conformers. Scheufler and co-workers demonstrated the presence of a cis-peptide bond for Pro present in the rhBMP-2 backbone [Scheufler et al., 1999], making isomerization at this site a thinkable scenario. For tissue plasminogen activator, peptide mapping in combination with mass spectrometric detection delivers four peaks, consistent with four possible isomers expected from two Pro residues in sequence [Ling et al., 1991]. But it was not possible to achieve distinct peaks with classic UV detection [Hancock, 1995]. Consequently, in our studies utilizing HPLC in combination with UV detection for mapping digested rhBMP-2 samples Pro isomerization is not expected to be detectable.

Another degradation process occurring in rhBMP-2 is the isomerization of aspartic acid (Asp). This pathway proceeds through a cyclic imide intermediate which might – depending on the environmental conditions - further degrade to isoAsp [Goolcharran et al., 2000]. X-isoAsp bonds are no longer cleaved by the enzyme Asp-N Endoproteinase deployed for peptide mapping. Therefore, the occurrence of uncleaved peptides which were formerly separated indicates Asp isomerization. This degradation is observed at two sites within rhBMP-2, but only alteration of Asp³³⁵ is used to monitor isomerization, as the second sensitive Asp is located in the propeptide sequence.

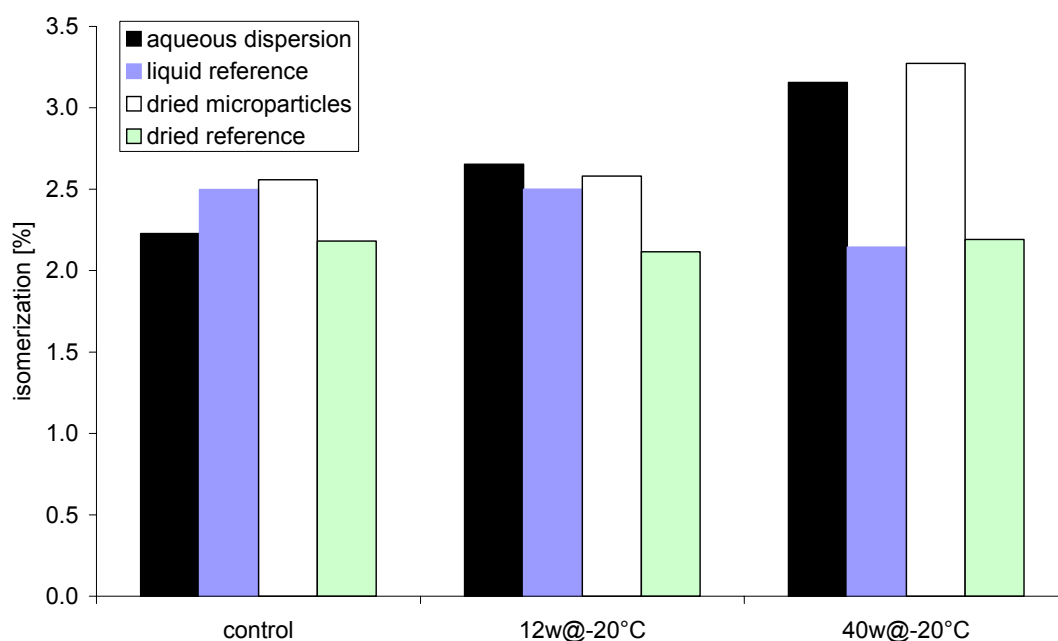


Figure 4-38: Isomerization of rhBMP-2 in different formulations after preparation (control), storage for 12 and 40 weeks at -20°C

Figure 4-38 depicts isomerization of Asp³³⁵ immediately after preparation (control) and after storage at -20°C. Within the controls, comparable values for isomerization were determined, ranging between 2.2 and 2.6 %. This indicates that neither the precipitation process nor supplementary lyophilization causes significant isomerization. Data for 12 and 40 weeks storage also do not suggest accelerated degradation in any of the four formulations, qualifying subzero temperatures for long time storage.

In Figure 4-39, the storage time at 5°C is plotted against isomerization with a logarithmic scale of the y-axis. Stability of the aqueous rhBMP-2 dispersion can be maintained, with values for isomerization not exceeding 5 % after 10 months storage. The liquid reference shows a clear tendency to isomerize, almost reaching 10 % degradation after 12 weeks and exceeding 20 % after 40 weeks. Both freeze dried formulations do not show significant changes over time, with isomerization values ranging between 2.7 and 3.5 % for the dried precipitate and slightly lower for the lyophilisate between 1.9 and 2.7 %. The subtle difference in isomerization levels between the two lyophilized samples is already seen after one week and continues over the whole storage time.

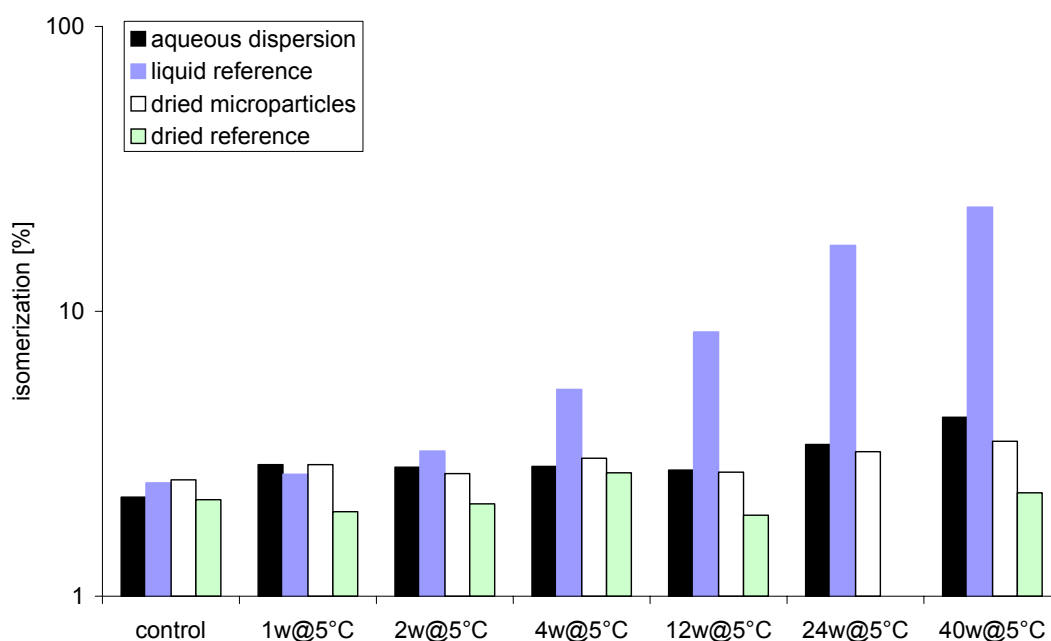


Figure 4-39: Isomerization over time of different rhBMP-2 formulations stored at 5°C

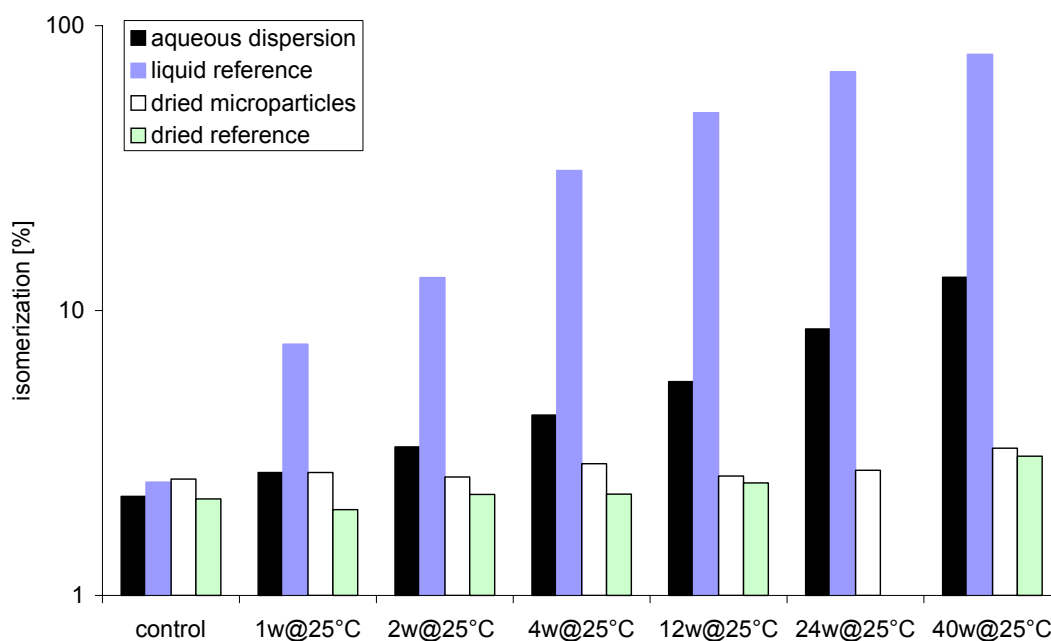


Figure 4-40: Isomerization of rhBMP-2 over time stored at 25°C

Figure 4-40 shows isomerization at 25°C, monitored over 10 months, again depicted on a logarithmic y-axis. The dramatic degradation of the liquid reference is dominating, leading to almost 80 % isoAsp formation after 6 months. Compared to this, the increase in isomerization in the aqueous dispersion is quite moderate, being below 10 % for 6 months and ending up to

13 % after 10 months. In analogy to the findings at 5°C, the dried precipitate still shows slightly higher levels as compared to the lyophilized reference.

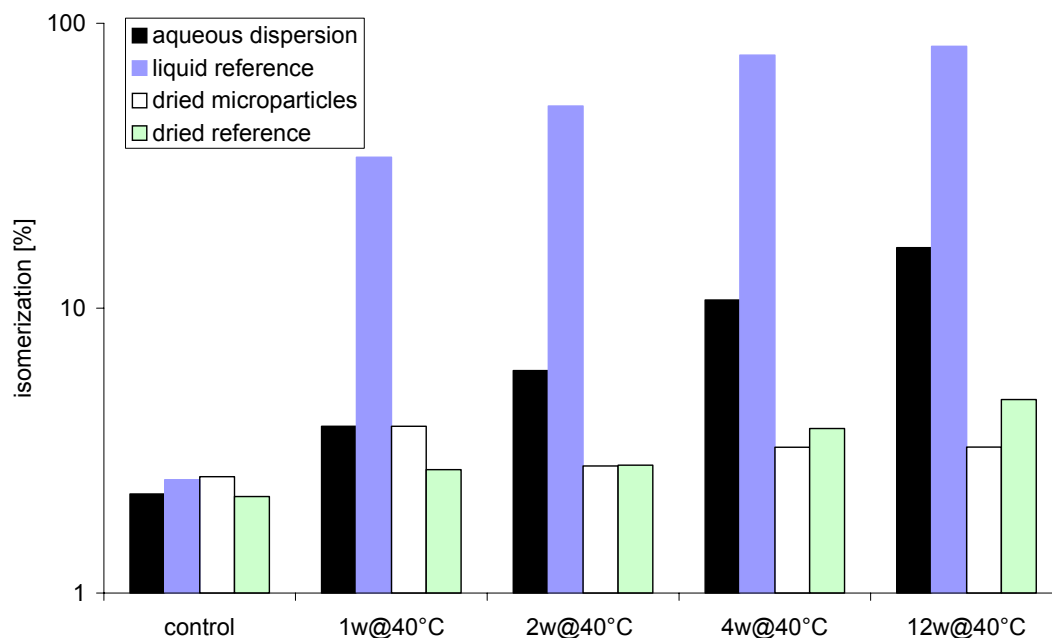


Figure 4-41: Isomerization over time in different rhBMP-2 formulations stored at 40°C

The conversion of Asp to isoAsp after storage at 40°C is given in Figure 4-41. Again, the liquid formulation is most prone to isomerization. Already after one week, approx. one third of the protein fall victim to this type of degradation, and a loss of almost 80 % is observed within 3 months. In contrast, isomerization is greatly decelerated in the aqueous dispersion, leading to 80 to 90 % lower levels relative to the liquid reference with total numbers exceeding the benchmark of 10 after one month. However, the tendency to degrade is also evident, and the total amount of isomerized rhBMP-2 exceeds the benchmark of 10 % after one month storage. Again, a strong positive effect on protein stability can be seen for the dried formulations. Both the dry precipitate and the lyophilisate stay below 5 % over the entire observation period. Whereas in the lyophilisate a trend might be concluded by the continuous increase from 2.7 % isomerization after one week to 4.7 % after 3 months, the dried precipitate did not reveal such a trend, and the tendentially lower isomerization values randomize between 2.8 to 3.8 %.

Within the tested formulations, the liquid reference formulation shows the highest isomerization rates, with 80 % loss after 6 months at 25°C or after 3 months at 40°C. Disregarding the small difference between body and storage temperature of 40°C and assuming that liquid rhBMP-2 obeys the same degradation kinetics in the body than as in vitro, almost 50 % would be lost due

to isomerization after two weeks. Under the same conditions, only 6 % of the aqueous dispersion would be degraded. For storage, isomerization can be further decelerated in this formulation by reduction of the storage temperature to 5°C, maintaining acceptable stability over 10 months. In both dried formulations, the discrepancy of isomerization levels is small. The difference is thought to be the consequence of unequal starting levels (Figure 4-38) which were preserved at 5 and 25°C over the course of the study. Thus, a definitive superiority of one formulation over the other cannot be derived from this data. At 40°C, however, the data suggest a slight advantage of the dried precipitate. Studies in aqueous solution with model hexapeptides containing Asp reveal a strong pH dependence of the degradation pathway, with basic pH values favoring isoAsp formation, whereas under acidic conditions, hydrolysis and cyclic imide formation are preferred. The reactivity of the carboxylic acid side chain is higher in the ionized form [Oliyai et al., 1993]. Consequently, higher isomerization is expected to occur in the liquid phase of the precipitated aqueous dispersion featuring a neutral pH. However, most of the protein molecules are existent as precipitate, thus minimizing the concentration of reactive molecules. In the precipitate, the molecules are separated from “mobile water”, leading to reduced protein mobility and therefore limiting the formation of the cyclic imide as intermediate step in isomerization.

In general, higher storage temperatures accelerate the degradation, especially in the liquid-containing formulations. This can be explained by the equation of Arrhenius, which predicts a two to threefold speeding up of a reaction by a temperature increase of 10°C [Martin et al., 1987]. Compared to the rapid deterioration of the liquid reference formulation, the aqueous precipitated dispersion explicitly shows lower oxidation and isomerization levels due to the exclusion of “mobile” water, thus immobilizing rhBMP-2 in the precipitate. At 25°C, the aqueous protein dispersion shows acceptable oxidation levels, but with 13 % isomerization, the degradation is quite high. At 5°C, stability over the entire observation period of 10 months is achieved without the need of drying or freezing, qualifying the aqueous precipitated dispersion as a long time storage candidate. Lyophilization is a well accepted and effective drying technique to gain protein pharmaceuticals with acceptable shelf lives [Wang, 2000]. Applying this approach on the liquid formulations effectively increases the chemical stability. At 5°C and 25°C storage, both the lyophilisate and the dried precipitate can be considered as equivalent. At 40°C, a slight superiority of the precipitated formulation for both isomerization and oxidation might be assumed.

4.2.2.4 Aggregation

Physical instabilities refer to changes in the higher order of protein structure, leading to denaturation, aggregation, adsorption or unwanted precipitation [Manning et al., 1989]. The native-like structure of rhBMP-2 precipitated under

controlled, physiological conditions and the reversibility of the precipitation process after immediate redissolution was already demonstrated (see 4.2.1). In the following, the maintenance of protein integrity during storage at reduced, ambient and accelerated temperatures should be investigated, focusing on the critical parameters aggregation, secondary structure and bioactivity.

4.2.2.4.1 Soluble Aggregates Determined by SEC

No difference in the aggregate content can be detected between the controls and the samples stored for 12 weeks at -20°C (Figure 4-42). The amount of aggregates found in the precipitated formulations is approximately half the amount found in the corresponding reference. As all formulations originate from the same protein stock solution, equal starting levels can be assumed. Consequently, higher aggregate contents would be expected for the precipitated formulations, as these samples have experienced additional stress (caused by additional process steps: dialysis, precipitation, and resolubilization). Several explanations can be given: (i) reduction of the aggregate content intrinsically present in the bulk solution, e.g. by redissolution during dialysis into low acidic pH or potential separation by adsorption to sterile filter membranes, (ii) removal of soluble aggregates with the supernatant after precipitation and concentration of the precipitate by centrifugation, (iii) removal of aggregates by the centrifugation step generally performed in sample preparation for SEC.

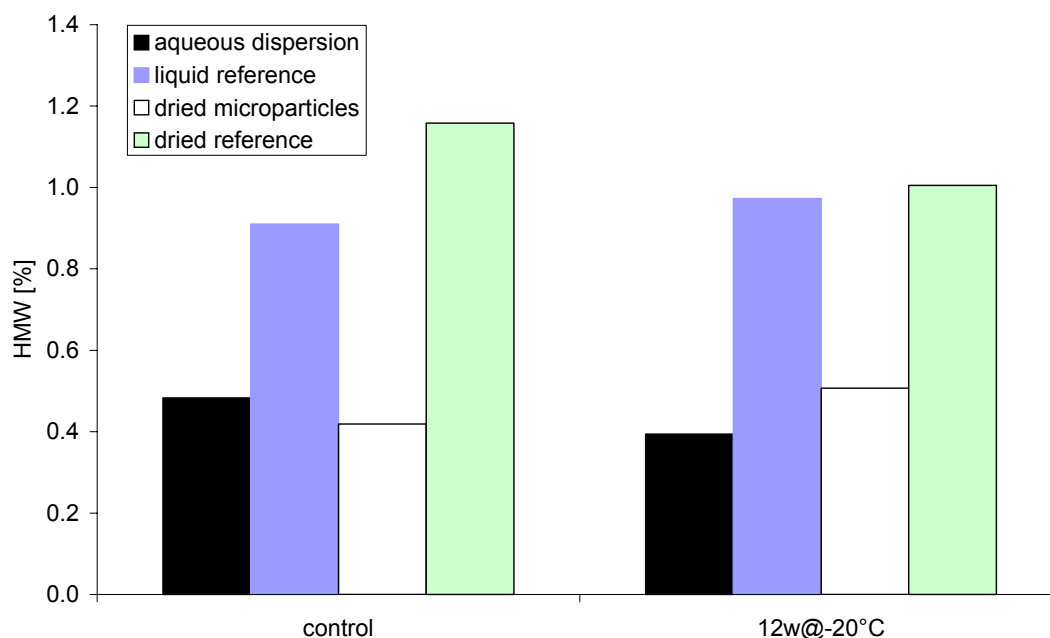


Figure 4-42: Soluble aggregates of rhBMP-2 in different formulations during storage at -20°C

At a storage temperature of 5°C, all formulations stay well below 2 % aggregate content, and the increase seen over time is only marginal. In general, lower amounts of aggregates are found in the precipitated formulations, compared to the references, most probably a consequence of lower initial levels. The relative increase in aggregate content, compared to the starting level, is highest in the aqueous precipitate dispersion, followed by the dried precipitate, the liquid formulation and finally the lyophilisate. The absolute aggregate content of both precipitated formulations is initially the same, so the slower escalation in the dried formulation is indicative for its superiority. Whereas the lyophilisate shows a higher absolute aggregate content, the escalation is more rapid in the liquid precipitated samples, arguing for the superiority of the lyophilisate with respect to long time storage (Figure 4-43).

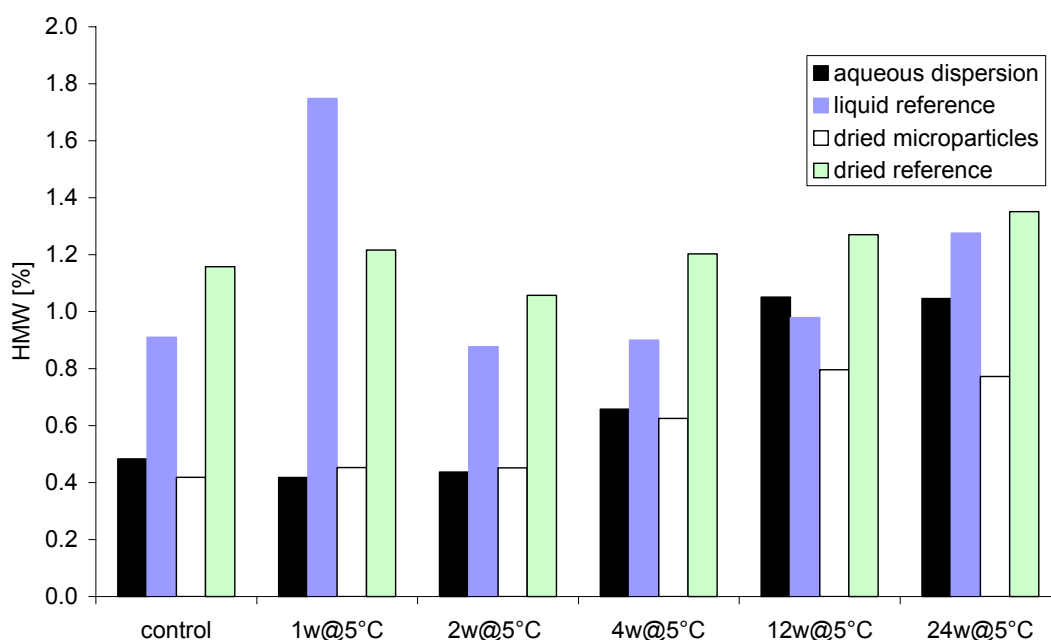


Figure 4-43: High molecular weight aggregate formation of rhBMP-2 in different formulations during storage at 5°C

After storage at 25°C, a increase in aggregate content can be observed in all formulations over time (Figure 4-44). Aggregation in the lyophilisate is well below 3 %. The advantage of lower initial starting levels in the precipitated formulations gets lost, and after 4 weeks storage, the aggregate content exceeds the one of the corresponding reference. This trend is continued, and after 3 months, almost 5 % aggregates are found in the precipitated formulations. Both the lyophilisate and the liquid reference stay well below 3 % aggregation, with slightly lower levels found in the latter.

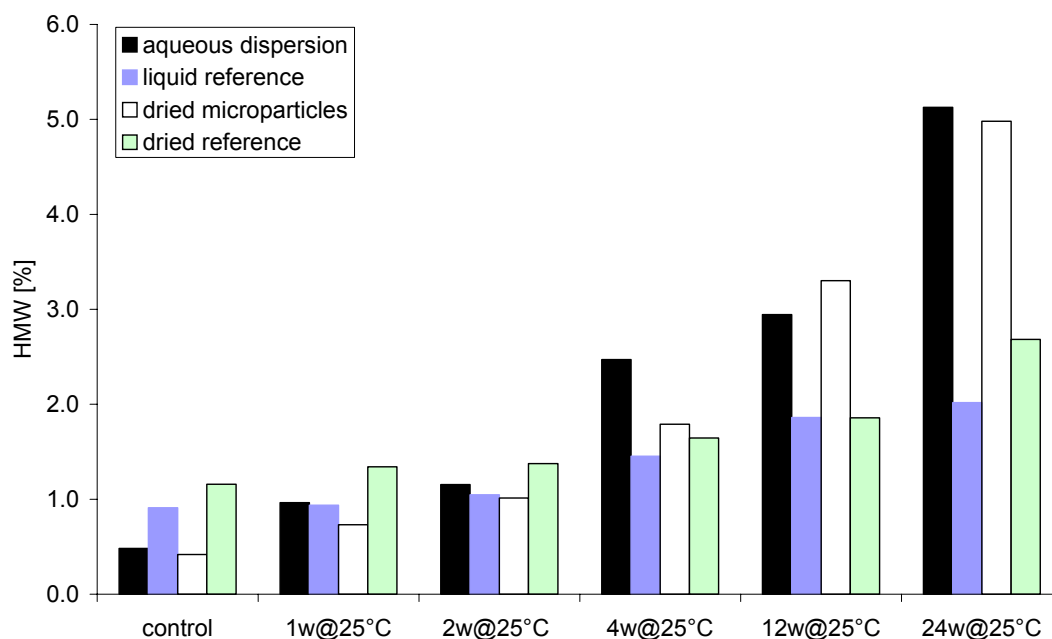


Figure 4-44: High molecular weight aggregate formation of rhBMP-2 in different formulations during storage at 25°C

The trend of higher aggregate content in the precipitated formulations, compared to the references, is even more pronounced in the 40°C storage samples (Figure 4-45), being obvious already after 1 week. After 3 months levels between 14-16 % are found in the aqueous precipitate dispersion and in the dried precipitate. Within the reference formulations, the aggregate content of the liquid reference formulation outran the value of the lyophilisate after 4 weeks storage. After 3 months, the absolute aggregate content is approx. 2.5 % higher than in the lyophilisate, which shows almost 5 % aggregates.

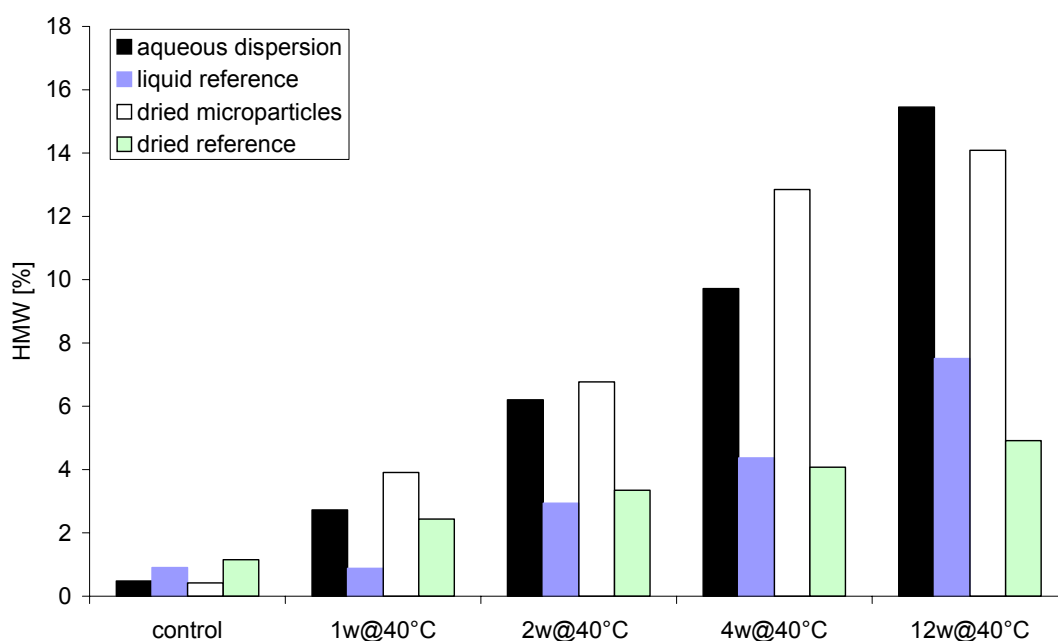


Figure 4-45: High molecular weight aggregate formation of rhBMP-2 in different formulations during storage at 40°C

As a prerequisite for SEC analytics, the precipitated and the lyophilized samples needed to be redissolved. Consequently, aggregates might either already exist in the solid material or could be created at the instant of reconstitution from conformationally altered species. An explanation for the high aggregation tendency observed in the precipitated formulations at high temperatures might be the intimacy of precipitated molecules, making a reaction among each other more probable. Higher temperatures deliver the energy necessary to overcome the limited molecular mobility. For such a mechanism however, Pikal and co-workers would expect an initial rapid increase in aggregates, followed by a decline as favorable configurations have already reacted. To explain a continuous increase – as it is seen in our experiments – they speculatively suppose that the formation of a conformationally altered intermediate might be the limiting factor for the rate of aggregation [Pikal et al., 1991]. The reduced aggregation tendency seen in the liquid reference can be explained by the presence of sucrose, which can act as thermodynamic stabilizer of the native conformation according to the concept of preferential exclusion [Kim et al., 2003].

4.2.2.4.2 Covalent and Non-covalent Aggregates by SDS-PAGE

SEC provides information about the total aggregate content. To verify the obtained results and to get a deeper insight into the nature of the aggregation mechanism, SDS-PAGE was performed, allowing a differentiation between covalently and non-covalently linked aggregates (under reducing and non

reducing conditions, respectively). Due to the higher sensitivity, silver staining was used, accepting that this staining technique does not allow for accurate quantification [Jones, 1994]. Comparison of band intensities between different gels documenting different storage times is difficult, as the staining intensity within the individual gels varies considerably and attempts to correct this mathematically by referencing to a standard failed. Therefore, a relative evaluation of aggregation was performed, given in Table 4-7.

Table 4-7: Aggregate content determined by SDS-PAGE: non-covalent aggregates were evaluated with ((-) < - < -- < --- < ----); samples containing covalent aggregates are with grey background (relative intensity parallels content)

time [weeks]	temperature [°C]	aqueous dispersion	liquid reference	dried precipitate	dried reference
0	RT				
	-20				
1	5	(-)	(-)		
	25	--	-	-	-
	40	---	--	---	--
2	5	(-)		(-)	
	25	--	-	--	--
	40	----	---	----	--
4	5	(-)		(-)	
	25	--	--	-	--
	40	----	---	----	---
12	-20				
	5			(-)	
	25	--	--	--	--
	40	----	---	----	--
24	-20				
	5	-	-	(-)	(-)
	25	---	--	---	--
60	5	--	--		(-)
	25	---	---	--	-

Non-reduced SDS-PAGE

No aggregates are detected in the controls and in the samples stored for -20°C for 3 and 6 months, respectively. After storage at 5°C for one week, the band pattern of both reference formulations are identical to the internal rhBMP-2 standard, with a very weak high molecular weight band indicating the presence of trace amounts of tetramer (consisting of four rhBMP-2 monomers, e.g. by combination of two naturally occurring dimers). In the aqueous dispersion and the dried precipitate, no high molecular weight species (HMWs) are present. At 25°, weak bands are found in all formulations, becoming more distinct at 40°C. With slight variations, this pattern is also found after 2, 4 and 12 weeks storage. A new quality is introduced after 24 weeks storage, with aggregates already present at 5°C in all formulations. In general, the HMW bands in the precipitated samples are more intense than in the references, especially after storage at higher temperatures.

Two distinct HMW species can be found in the aqueous dispersion, with molecular weights of 57-60 kDa and approx. 78-80 kDa. Aggregates in the liquid reference formulation and the dried formulations have molecular weights of 56-60 kDa and 69-73 kDa. With a molecular weight of 28-33 kDa for the native dimer and 14-17 kDa for the naturally occurring monomers, a molecular weight in the range of 56-60 kDa is consistent with a tetramer. After two week's storage at 40°C, the aqueous precipitate dispersion exhibits an additional band with a molecular weight of approx. 44 kDa. After 4 weeks, the formation of hexamers is indicated by a band of 97 kDa, which fits well to the theoretical expectation of 84-100 kDa for this aggregate.

The semi-quantitative analysis by visual comparison of band intensities delivers results which are in good agreement with SEC data. Both methods demonstrate a lower aggregate content at 5°C and higher levels after storage at elevated temperatures for the precipitated formulations as compared to the references.

Reduced SDS-PAGE

The gels performed under reducing conditions deliver additional information about the binding within the aggregates. In the dried precipitate stored at 40°C, covalent aggregates with a molecular weight of approx. 30 kDa are present after one week (Table 4-7). After two weeks storage at the same temperature, covalent aggregates are also found in the aqueous dispersion and the liquid reference. After 4 weeks, a faint band indicates the presence of covalently linked rhBMP-2 species in the lyophilized reference. The band intensities and thus the amounts of covalent aggregates differ considerably, with the bands of the precipitated formulations being more pronounced than in the references. The positive outcome at low storage temperatures, with absence of covalent aggregates at 5 and 25°C leads to a focus in the follow-up studies at these temperatures. After 6 and 10 months, small amounts of covalently linked

species are found in all formulations stored at 25°C. Therefore, only storage at 5°C is useful to completely prevent covalent aggregate formation over 10 months in all formulations.

The covalently linked aggregates seen after reduction have molecular weights comparable to the native, non-reduced dimer. The band shape is consistent with the shape of the native, non-reduced rhBMP-2 dimer, featuring band doubling due to the naturally occurring isoforms of the differentiation factor. No high molecular weight aggregates, with masses comparable to those detected under non-reducing conditions can be found. This allows the conclusion that all HMW species detected under non-reducing conditions were non-covalent, and the covalent aggregate on reduced gels is most probably a rhBMP-2 dimer which has experienced some modifications so that it can no longer be separated into monomers under the applied reducing conditions.

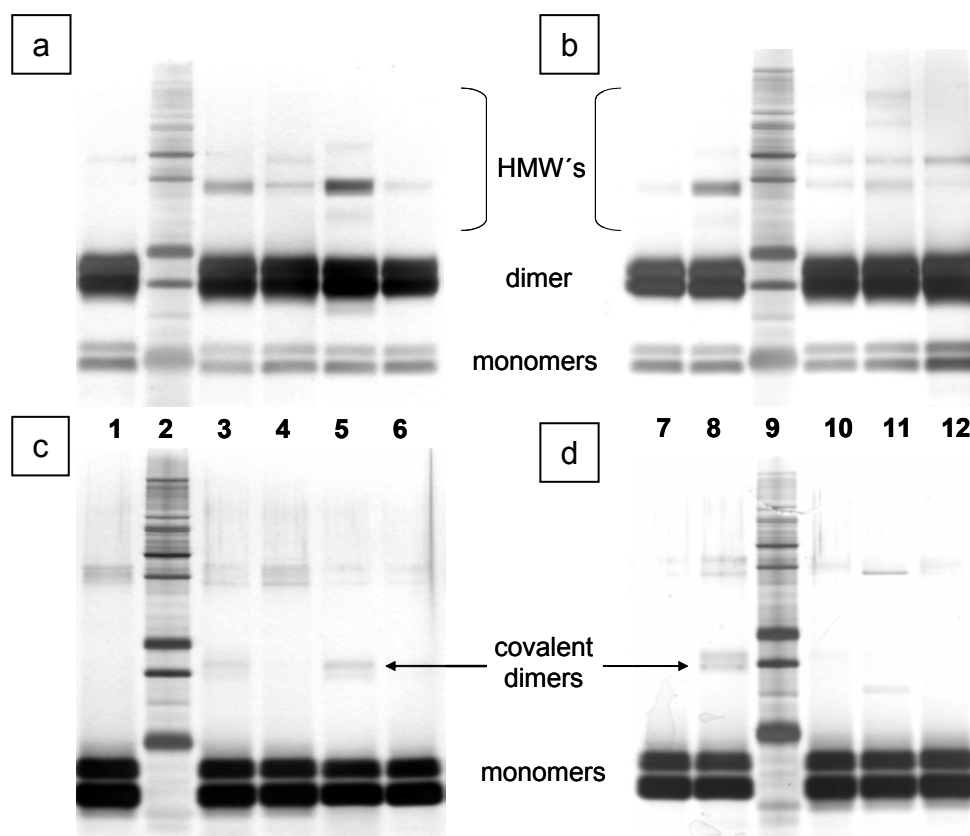


Figure 4-46: Selected silver stained SDS-page gels, both non-reduced (a, b) and reduced (c, d): native rhBMP-2 reference (lane 1, 12); MARK12™ wide range standard (lane 2, 9); storage for 6 months of liquid formulation at 25°C (lane 3) and 5°C (lane 4), aqueous precipitated dispersion stored at 25°C (lane 5) and 5°C (lane 6), dried precipitate stored at 5°C (lane 7) and 25°C (lane 8), lyophilisate, stored at 5°C (lane 10) and 25°C (lane 11)

4.2.2.4.3 Secondary Structure Investigation by ATR FTIR

It could be demonstrated by ATR-FTIR measurements that the precipitation process does not alter the secondary structure when redissolution is performed within a few hours (Figure 4-26). To study whether precipitate aging induces detectable conformational changes, samples of the precipitate in aqueous dispersion stored for 6 months at 5°C and 25°C were analyzed by ATR-FTIR and compared to both native liquid standard and the liquid reference treated at the same conditions. Figure 4-47 shows the area normalized second derivative spectra. No major difference can be detected between the samples stored for 6 months and the control spectra of native rhBMP-2. Thus, as shown previously, aggregates detectable with SEC and SDS-PAGE in the stored samples at 5°C and 25°C cannot be picked up by FTIR which would pick up strong changes in the secondary structure.

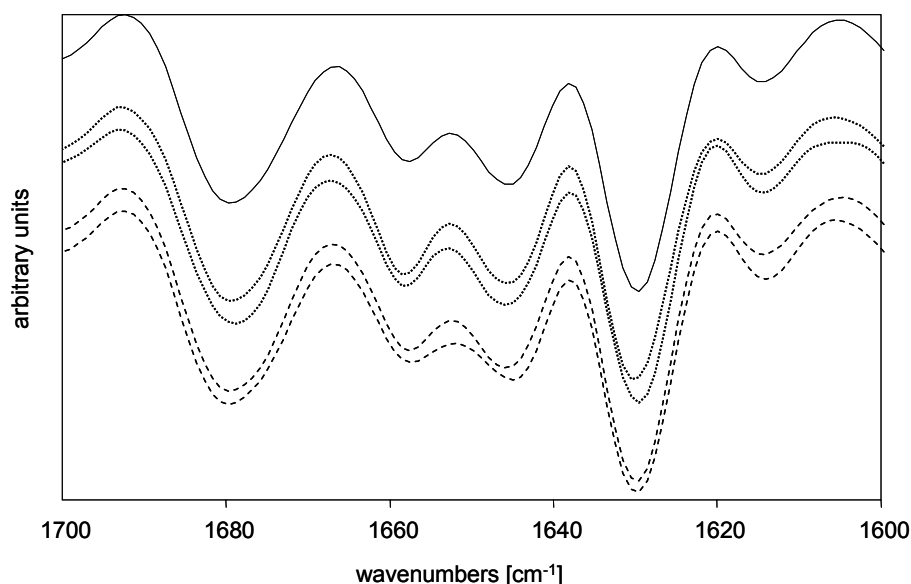


Figure 4-47: Spectra of native liquid rhBMP-2 (—), aqueous precipitate dispersion stored at 5°C (·····) and 25°C (----) and liquid rhBMP-2 reference formulation stored at 5°C (-·-·-) and 25°C (- - - -) for 6 months.

4.2.2.4.4 Bioactivity Testing of Aqueous Precipitate Dispersion

In a small study, the intactness of precipitated rhBMP-2 was evaluated by bioactivity determination as a function of time and temperature. Non-preserved sterile aqueous dispersions were prepared. After storage at designated times and temperatures, the microparticles were concentrated by centrifugation, the supernatant was removed and the remaining pellet was redissolved in formulation buffer, frozen in liquid nitrogen and stored at -80°C until analysis. Dialyzed rhBMP-2 (1 mM HCl), which was used as starting material for the precipitated formulations, was included as standard. Furthermore, aqueous

dispersions of the storage stability study were also subjected to bioactivity determination. In Figure 4-48, each sample is faced with the internal control of fully bioactive protein.

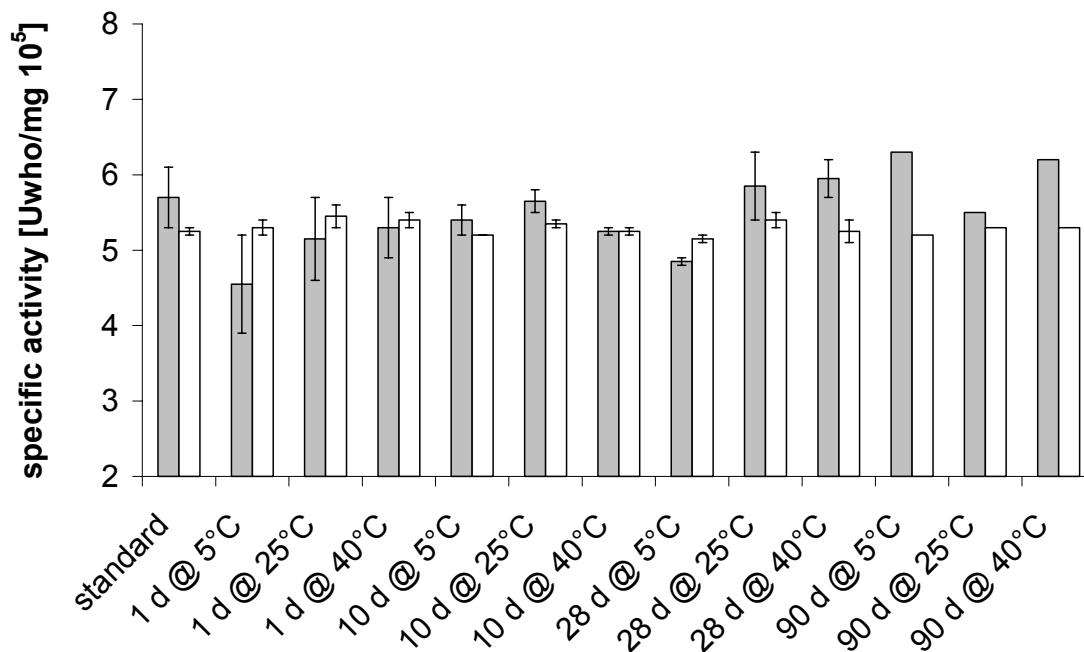


Figure 4-48: Specific activity of precipitated rhBMP-2 after storage at different temperatures for 1, 10 and 28 and 90 days; grey bars represent samples, white bars the corresponding internal control

Fully bioactive samples deliver specific activities in the magnitude of $5 \cdot 10^5$ Uwho/mg, and a reduction by more than $2 \cdot 10^5$ units suggests serious damage of the protein. Accordingly, full bioactivity could be demonstrated for the aqueous dispersion. The absence of a systematic trend gives rise to the assumption that bioactivity will not be reduced during long time storage. The results also confirm full intactness of rhBMP-2 dialyzed into 1 mM HCl – the starting material for the precipitated formulation.

4.2.3 Summary

Evidence is provided that the controlled precipitation process does not disturb the integrity of rhBMP-2. Analysis with ATR-FTIR proves a native-like secondary structure of rhBMP-2 precipitated under controlled physiological conditions. Subsequent redissolution did not induce any changes demonstrating full reversibility. Further proof for the reversibility of rhBMP-2 precipitation is provided by DSC measurements, showing conformity of the melting temperatures before precipitation and after precipitation and redissolution. Furthermore, the precipitate features an intense endotherm peak in the DSC thermogram, indicating that the protein is not unfolded and still possesses secondary struc-

ture. Alterations in secondary structure of precipitated rhBMP-2, as seen during thermal unfolding in ATR-FTIR measurements, are non permanent and reversible, as demonstrated in the unfolding spectra of the resolubilized sample. In addition, samples dissolved immediately after precipitation did not show a higher aggregate content and were fully bioactive in cell culture experiments.

Precipitation shows a high potential to minimize the chemical instabilities isomerization and oxidation. With respect to the latter, the extensive degradation seen in the liquid reference can be greatly reduced, and rhBMP immobilized in the precipitated state maintains acceptable low oxidation levels at 25°C storage for 40 weeks. Quite impressive stabilization is also achieved regarding isomerization. Whereas the liquid reference formulation loses more than 68 % due to isoAsp formation, the aqueous precipitate dispersion shows only approx. 8.6 % after 24 weeks at 25°C, and keeps well below 5 % at 5°C storage. Thus, the liquid reference formulation would require storage at 5°C, the aqueous precipitate dispersion can be stored at the higher temperature of 25°C and still maintains acceptable stability. Freeze drying of the aqueous precipitate dispersion delivers a stable formulation, enabling storage at 40°C for 40 weeks without significant increase in oxidation or isomerization. In addition, the 40°C data suggest a slight advantage of the precipitate, with otherwise comparable stability to the lyophilisate. The advantage, however, is alleviated by the fact that the precipitated formulation requires longer times for complete redissolution. Especially after long time storage at high temperatures, additional shaking was necessary to get a clear solution, with reconstitution times exceeding several minutes.

The behavior of precipitation based formulations towards aggregation is ambivalent and strongly dependent on the temperature. At high storage temperatures, the reference formulations were superior, staying below 3 % aggregate content over 24 weeks at 25°C and 1 to 2 weeks at 40°C. Furthermore, irreversibly crosslinked rhBMP-2 dimers preferably occur in the precipitated formulations stored at higher temperatures, being slightly more pronounced in the dried precipitate. At 5°C, both the aqueous precipitate dispersion and the dried precipitate show lower absolute levels for aggregation than the corresponding liquid and freeze dried references. The maintenance of bioactivity in the aqueous dispersion was demonstrated over a period of three months at all temperatures tested, confirming the integrity of the protein. Consequently, precipitation can be used as a suitable tool for the preparation of highly concentrated rhBMP-2 formulations, and storage of the precipitated formulation at 5°C provides an alternative to lyophilization.

ATR-FTIR is a useful tool to analyze and quantify the overall secondary structure of proteins. However, this technique does not allow the detection of aggregate formation in the dimension of 5 %. In addition, in a sample showing

17 % oxidation and 79 % isomerization (determined by peptide mapping), no change could be seen with ATR-FTIR.

4.3 In-vitro Release from rhBMP-2 Microparticles

4.3.1 Considerations and Setup

Geiger describes the development of a suitable in-vitro release assay for a sustained release rhBMP-2 formulation based on ceramic/collagen composites [Geiger, 2001]. The major obstacles turned out to be the low solubility of rhBMP-2 in physiological fluids, the difficulty of quantifying small amounts of protein in large volumes of release medium and system inherent problems, such as interference of carrier decomposition products with the applied detection method. In addition, release could be greatly manipulated by the properties of the release medium, as the solubility of rhBMP-2 is very sensitive to the ionic strength and the presence of sulphate and chloride. Therefore, artificial buffer systems are considered to be no suitable release buffer candidates, and in-vitro release studies should be performed with serum.

The development of an in-vitro release assay utilizing serum as release medium and at the same time avoiding radioactive labelling or ELISA is challenging. To overcome the above described obstacles, release from rhBMP-2 microspheres should be determined indirectly by quantifying the amount of protein still present in the microparticles at the designated time points. This approach has two advantages: (i) due to the sustained release of rhBMP-2 from disintegrating microparticles, a sufficient amount of protein is initially present, enabling rationale quantification; (ii) solid rhBMP-2 microparticles can be separated from serum by centrifugation, thus minimizing its interfering protein content. Figure 4-49 shows a microscopic image of rhBMP-2 microparticles suspended in human serum.

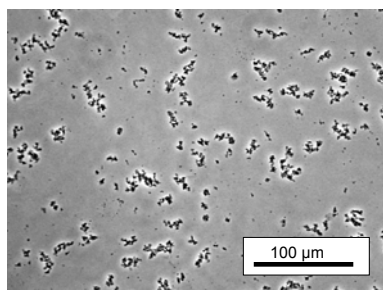


Figure 4-49: *rhBMP-2 microparticles suspended in human serum*

4.3.2 Analytic Development

The feasibility of RP-HPLC and SDS-PAGE to separate rhBMP-2 from serum was tested, assuming that approx. 0.1 % serum will still be present in the sample after centrifugation, removal of the supernatant, and redissolution of the protein pellet.

The applied RP-HPLC method does deliver two peaks, but baseline separation could not be achieved (Figure 4-50a). Variations in the performance parameters (decrease in flow rate, slower increase of organic solvent, longer run time) did improve the separation (Figure 4-50b). Nevertheless, the rhBMP-2 monomers were clearly eluted together with the major serum albumin peak. In addition, the modified run required higher sample volumes (100 μ l instead of 50 μ l), thus increasing the total amount of protein necessary for the analytic.

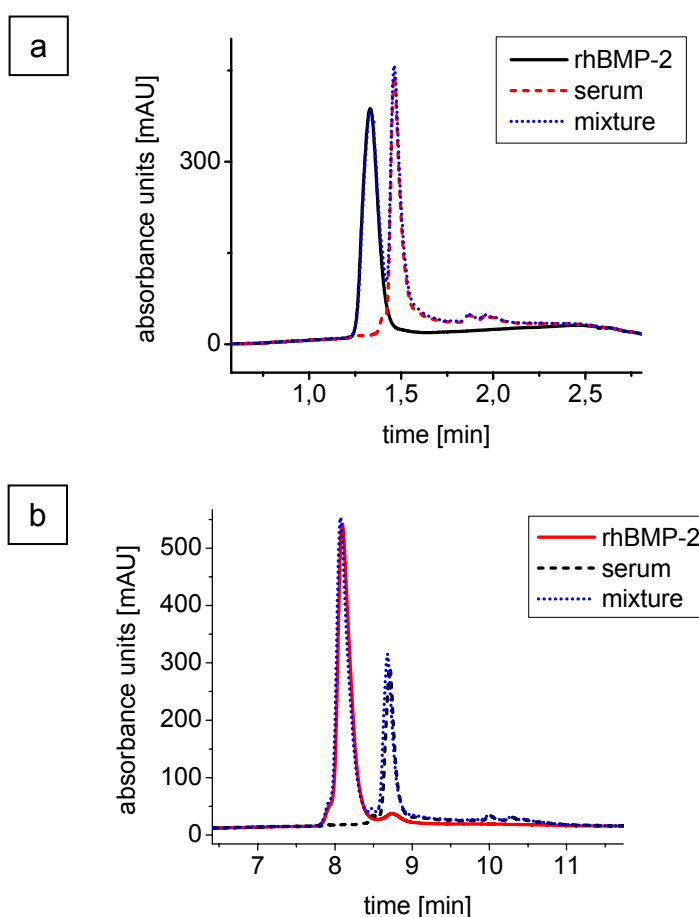


Figure 4-50: RP-HPLC chromatograms of artificial serum/rhBMP-2 mixtures: (a) standard run with 50 μ l injection volume containing 0.1 mg/ml rhBMP-2 in 0.1 % serum (b) modified run conditions with an injection volume of 100 μ l containing 0.2 mg/ml rhBMP-2 in 0.1 % serum

The results suggest that the applied HPLC approach is principally suitable to separate rhBMP-2 from trace amounts of serum. For quantification, the small overlapping zone of the dimer peak with the serum could be overcome by a calibration based on peak high instead of peak area.

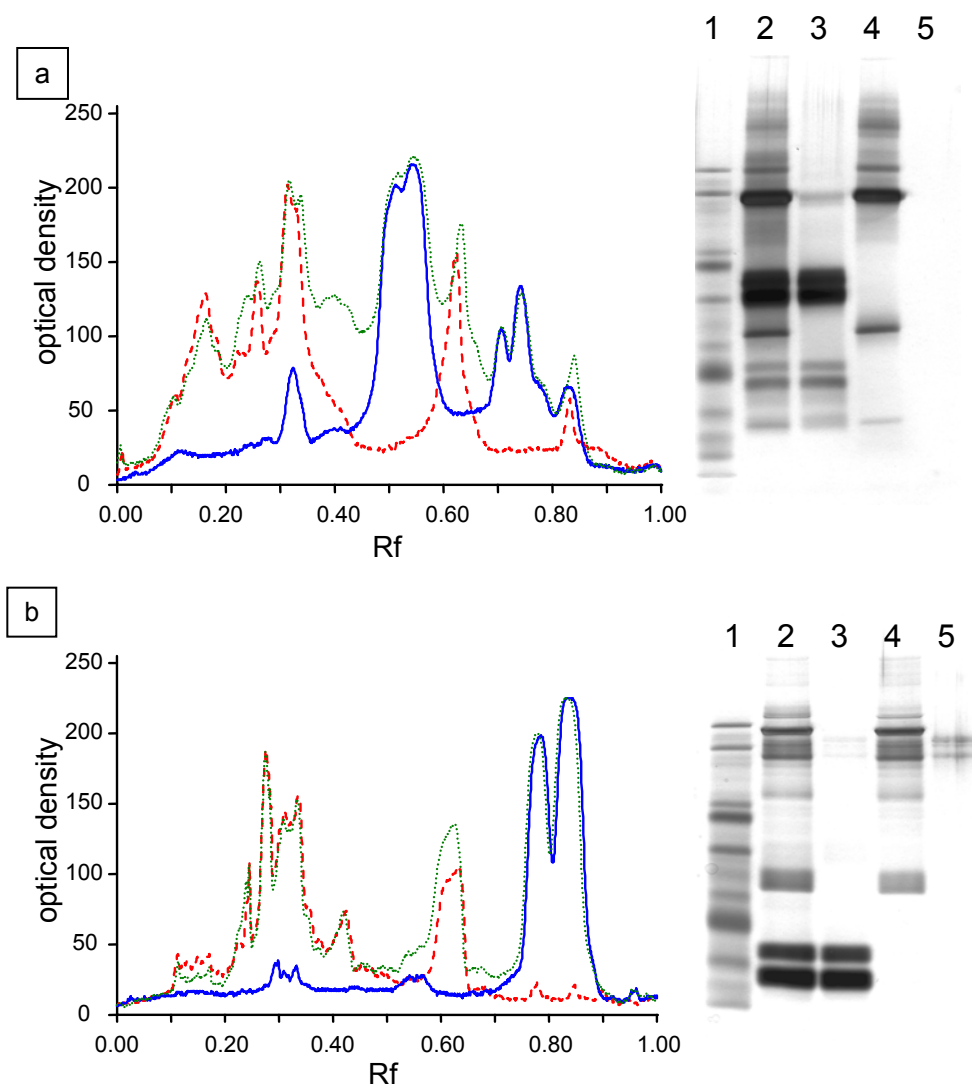


Figure 4-51: SDS-PAGE gel electrophoretic separation of artificial rhBMP-2/serum mixtures: densitographs and corresponding gels (lane 1: marker, lane 2: serum / rhBMP-2 mixture (dotted), lane 3: rhBMP-2 (solid), lane 4: serum (dashed), lane 5: running buffer) for (a) non reduced (b) reduced samples.

As an alternative quantification method, SDS-PAGE was tested. The densitographs of non-reduced samples show interference of both monomeric and dimeric rhBMP-2 signals with the background derived from serum (Figure 4-51a). In the reduced samples, serum depicts only very weak signals in the region of the rhBMP-2 monomer bands (Figure 4-51b). Furthermore, reduction was thought to be an elegant way to increase the sensitivity by an increase of

the calibration peak area, which is then composed of the naturally occurring monomers and the monomers created by the conversion of the dimer into monomers. Consequently, the reduced variant is to be preferred.

4.3.3 Calibration of Concentration Determination with SDS-PAGE

Figure 4-52 shows the integrated optical density (IOD) of rhBMP-2 calibration samples, acquired with gel electrophoresis under reducing conditions and subsequent silver staining. No linearity is obtained within the concentration range of 0.01 - 0.4 μg protein load per lane. Furthermore, identical protein loads analyzed on different gels resulted in different IODs, indicating a high variation of staining intensity. The non-linearity of silver staining is also reported in literature, rendering this dye to be unsuitable for quantification [Jones, 1994].

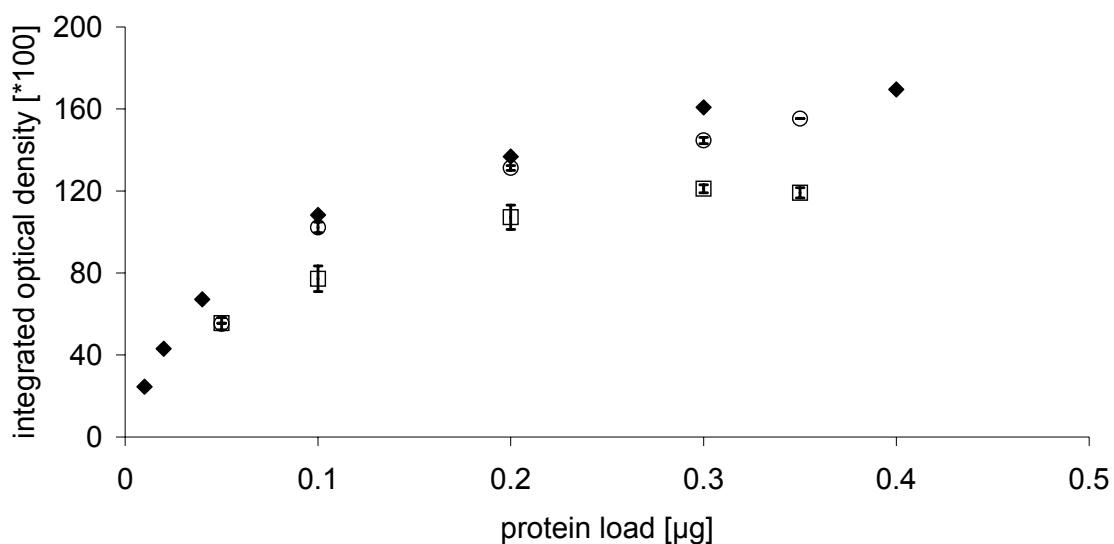


Figure 4-52: Integrated optical density of silver stained calibration samples (reduced conditions) analyzed on three different gels: gel I (♦) with 7 different concentrations, gel II (○) and III (□) with 5 calibration samples measured in duplicate.

In contrast to silver staining, Coomassie blue staining is less sensitive, and protein loads of 0.1 to 1 μg were used for quantification. With this dye, an acceptable calibration can be achieved (Figure 4-53, $R^2 = 0.9881$), and repeated analysis on different gels confirmed the linearity and the slope of the calibration.

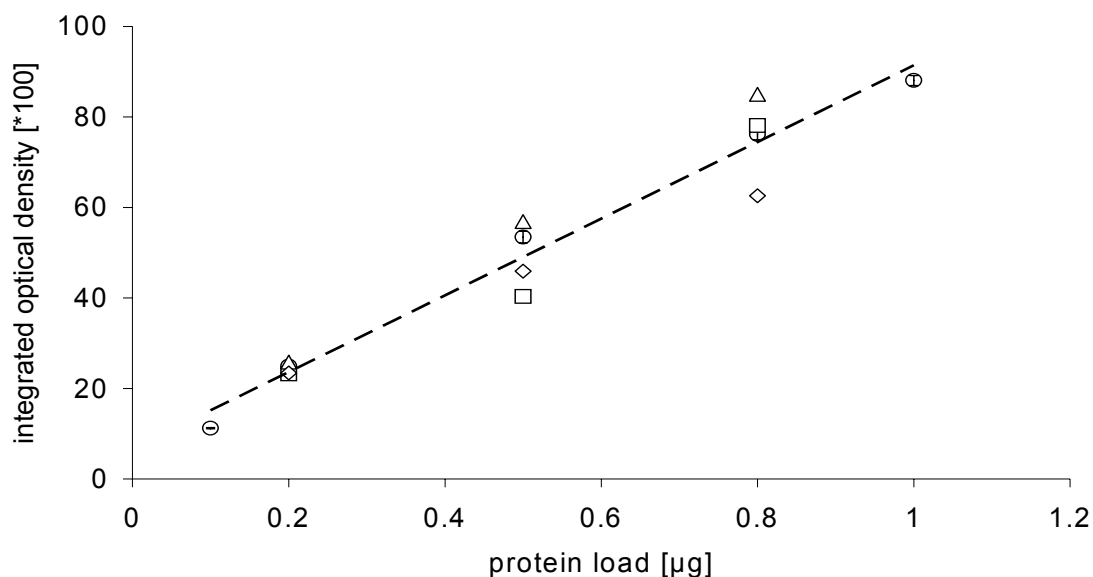


Figure 4-53: Calibration curves for SDS-PAGE after Coomassie blue staining (reducing conditions): linear fit (—) for a five point calibration (○) with samples run in duplicate; (□, ◇, △) three point calibrations performed on different gels

In respect of sensitivity, Coomassie blue stained gels and the HPLC-analysis are quite similar. For the HPLC-approach, Geiger has determined the lower limit of detection in rhBMP-2 samples without an interfering serum peak to be approx. 0.1 µg per injection. Calibration of Coomassie blue stained gels was performed in the same concentration range. The gel electrophoretic separation is favored for two reasons. At first, separation from serum was more pronounced in the reduced gels than in the HPLC-approach. Secondly, samples containing high amounts of serum have been shown to negatively affect the performance of the employed separation column, possibly due to accumulation of serum proteins on the column [Geiger, 2001]. Consequently, there has been concern of a possible damage to the column by injecting serum containing samples, leading to reduced reproducibility.

4.3.4 In-Vitro Release of rhBMP-2 from Microparticles in Serum

D'Augusta investigated the release of radioactively labeled rhBMP-2 from collagen sponges in serum, performing full serum exchange at each sampling point [D'Augusta et al., 2000]. His work provides the framework of the experimental setup. RhBMP-2 release studies from microparticles were performed without and with partial serum exchange. 100 µl microparticle suspension containing 200 µg rhBMP-2 were added to 1 ml serum and equilibrated in eppendorff caps at 37°C in a shaking water bath. Serum exchange was performed by centrifugation to concentrate the rhBMP-2 microparticles at the bottom of the vial, replacement of 500 µl serum with fresh

one, vortexing of the sample and putting it back into the shaking water bath. At designated time points, the sample was centrifuged, the supernatant completely removed, the residual protein microparticles present as pellet redissolved and stored at -20°C until analysis. The scheme of serum exchange and sampling for the setup with partial serum exchange is illustrated in Table 4-8.

Table 4-8: Sample drawing and serum exchange scheme for in vitro release testing (① symbolizes sample #1, etc.)

time [h]	1	4	24	72	168	336
sampling	①	②	③	④	⑤	⑥
exchange	② ③ ④ ⑤ ⑥	③ ④ ⑤ ⑥	④ ⑤ ⑥	⑤ ⑥	⑥	

Figure 4-54 shows the release profiles for both setups. For comparison, the data obtained by D'Augusta for in-vitro release of rhBMP-2 from collagen sponge, with complete serum exchange at designated times, are also included. The release after 1 hour is the same for both setups, resulting in over 40 %. Without medium exchange, approx. 50 % is released after one day. The initial burst is followed by a period of minimal release, and after 14 days, 32 % of the initial protein content can be recovered as undissolved microparticles. Release is more rapid in the setup with partial serum exchange, increasing the release from 53 % to 85 % within the first day (with a total of 90 % of initial volume being replaced at this time point). After 14 days, no residual protein particles can be found, suggesting complete redissolution.

D'Augusta obtained a release of 48 % within 1 day (the first measuring time point), increasing to 81 % after 14 days (Figure 4-54). The release profile of the microparticulate system shows a higher initial burst. At later time points, the obtained curve progression for the approach with serum exchange is similar to the release determined by D'Augusta. A difference can be seen in the total recovery. Whereas the microparticle system is completely dissolved after 14 days, irreversible binding of rhBMP-2 on the sponge leads to a reduced recovery in this system. The approach without serum exchange shows enhanced retention, revealing the importance of medium exchange to reflect the in vivo situation.

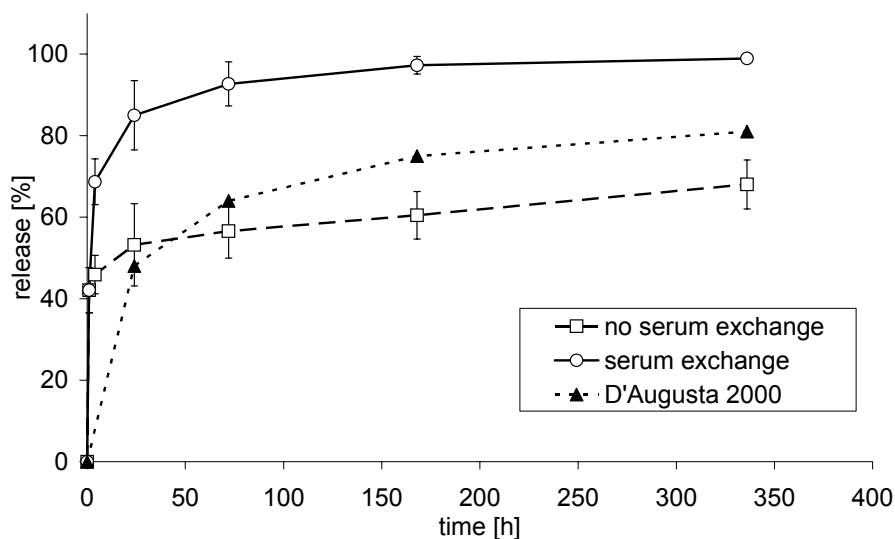


Figure 4-54: Cumulative in-vitro release of rhBMP-2 in serum: rh BMP-2 microparticles without (\square) and with approx. 45 % serum exchange (\circ) at each sampling time point; (\blacktriangle) rhBMP-2 loaded collagen sponge with total serum exchange at each sampling point

A different behavior of the monomers building up the native rhBMP-2 dimer can be observed on the reduced gels, with the higher molecular weight monomer (representing the extended T form, see Figure 1-2) disappearing faster than the isomers of lower molecular weight (build up by the Q and <Q form). The faster fading of the high molecular weight monomer might be caused by the high hydrophilicity of the double extended homodimer (T/T isoform), thus redissolving faster than the more hydrophobic isoforms [Friess, 2000].

4.3.5 Summary

An in-vitro release assay was developed for rhBMP-2 microparticle formulation that allows the use of serum as release medium and utilizes SDS-PAGE for protein quantification. Whereas silver staining has proven to be unsuitable, good results are obtained with the Comassie blue dye. It could be demonstrated that the applied RP-HPLC is principally feasible to separate rhBMP-2 from serum. The obtained release profile for the microparticles is in good correlation to the data obtained for the release of rhBMP-2 from a collagen sponge. In contrast to the protein/carrier combination, 100 % release can be achieved from the microparticulate system. A difference in the dissolution behavior of rhBMP-2 isoforms is suggested, with dimers containing the extended monomer disappearing faster than the isoforms build up of the mature and isomerized monomers.

4.4 Efficacy Study in the Rabbit Distal Femur Intraosseous Model

4.4.1 Study Design

The efficacy of precipitated rhBMP-2 delivered as an injectable microparticle suspension to induce bone formation was evaluated. Rabbits serve as a qualified screening model as they feature a region at the distal femur between the condyles of very low bone density (Figure 4-55). The rationale is to inject the rhBMP-2 formulation intraosseous into this region to augment bone density.

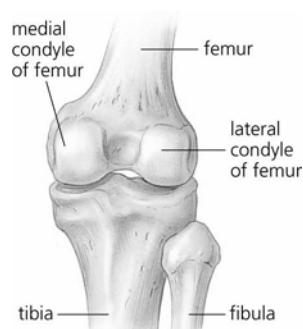


Figure 4-55: Illustration of anatomic localization of injection site (adapted from www.freedictionary.com/chondyle)

The study included 4 animals. A unilateral design was applied, i.e. one limb was treated with a total dose of 0.12 mg precipitated rhBMP-2 (300 μ l microparticle suspension with a concentration of 0.4 mg/ml), whereas the contralateral limb serves as untreated control. Four weeks after injection, the rabbits were sacrificed. Analysis was performed by radiography and histology and data were compared with historic data of pure buffer and sustained releasing gel formulations. In-life radiographs were assessed at the time of surgery and two and four weeks post surgery. The trabecular bone volume was calculated as % bone area from VonKossa stained slides in the epiphyseal region (Figure 4-56). Furthermore, the % difference from untreated controls was calculated. De-novo bone formation was qualitatively assessed by estimating the % surface of labeled trabecular bone area by visual inspection with a fluorescence microscope. Fluorochrome labelling was achieved by systemic administration of tetracycline 10 and 25 days post-op. The antibiotic forms chelate complexes with apatite, thus marking tissues which were mineralized at the time of dye administration.

4.4.2 Study Outcome

Radiography did not reveal dramatic differences in bone density both for the rhBMP-2 treated and the untreated control group (data not shown). The results of histomorphometric evaluation are listed in Table 4-9. Only a moderate

increase in trabecular bone volume, with a difference of approx. 9.5 % between rhBMP-2 microparticle-treated and untreated controls was found. 20-30 % of the bone surface area was labeled, suggesting a moderate bone formation activity. Compared to historic data of rhBMP-2 delivered in buffer, which shows an increase in trabecular bone area of approx. 8 % and de-novo bone formation in the range of 10-30 %, there seems to be no advantage of the precipitated formulation in this model.

Table 4-9: Trabecular bone areas assessed by histomorphometry and fluorochrome labeling

animal	control (left) [%]	treated (right) [%]	difference [%]	fluorochrome label [%]
1	25.02	25.45	2	30
2	37.70	40.41	7	30
3	36.02	39.86	11	20
4	28.00	32.96	18	20
average	31.68	34.67	9.48	25.00
SD	6.14	7.02	6.84	5.77

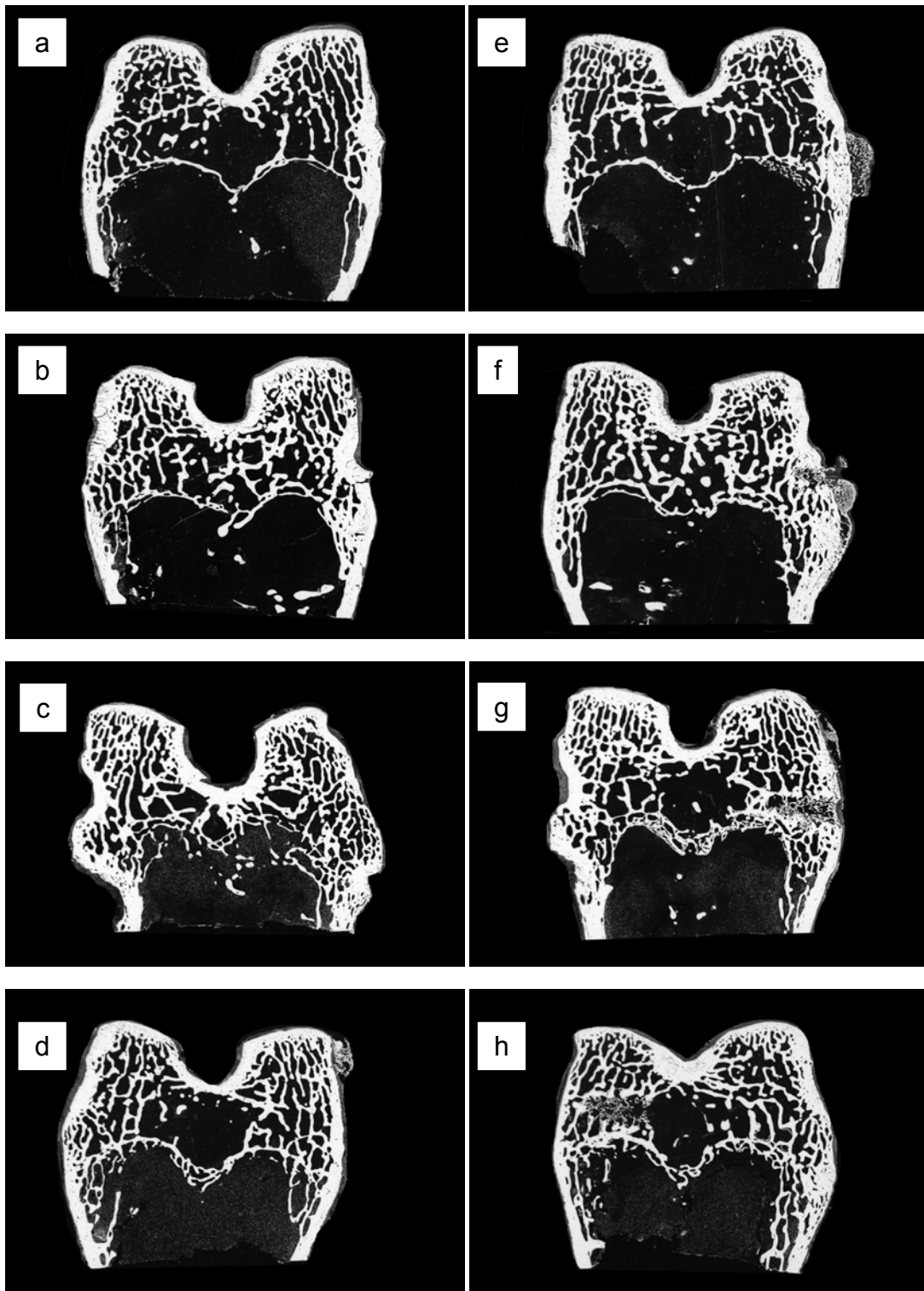


Figure 4-56: Sections of rabbit distal femurs after VonKossa silver staining and thresholding to black: (a-d) untreated controls (left femur of four animals) and right femurs (e-h) treated with rhBMP-2 microparticle suspension

In general, bone formation in small animals is much more rapid than in humans. Therefore, successful candidates in small animals will not necessarily lead to a positive result in large animals. In reverse, negative outcomes are likely to predict failure in large animals and humans [Seeherman et al., 2003]. With this respect, the identical outcome of the precipitated formulation compared to the liquid buffer formulation is disappointing. A possible explanation for the marginal effect might be an insufficient retention of rhBMP-2 the site of action. Either the microparticles themselves are quickly cleared off the injection site due to the high liquid exchange rate, or the release from the microparticles is too rapid, as indicated by the high in-vitro release obtained in the setup with serum exchange (Figure 4-54). A pharmacokinetic study with radioactively labeled protein would be helpful to identify the fundamental reason.

A positive evaluation can be given with respect of immunogenicity. Although not explicitly tested, i.e. by monitoring inflammatory markers or specific anti-rhBMP-2 antibody titers, the smooth course of the study, with any side reaction absent, suggests a good in-vivo tolerance of precipitated rhBMP-2 in the tested animal model.

5 Summary

The present thesis focuses on the development and characterization of a novel formulation for the sustained delivery of recombinant human bone morphogenetic protein-2 (rhBMP-2). Based on the concept of precipitation, the known low solubility of the protein at physiological conditions was utilized to generate microparticles, delivering an aqueous protein suspension.

RhBMP-2 has proven to induce bone formation. This ability can be applied to the field of bone tissue engineering, e.g. to support and accelerate bone regeneration at a skeletal site after fracture or in plastic surgery. For an optimal therapeutic effect, a prolonged presence of the morphogen at the site of action is required. As rhBMP-2 is rapidly cleared from the application site when administered as solution, it is usually combined with a carrier which retains the morphogen at the implantation site and provides its prolonged presence by sustained release. In the commercially available product the protein is soaked on a collagen sponge prior to implantation. The major disadvantage of this formulation is the necessity for invasive surgery to introduce the graft. With an injectable formulation, surgery could be avoided. In cases where operative treatment is necessary, an injectable formulation will be helpful in conjunction with a minimally invasive surgical technique. In addition, the treatment of fractures that do not require surgery will benefit from such a formulation (e.g. to enhance healing of simple, closed fractures). Finally, novel indications may arise for the multifunctional morphogen which extend beyond the treatment of skeletal diseases due to benefits from an injectable, sustained release formulation. Driven by the need, a number of injectable carriers for rhBMP-2 are currently under investigation, including calcium phosphate and sulphate cements, synthetic and natural polymers as gels or pastes and combinations thereof.

The approach of this work was to create a "carrier free", injectable formulation which contains the protein as precipitated particles thus providing its own matrix. Release of active rhBMP-2 is thought to occur by sustained dissolution of the microparticles. In contrast to other micoparticulate approaches, a high protein load can be achieved with precipitation. In addition, the generated particles are already suspended in an aqueous vehicle, thus avoiding difficulties which may arise by dispersion of dry particles in a liquid.

The first part of the thesis describes the development of a controlled precipitation process which allows the generation of uniformly sized microparticles. A simple experimental setup has proven to be suitable to obtain protein microparticles: in a batch mode, a turbulent rhBMP-2 bulk solution was

created with the help of vortexing and combined with a precipitation solution, and mixing was continued for a minute. Due to the composition of the solutions, an artificial physiological environment is created, forcing rhBMP-2 to precipitate. Laser light diffraction (LLD) with a modified sample cell which allows measurement of small sample volumes (< 5 ml) was deployed to characterize the precipitated microparticles. Particle formation was a time dependent process. Starting from an initially formed monomodal distribution, a second, larger population developed, leading to a bimodal distribution with maxima of approx. 7 μm and 35 μm after equilibration for one hour. Moderate centrifugation was reversible. After lyophilization and resuspension, the underlying bimodal distribution was broadened by an additional particle fraction exceeding 200 μm , observable both with LLD and in scanning electron microscopy (SEM) images. Lyophilization of highly concentrated precipitates greatly altered the particle distribution. Scaling-up of the batch precipitation process by increasing the final protein concentration and the batch volume was principally feasible, but is accompanied by the formation of associate species exceeding 200 μm . Improved scaling-up was obtained with a continuously operating precipitation procedure, utilizing a laminar mixing device. Independently from protein concentration and flow rate, similar particle size distributions were obtained than in the batch approach, but without the less desired large associates.

Optimization of the formulation composition included the introduction of a suitable buffer system, elucidated by solubility studies of rhBMP-2 in various phosphate buffer systems. Clearance of excipients derived from the original protein stock formulation led to a basic standard formulation composed of rhBMP-2, phosphate buffer (50 mM, pH 7.4) and potassium chloride. Using this formulation, both the batch process and the continuous micromixer approach delivered similar bimodal distributions with prominent maxima at approx. 7 and 34 μm . A slight advantage was seen for the laminar mixing approach due to the absence of any particles larger than 200 μm .

In the course of the optimization process, phase contrast microscopy was evaluated as additional analysis tool. The images revealed particle sizes in the range of 1 to 10 μm , and loosely associated small particles form larger agglomerates which could easily be separated by slight shear forces. Consequently, the large aggregates detected with LLD had to be agglomerates of small particles. This finding was also confirmed by laser light blockade measurements, showing that approx. 30 % of all particles have diameters of approx. 1.4 μm , and no particle is larger than 50 μm (based on number distribution). Other visualization techniques, like (Environmental) SEM, delivered only limited information on the genuine particle distribution in suspension.

The addition of selected polyanionic biopolymers intended to achieve larger and more stable particles by coprecipitation as well as the addition of surfactants to prevent particle association did not lead to the desired effect. Homogeneous suspensions, with a particle size of 1-2 μm were achieved by increasing the viscosity of the aqueous vehicle. The primary particles were separated by the shear forces and reassembly is prevented by the limited mobility of the particles in the dispersant.

The second part deals with the integrity of rhBMP-2 in the precipitated state and after redissolution. It was demonstrated that controlled precipitation did not harm rhBMP-2 and is fully reversible. With ATR-FTIR, native-like secondary structure was found in the precipitated microparticles. Secondary structure element determination resulted in 5 % α -helix and 25 % β -sheet content. RhBMP-2 from redissolved microparticles also delivered native conformation, showing full reversibility of the precipitation process. The aggregate content after precipitation and resolubilization was not increased as compared to the starting material, proving that the precipitation process did not induce the formation of aggregation competent intermediates. Further evidence for the reversibility of precipitation derived from DSC measurements. Essentially the same melting temperatures were obtained before precipitation and after redissolution of precipitated microparticles. In addition, improved thermal stability for the precipitated material was indicated by a higher melting temperature and a higher value for the calorimetric enthalpy, as compared to the liquid formulation. Temperature dependent ATR-FTIR measurements of both the precipitated and the redissolved sample revealed a loss of α -helical and β -turn structures. This loss of native-like structure was not accompanied by an increase in unordered structures, but intermolecular antiparallel β -sheet structures were formed which are typical for thermally unfolded proteins. Analysis of redissolved rhBMP-2 in cell culture demonstrated full bioactivity.

In addition, the potential of two precipitated formulation candidates – an aqueous dispersion and a freeze dried precipitate - to maintain protein stability over time was analyzed. Peptide mapping was implemented for the analysis of isomerization and oxidation during storage. Increased chemical stability was found for precipitated material, greatly reducing oxidation and isomerization compared to a liquid reference. Chemical degradation in the freeze dried precipitate was further reduced and comparable to the commercially available lyophilisate, meeting the stability criteria over the whole observation period. Aggregation as the major physical instability was monitored with SEC and gel electrophoresis. At high storage temperatures, both precipitated formulations showed higher sensitivity to aggregation than the references as indicated by increased aggregate contents and the appearance of covalently linked dimers. At 5°C storage, aggregation was reduced, leading to values comparable to the references. For up to 3 months, full bioactivity was demonstrated for the

aqueous precipitate formulation, and maintenance of conformational integrity was demonstrated over 6 months.

ATR-FTIR has proven to be a good tool for determining the overall secondary structure of proteins. However, it failed to uncloset an aggregate content in the order of 5 %, as determined by SEC, and high levels of isomerization and oxidation, as demonstrated by peptide mapping, suggesting that chemical degradation processes have no effect on the secondary structure of rhBMP-2.

In the last part, the ability of the microparticle formulation to deliver rhBMP-2 in a sustained manner was tested. An in-vitro assay utilizing serum as release medium was developed. The difficulty to quantify rhBMP-2 in presence of serum was coped with a gel electrophoretic approach. In a setup with partial medium exchange, a high initial burst is followed by moderate release, suggesting a rapid dissolution, and complete disappearance of the particles within 14 days. The efficacy of the aqueous protein suspension to augment bone density was tested in rabbits. Compared to the untreated control, a moderate increase in trabecular bone volume of approx. 9.5 % was found. De-novo bone formation of 20-30 % indicated a moderate bone formation activity. The results were comparable to the outcome for a liquid rhBMP-2 formulation. Thus, accelerated bone formation with the developed aqueous microparticulate formulation could not be shown in this animal model. For optimization, the approach of increasing the viscosity of the dispersant appears promising.

In conclusion, a simple precipitation step is useful to minimize chemical degradation of rhBMP-2 and can be utilized as alternative storage form at low temperatures. In addition, precipitation provides a useful tool for the preparation of highly concentrated formulations. Finally, the generation of microparticles by controlled precipitation is feasible. Consequently, controlled precipitation does have a great potential in formulation development, and transfer of this technique to other proteins is awaited.

6 References

- Abbatiello, S. E., Porter, T. J., Anion-mediated precipitation of recombinant human bone morphogenetic protein (rhBMP-2) is dependent upon heparin binding N-terminal region, *Protein Science* (1997) 99.
- Aigner, T., Stove, J., Collagens-major component of the physiological cartilage matrix, major target of cartilage degeneration, major tool in cartilage repair, *Advanced Drug Delivery Reviews*, 55 (2003) 1569-1593.
- Atha, D. H., Ingham, K. C., Mechanism of precipitation of proteins by polyethylene glycols: analysis in terms of excluded volume, *J. Biol. Chem.*, 256 (1981) 12108-12117.
- Bahamonde, M. E., Lyons, K. M., BMP-3: to be or not to be a BMP, *Journal of bone and joint surgery*, 83-A Suppl 1 (2001) S56-S62.
- Barth, A., Zscherp, C., What vibrations tell us about proteins, *Quarterly reviews of biophysics*, 35 (2002) 369-430.
- Bauer, T. W., Smith, S. T., Bioactive materials in orthopaedic surgery: overview and regulatory considerations, *CLINICAL ORTHOPAEDICS AND RELATED RESEARCH*, (2002) 11-22.
- Bechthold-Peters, K., Crystallization and precipitation as tools to stabilize therapeutic proteins and peptides, *Controlled Release Society German Chapter Annual Meeting*, Munich, 2003.
- Bell, D. J., Heywood-Waddington, D., Hoare, M., Dunnill, P., The density of protein precipitates and its effect on centrifugal sedimentation, *Biotechnology and Bioengineering*, 24 (1982) 127-141.
- Bell, D. J., Hoare, M., Dunnill, P., The formation of protein precipitates and their centrifugal recovery, *Advances in Biochemical Engineering/Biotechnology*, 26 (1983) 1-72.
- Bertini, I., F. Briganti, and A. Scozzafava, Specificity factors in metal ion-macromolecular ligand interactions, 1995.
- Blum, J. S., Li, R. H., Mikos, A. G., Barry, M. A., An optimized method for the chemiluminescent detection of alkaline phosphatase levels during osteodifferentiation by bone morphogenetic protein 2, *Journal of Cellular Biochemistry*, 80 (2000) 532-537.
- Boden, S. D., Martin, G. J., Jr., Horton, W. C., Truss, T. L., Sandhu, H. S., Laparoscopic anterior spinal arthrodesis with rhBMP-2 in a titanium interbody threaded cage, *Journal of spinal disorders*, 11 (1998) 95-101.
- Boden, S. D., Martin, G. J., Jr., Morone, M. A., Ugbo, J. L., Moskowitz, P. A., Posterolateral lumbar intertransverse process spine arthrodesis with recombinant human bone morphogenetic protein 2/hydroxyapatite-tricalcium phosphate after laminectomy in the nonhuman primate, *Spine*, 24 (1999) 1179-1185.

- Boden, S. D., Zdeblick, T. A., Sandhu, H. S., Heim, S. E., The use of rhBMP-2 in interbody fusion cages. Definitive evidence of osteoinduction in humans: a preliminary report, *Spine*, 25 (2000) 376-381.
- Boden, S. D., Kang, J., Sandhu, H., Heller, J. G., Use of recombinant human bone morphogenetic protein-2 to achieve posterolateral lumbar spine fusion in humans: a prospective, randomized clinical pilot trial: 2002 Volvo Award in clinical studies, *Spine*, 27 (2002) 2662-2673.
- Botchkarev, V. A., Bone morphogenetic proteins and their antagonists in skin and hair follicle biology, *Journal of Investigative Dermatology*, 120 (2003) 36-47.
- Boyne, P. J., Application of bone morphogenetic proteins in the treatment of clinical oral and maxillofacial osseous defects, *Journal of bone and joint surgery*, 83-A Suppl 1 (2001) S146-S150.
- Boyne, P. J., Marx, R. E., Nevins, M., Triplett, G., Lazaro, E., Lilly, L. C., Alder, M., Nummikoski, P., A feasibility study evaluating rhBMP-2/absorbable collagen sponge for maxillary sinus floor augmentation, *International journal of periodontics & restorative dentistry*, 17 (1997) 11-25.
- Brange, J., Physical stability of proteins, 2000.
- Chechin, R., Thorolfsson, M., Knappskog, P. M., Domain structure and stability of human phenylalanine hydroxylase inferred from infrared spectroscopy, *FEBS Letters*, (1998) 225-230.
- Chi, E. Y., Krishnan, S., Randolph, T. W., Carpenter, J. F., Physical Stability of Proteins in Aqueous Solution: Mechanism and Driving Forces in Nonnative Protein Aggregation, *Pharmaceutical Research*, 20 (2003) 1325-1336.
- Cook, S. D., Baffes, G. C., Wolfe, M. W., Sampath, T. K., Rueger, D. C., Whitecloud, T. S., III, The effect of recombinant human osteogenic protein-1 on healing of large segmental bone defects, *Journal of bone and joint surgery*, 76 (1994) 827-838.
- Coppi, G., Iannuccelli, V., Leo, E., Bernabei, M. T., Cameroni, R., Protein immobilization in crosslinked alginate microparticles, *Journal of Microencapsulation*, 19 (2002) 37-44.
- Cueto, M., Dorta, M. J., Munguia, O., Llabres, M., New approach to stability assessment of protein solution formulations by differential scanning calorimetry, *International Journal of Pharmaceutics*, 252 (2003) 159-166.
- D'Augusta, D. A., K. McCarthy, H. D. Kim, and R. H. Li, Methods for In Vitro Characterization of rhBMP-2 Carriers, Kamuela, Hawaii, USA, 2000, p. 1254.
- Defelippis, M. R. and M. J. Akers, Peptides and proteins as parenteral suspensions: an overview of design, development, and manufacturing considerations, 2000.
- Dong, A., Prestrelski, S. J., Allison, S. D., Carpenter, J. F., Infrared spectroscopic studies of lyophilization- and temperature-induced protein aggregation, *Journal of Pharmaceutical Sciences*, 84 (1995) 415-424.

- Dong, A., Huang, P., Caughey, W. S., Protein secondary structures in water from second-derivative amide I infrared spectra, *Biochemistry*, 29 (1990) 3303-3308.
- Ducruix, A. F., Ries-Kautt, M. M., Solubility diagram analysis and the relative effectiveness of different ions on protein crystal growth, *Methods (San Diego, CA, United States)*, 1 (1990) 25-30.
- Dumitriu, S., Chornet, E., Inclusion and release of proteins from polysaccharide-based polyion complexes, *Advanced Drug Delivery Reviews*, 31 (1998) 223-246.
- Edsall, J. T., Plasma proteins and their fractionation, *Advances in Protein Chemistry (Pub. by Academic Press Inc. , New York)*, 3 (1947) 383-479.
- Einhorn, T. A., Clinical applications of recombinant human BMPs: early experience and future development, *Journal of bone and joint surgery, American volume*, 85-A Suppl 3 (2003) 82-88.
- Einhorn, T. A., Majeska, R. J., Mohaideen, A., Kagel, E. M., Bouxsein, M. L., Turek, T. J., Wozney, J. M., A single percutaneous injection of recombinant human bone morphogenetic protein-2 accelerates fracture repair, *Journal of bone and joint surgery*, 85-A (2003) 1425-1435.
- Englard, S., Seifter, S., Precipitation techniques, *Methods in Enzymology*, 182 (1990) 285-300.
- Fabian, H., Schultz, C. P., Fourier transform infrared spectroscopy in peptide and protein analysis, in: R. A. Meyers (Ed.), *Encyclopedia of Analytical Chemistry*, John Wiley & Sons Ltd, Chichester, 2000, pp. 5779-5803.
- Fairbank, J. C., Couper, J., Davies, J. B., O'Brien, J. P., The Oswestry low back pain disability questionnaire, *Physiotherapy*, 66 (1980) 271-273.
- Feher, G., Kam, Z., Nucleation and growth of protein crystals: general principles and assays, *Methods in Enzymology*, 114 (1985) 77-112.
- Fornasiero, F., Ulrich, J., Prausnitz, J. M., Molecular thermodynamics of precipitation, *Chemical Engineering and Processing*, 38 (1999) 463-475.
- Forslund, C., Rueger, D., Aspenberg, P., A comparative dose-response study of cartilage-derived morphogenetic protein (CDMP)-1, -2 and -3 for tendon healing in rats, *Journal of Orthopaedic Research*, 21 (2003) 617-621.
- Friedlaender, G. E., Perry, C. R., Cole, J. D., Cook, S. D., Cierny, G., Muschler, G. F., Zych, G. A., Calhoun, J. H., LaForte, A. J., Yin, S., Osteogenic protein-1 (bone morphogenetic protein-7) in the treatment of tibial nonunions, *Journal of bone and joint surgery*, 83-A Suppl 1 (2001) S151-S158.
- W. Friess, *Drug Delivery Systems Based on Collagen*, Shaker Verlag, Aachen 2000.
- Friess, W., Sargeant, C., In vitro evaluation of rhBMP-2 in combination with a porous calcium phosphate device for bone regeneration, *Proceedings of the International Symposium on Controlled Release of Bioactive Materials*, 24th (1997) 895-896.

- Fromigue, O., Modrowski, D., Marie, P. J., Growth factors and bone formation in osteoporosis: Roles for fibroblast growth factor and transforming growth factor beta, *Current Pharmaceutical Design*, 10 (2004) 2593-2603.
- Geesink, R. G., Hoefnagels, N. H., Bulstra, S. K., Osteogenic activity of OP-1 bone morphogenetic protein (BMP-7) in a human fibular defect, *Journal of bone and joint surgery*, 81 (1999) 710-718.
- Geiger, M., Porous Collagen/Ceramic Composite Carriers for Bone Regeneration Using Recombinant Human Bone Morphogenetic Protein-2 (rhBMP-2). Dissertation (2001), FAU Erlangen-Nuernberg.
- Gelse, K., Jiang, Q. J., Aigner, T., Ritter, T., Wagner, K., Poschl, E., der Mark, K., Schneider, H., Fibroblast-mediated delivery of growth factor complementary DNA into mouse joints induces chondrogenesis but avoids the disadvantages of direct viral gene transfer, *Arthritis & Rheumatism*, 44 (2001) 1943-1953.
- Glatz, C. E., Modelling of Aggregation-Precipitation Phenomena, in: T. J. Ahern, M. C. Manning, and Editors. (Eds.), *Stability of Protein Pharmaceuticals, Part A: Chemical and Physical Pathways of Protein Degradation*. [In: *Pharm. Biotechnol.*, 1992; 2], Plenum Press, London and New York, 1992, pp. 135-167.
- Gombotz, W. R., Wee, S., Protein release from alginate matrixes, *Advanced Drug Delivery Reviews*, 31 (1998) 267-285.
- Goolcharran, C., M. Khosravi, and R. T. Borchardt, *Chemical pathways of peptide and protein degradation*, 2000.
- Gurd, F. R. N., The specificity of metal-protein interactions, *Ion Transport Across Membranes* (Academic Press Inc. , New York, N. Y.), (1954) 246-272.
- Hancock W. S., *New Methods in Peptide Mapping for the Characterization of Proteins*, 1995.
- Hao, Y. L., Ingham K. C., Wickerhauser M., *Fractional precipitation of proteins with polyethylene glycol*, 1980.
- Hartwig, C.-H., Esenwein, S. A., Pfund, A., Kusswetter, D. W., Herr, G., Improved osseointegration of titanium implants of different surface characteristics by the use of bone morphogenetic protein (BMP-3): an animal study performed at the metaphyseal bone bed in dogs, *Zeitschrift fur Orthopadie und ihre Grenzgebiete*, 141 (2003) 705-711.
- Hecht, B. P., Fischgrund, J. S., Herkowitz, H. N., Penman, L., Toth, J. M., Shirkhoda, A., The use of recombinant human bone morphogenetic protein 2 (rhBMP-2) to promote spinal fusion in a nonhuman primate anterior interbody fusion model, *Spine*, 24 (1999) 629-636.
- Hessel, V., Ehrfeld, W., Haverkamp, V., Lowe, H., Schiewe, J., Generation of dispersions using multilamination of fluid layers in micromixers, *Paperback APV*, 42 (2001) 45-59.
- Hilbrig, F., Freitag, R., Protein purification by affinity precipitation, *Journal of Chromatography, B: Analytical Technologies in the Biomedical and Life Sciences*, 790 (2003) 79-90.

- Hoare, M., Protein precipitation and precipitate aging. Part I. Salting-out and ageing of casein precipitates, *Transactions of the Institution of Chemical Engineers*, 60 (1982) 79-87.
- Hofbauer, L. C., Heufelder, A. E., Updating the metalloprotease nomenclature: bone morphogenetic protein 1 identified as procollagen C proteinase, *European Journal of Endocrinology*, 135 (1996) 35-36.
- Hofmeister, F., Instructions on the effects of mineral salts: Mechanisms of protein precipitation by mineral salts and their role in protein function, *Arch Exp Pathol Pharmacol*, 24 (1888) 247-260.
- Howell, T. H., Fiorellini, J., Jones, A., Alder, M., Nummikoski, P., Lazaro, M., Lilly, L., Cochran, D., A feasibility study evaluating rhBMP-2/absorbable collagen sponge device for local alveolar ridge preservation or augmentation, *International journal of periodontics & restorative dentistry*, 17 (1997) 124-139.
- Hunziker, E. B., Driesang, I. M., Morris, E. A., Chondrogenesis in cartilage repair is induced by members of the transforming growth factor-beta superfamily, *CLINICAL ORTHOPAEDICS AND RELATED RESEARCH*, (2001) S171-S181.
- T. A. Jennings, *Lyophilization: Introduction and Basic Principles*, 1999.
- Jones, A. J. S., Analytical methods for the assessment of protein formulations and delivery systems, *ACS Symposium Series*, 567 (1994) 22-45.
- Juckes, I. R. M., Fractionation of proteins and viruses with polyethylene glycol, *Biochimica et Biophysica Acta*, 229 (1971) 535-546.
- Kaps, C., Bramlage, C., Smolian, H., Haisch, A., Ungethum, U., Burmester, G. R., Sittinger, M., Gross, G., Haupl, T., Bone morphogenetic proteins promote cartilage differentiation and protect engineered artificial cartilage from fibroblast invasion and destruction, *Arthritis & Rheumatism*, 46 (2002) 149-162.
- Kendrick, B. S., Cleland, J. L., Lam, X., Nguyen, T., Randolph, T. W., Manning, M. C., Carpenter, J. F., Aggregation of Recombinant Human Interferon Gamma: Kinetics and Structural Transitions, *Journal of Pharmaceutical Sciences*, 87 (1998) 1069-1076.
- Kim, Y. S., Jones, L. S., Dong, A., Kendrick, B. S., Chang, B. S., Manning, M. C., Randolph, T. W., Carpenter, J. F., Effects of sucrose on conformational equilibria and fluctuations within the native-state ensemble of proteins, *Protein Science*, 12 (2003) 1252-1261.
- Kirker-Head, C. A., Potential applications and delivery strategies for bone morphogenetic proteins, *Advanced Drug Delivery Reviews*, 43 (2000) 65-92.
- Kistler, P. and H. Friedli, *Ethanol precipitation of proteins*, 1980.
- Kohnert, U., Growth factors in bone regeneration, *Controlled Release Society German Chapter Annual Meeting*, Munich, 2003.
- Koida, M., Fukuyama, R., Nakamuta, H., Osteoporosis requires bone-specific statins, *Current Pharmaceutical Design*, 10 (2004) 2605-2613.

- Korchynsky, O. and P. ten Dijke, Bone morphogenetic protein receptors and their nuclear effectors in bone formation, 2002.
- Langer, K., Balthasar, S., Vogel, V., Dinauer, N., von Briesen, H., Schubert, D., Optimization of the preparation process for human serum albumin (HSA) nanoparticles, *International Journal of Pharmaceutics*, 257 (2003) 169-180.
- Latner, A. L., Hodson, A. W., Differential precipitation with concanavalin A as a method for the purification of glycoproteins: human alkaline phosphatase, *Analytical Biochemistry*, 101 (1980) 483-487.
- Lee, G., Spray-drying of proteins, *Pharmaceutical Biotechnology*, 13 (2002) 135-158.
- Lieberman, J. R., Daluiski, A., Einhorn, T. A., The role of growth factors in the repair of bone. Biology and clinical applications, *Journal of bone and joint surgery*, 84-A (2002) 1032-1044.
- T. S. Lindholm, *Bone Morphogenetic Proteins: Biology, Biochemistry and Reconstructive Surgery*, 1996.
- Ling, V., Guzzetta, A. W., Canova-Davis, E., Stults, J. T., Hancock, W. S., Covey, T. R., Shushan, B. I., Characterization of the tryptic map of recombinant DNA derived tissue plasminogen activator by high-performance liquid chromatography-electrospray ionization mass spectrometry, *Analytical Chemistry*, 63 (1991) 2909-2915.
- Maa, Y. F., Prestrelski, S. J., Biopharmaceutical powders: particle formation and formulation considerations, *Current Pharmaceutical Biotechnology*, 1 (2000) 283-302.
- Manning, M. C., Patel, K., Borchardt, R. T., Stability of protein pharmaceuticals, *Pharmaceutical Research*, 6 (1989) 903-918.
- A. Martin, J. Swarbrick, and A. Cammarata, *Physikalische Pharmazie*, Wissenschaftliche Verlagsgesellschaft, Stuttgart 1987.
- Martin, G. J., Jr., Boden, S. D., Marone, M. A., Marone, M. A., Moskovitz, P. A., Posterolateral intertransverse process spinal arthrodesis with rhBMP-2 in a nonhuman primate: important lessons learned regarding dose, carrier, and safety, *Journal of spinal disorders*, 12 (1999) 179-186.
- Martinovic, S., F. Borovecki, K. T. Sampath, and S. Vukicevic, *Biology of bone morphogenetic proteins*, 2002.
- Marukawa, E., Asahina, I., Oda, M., Seto, I., Alam, M., Enomoto, S., Functional reconstruction of the non-human primate mandible using recombinant human bone morphogenetic protein-2, *International journal of oral and maxillofacial surgery*, 31 (2002) 287-295.
- Melander, W., Horvath, C., Salt effects on hydrophobic interactions in precipitation and chromatography of proteins: an interpretation of the lyotropic series, *Archives of biochemistry and biophysics*, 183 (1977) 200-215.
- Moore, B. D., Parker, M. C., Halling, P. J., Partridge, J., Rapid dehydration of proteins. University of Strathclyde, University Court of the University of Glasgow., WO069887 (2000).

- Morita, T., Horikiri, Y., Yamahara, H., Suzuki, T., Yoshino, H., Formation and isolation of spherical fine protein microparticles through lyophilization of protein-poly(ethylene glycol) aqueous mixture, *Pharmaceutical Research*, 17 (2000) 1367-1373.
- Nakashima, M., Reddi, A. H., The application of bone morphogenetic proteins to dental tissue engineering, *Nature Biotechnology*, 21 (2003) 1025-1032.
- Nemec, K., Schubert-Zsilavec, M., Future therapies for metabolic bone diseases. New concepts and targets, *Pharmazie in unserer Zeit*, 30 (2001) 548-552.
- Niederauer, M. Q., Glatz, C. E., Selective precipitation, *Advances in Biochemical Engineering/Biotechnology*, 47 (1992) 159-188.
- Oliyai, C., Borchardt, R. T., Chemical pathways of peptide degradation. IV. Pathways, kinetics, and mechanism of degradation of an aspartyl residue in a model hexapeptide, *Pharmaceutical Research*, 10 (1993) 95-102.
- P.Kistler, H. F., P.R.Foster, J. G. W., M.Steinbuch, Y.L.Hao, K. C. I. M. W., Fractionation by precipitation, in: J.M.Curling (Ed.), *Methods of plasma fractionation*, Academic Press, London, 1980, pp. 3-70.
- Pikal, M. J., Dellerman, K. M., Roy, M. I., Riggin, R. M., The effects of formulation variables on the stability of freeze-dried human growth hormone, *Pharmaceutical Research*, 8 (1991) 427-436.
- Privalov, P. L., Gill, S. J., The hydrophobic effect: a reappraisal, *Pure and Applied Chemistry*, 61 (1989) 1097-1104.
- Reddi, A. H., Bone morphogenetic proteins and skeletal development: the kidney-bone connection, *Pediatric nephrology (Berlin, Germany)*, 14 (2000) 598-601.
- Reddi, A. H., Bone morphogenetic proteins: from basic science to clinical applications, *Journal of bone and joint surgery*, 83-A Suppl 1 (2001) S1-S6.
- Remmele, R. L., Jr., Gombotz, W. R., Differential scanning calorimetry: a practical tool for elucidating stability of liquid biopharmaceuticals, *BioPharm (Duluth, Minnesota)*, 13 (2000) 36-46
- Rothstein, F., Differential precipitation of proteins: science and technology, *Bioprocess Technology*, 18 (1994) 115-208.
- Rueger, D. C., *Biochemistry of bone morphogenetic proteins*, 2002.
- Ruhe, P. Q., Hedberg, E. L., Padron, N. T., Spauwen Paul, H. M., Jansen, J. A., Mikos, A. G., rhBMP-2 release from injectable poly(DL-lactic-co-glycolic acid)/calcium-phosphate cement composites, *Journal of bone and joint surgery*, 85-A Suppl 3 (2003) 75-81.
- Ruppert, R., Hoffmann, E., Sebald, W., Human BMP-2 contains a heparin-binding site which modifies its biological activity, *European Journal of Biochemistry*, 237 (1996) 295-302.
- Sabulal, B., Kishore, N., Amino acids and short peptides do not always stabilize globular proteins: a differential scanning calorimetric study on their interactions with bovine α -lactalbumin, *Journal of the Chemical Society, Faraday Transactions*, 93 (1997) 433-436.

- Sampath, T. K., Reddi, A. H., Dissociative extraction and reconstitution of extracellular matrix components involved in local bone differentiation, *Proceedings of the National Academy of Sciences of the United States of America*, 78 (1981) 7599-7603.
- Sanchez-Ruiz, J. M., Differential scanning calorimetry of proteins, *Subcellular Biochemistry*, 24 (1995) 133-176.
- Sandhu, H. S., Khan, S. N., Recombinant human bone morphogenetic protein-2: use in spinal fusion applications, *Journal of bone and joint surgery*, 85-A Suppl 3 (2003) 89-95.
- Sandhu, H. S., Toth, J. M., Diwan, A. D., Seim, H. B., III, Kanim Linda, E. A., Kabo, J. M., Turner, A. S., Histologic evaluation of the efficacy of rhBMP-2 compared with autograft bone in sheep spinal anterior interbody fusion, *Spine*, 27 (2002) 567-575.
- Scheufler, C., Sebald, W., Hulsmeier, M., Crystal structure of human bone morphogenetic protein-2 at 2.7 Å resolution, *Journal of Molecular Biology*, 287 (1999) 103-115.
- Schimandle, J. H., Boden, S. D., Hutton, W. C., Experimental spinal fusion with recombinant human bone morphogenetic protein-2, *Spine*, 20 (1995) 1326-1337.
- R. K. Scopes, *Protein Purification*. 3rd Ed, 1995.
- Seeherman, H., Li, R., Wozney, J., A review of preclinical program development for evaluating injectable carriers for osteogenic factors, *Journal of bone and joint surgery*, 85-A Suppl 3 (2003) 96-108.
- Segura, T., Anderson, B. C., Chung, P. H., Webber, R. E., Shull, K. R., Shea, L. D., Crosslinked hyaluronic acid hydrogels: a strategy to functionalize and pattern, *Biomaterials*, 26 (2005) 359-371.
- Sellers, R. S., Zhang, R., Glasson, S. S., Kim, H. D., Peluso, D., D'Augusta, D. A., Beckwith, K., Morris, E. A., Repair of articular cartilage defects one year after treatment with recombinant human bone morphogenetic protein-2 (rhBMP-2), *Journal of bone and joint surgery*, 82 (2000) 151-160.
- Shah, A. K., Lazatin, J., Sinha, R. K., Lennox, T., Hickok, N. J., Tuan, R. S., Mechanism of BMP-2 stimulated adhesion of osteoblastic cells to titanium alloy, *Biology of the Cell*, 91 (1999) 131-142.
- Simpson, R. J., An overview of protein structure, 2004a.
- Simpson, R. J., Concentrating solutions of proteins, 2004b.
- Smith, J., Implantation of rhBMP-2 devices in the rat femoral defect model. BBA-940171994, Cambridge MA.
- Steinbuch, M., Protein fractionation by ammonium sulfate, Rivanol and caprylic acid precipitation, 1980.
- Stratton, L. P., Dong, A., Manning, M. C., Carpenter, J. F., Drug Delivery Matrix Containing Native Protein Precipitates Suspended in a Poloxamer Gel, *Journal of Pharmaceutical Sciences*, 86 (1997) 1006-1010.

- Subramaniam, B., Rajewski, R. A., Snavely, K., Pharmaceutical processing with supercritical carbon dioxide, *Journal of Pharmaceutical Sciences*, 86 (1997) 885-890.
- Sucato, D. J., Hedequist, D., Zhang, H., Pierce, W. A., O'Brien, S. E., Welch, R. D., Recombinant human bone morphogenetic protein-2 enhances anterior spinal fusion in a thoracoscopically instrumented animal model, *Journal of bone and joint surgery*. 86-A (2004) 752-762.
- Susi, H. and D. M. Byler, Fourier transform infrared spectroscopy in protein conformation studies, 1988.
- Tabata, Y., Ikada, Y., Protein release from gelatin matrixes, *Advanced Drug Delivery Reviews*, 31 (1998) 287-301.
- Thews, Mutschler, and Vaupel, *Anatomie Physiologie Pathophysiologie des Menschen*, WissenschaftlicheVerlagsgesellschaft mbH, Stuttgart 2004.
- Thies, R. S., Bauduy, M., Ashton, B. A., Kurtzberg, L., Wozney, J. M., Rosen, V., Recombinant human bone morphogenetic protein-2 induces osteoblastic differentiation in W-20-17 stromal cells, *Endocrinology*, 130 (1992) 1318-1324.
- Uludag, H., Gao, T., Porter, T. J., Friess, W., Wozney, J. M., Delivery systems for BMPs: factors contributing to protein retention at an application site, *Journal of bone and joint surgery*, 83-A Suppl 1 (2001) S128-S135.
- Urist, M. R., Bone: formation by autoinduction, *Science*, 150 (1965) 893-899.
- Urist, M. R., Strates, B. S., Bone morphogenetic protein, *Journal of dental research*, 50 (1971) 1392-1406.
- Valentin-Opran, A., Wozney, J., Csimma, C., Lilly, L., Riedel, G. E., Clinical evaluation of recombinant human bone morphogenetic protein-2, *CLINICAL ORTHOPAEDICS AND RELATED RESEARCH*, (2002) 110-120.
- van Beuningen, H. M., Glansbeek, H. L., van der Kraan, P. M., van den Berg, W. B., Differential effects of local application of BMP-2 or TGF-beta 1 on both articular cartilage composition and osteophyte formation, *Osteoarthritis and cartilage/OARS*, 6 (1998) 306-317.
- Von Hippel, P. H. and T. Schleich, Effects of neutral salts on the structure and conformational stability of macromolecules in solution, 1969.
- Wang, E. A., Rosen, V., Cordes, P., Hewick, R. M., Kriz, M. J., Luxenberg, D. P., Sibley, B. S., Wozney, J. M., Purification and characterization of other distinct bone-inducing factors, *Proceedings of the National Academy of Sciences of the USA*, 85 (1988) 9484-9488.
- Wang, E. A., Wozney, J. M., Rosen, V. A., Purification of bovine bone inductive factor and cloning and expression of human cDNA encoding same. Genetics Institute, WO8800205 (1987).
- Wang, E. A., Wozney, J. M., Rosen, V. A., DNA sequences encoding the osteoinductive proteins and expression of these DNA sequences in transgenic cells. Genetics Institute, US5166058 (1989).

- Wang, W., Instability, stabilization, and formulation of liquid protein pharmaceuticals, *International Journal of Pharmaceutics*, 185 (1999) 129-188.
- Wang, W., Lyophilization and development of solid protein pharmaceuticals, *International Journal of Pharmaceutics*, 203 (2000) 1-60.
- Winn, S. R., Uludag, H., Hollinger, J. O., Carrier systems for bone morphogenetic proteins, *CLINICAL ORTHOPAEDICS AND RELATED RESEARCH*, (1999) S95-106.
- Winn, S. R., Uludag, H., Hollinger, J. O., Sustained release emphasizing recombinant human bone morphogenetic protein-2, *Advanced Drug Delivery Reviews*, 31 (1998) 303-318.
- Winters, M. A., Knutson, B. L., Debenedetti, P. G., Sparks, H. G., Przybycien, T. M., Stevenson, C. L., Prestrelski, S. J., Precipitation of Proteins in Supercritical Carbon Dioxide, *Journal of Pharmaceutical Sciences*, 85 (1996) 586-594.
- Woiszwilllo, J. E., Macromolecular microparticles, methods of production, and diagnostic, therapeutic, and other uses thereof. Middlesex Sciences, US9420856 (1994).
- Wozney, J. M., Rosen, V., Celeste, A. J., Mitscock, L. M., Whitters, M. J., Kriz, R. W., Hewick, R. M., Wang, E. A., Novel regulators of bone formation: molecular clones and activities, *Science* (Washington, DC, United States), 242 (1988) 1528-1534.
- www.espineinstitute.com
- www.fda.gov/
- www.roteliste.de
- www.spineuniverse.com
- Yakovlevsky, K., Chamachkine, M., Khalaf, N., Govardhan, C. P., Jung, C. W., Spherical protein particles and methods for preparation and use as in drug delivery systems and diagnostic agents. Altus Biologics, WO2002US19870.
- Zdeblick, T. A., Ghanayem, A. J., Rapoff, A. J., Swain, C., Bassett, T., Cooke, M. E., Markel, M., Cervical interbody fusion cages. An animal model with and without bone morphogenetic protein, *Spine*, 23 (1998) 758-765.
- Zhao M., Chen D., Expression of rhBMP-2 in *Escherichia coli* and its Activity in Inducing Bone Formation, in: T. S. Lindholm (Ed.), *Advances in skeletal reconstruction using bone morphogenetic proteins*, World Scientific, River Edge, NJ, 2002, pp. 1-18.

Curriculum Vitae

Personal data

Name Daniel Hans Schwartz
Born November 22, 1975 in Pegnitz, Germany
Material status single
Nationality German

Professional and academic training

Since 01/2005 research scientist at Merck KGaA, Darmstadt, Germany

10/2001–12/2004 Continuation of the Ph. D. thesis at the Department of Pharmacy, Pharmaceutical Technology and Biopharmaceutics at the Ludwig-Maximilians-University of Munich

02/2001–09/2001 Ph. D. student at the Institute of Pharmaceutical Technology at the Friedrich-Alexander-University Erlangen-Nuremberg: Start of the Ph. D thesis in cooperation with Wyeth BioPharma, Andover, MA, USA

23.01.2001 Licensed Pharmacist (Germany)

18.12.2000 Certificate of the Pharmaceutic examination

06.12.2000 3rd part of the German examination in Pharmacy

11/1999–02/2001 One year internship in a public pharmacy (Zeil-Apotheke in Frankfurt/Main, Germany); subsequent employment as Pharmacist

11/1995–10/1999 Studying Pharmacy at the Friedrich-Alexander-University Erlangen-Nuremberg

25.10.1999 2nd part of the German examination in Pharmacy

29.08.1997 1st part of the German examination in Pharmacy

03/1996–04/1996 Internship at the „Zeil-Apotheke“ in Frankfurt

30.06.1995 Graduation with Abitur (German High School Diploma) at the Staatlichen Gymnasium Lauf an der Pegnitz